NTNU – Trondheim
Norwegian University of
Science and Technology

Ion Exchange

- A Treatment Option for Acid Mine Drainage

Amita Khan

Civil and Environmental Engineering
Submission date: June 2014
Supervisor: Cynthia Halle, IVM
Co-supervisor: Stein Wold Østerhus, IVM

Norwegian University of Science and Technology
Department of Hydraulic and Environmental Engineering

NORWEGIAN UNIVERSITY OF SCIENCE AND TECHNOLOGY
DEPARTMENT OF CIVIL AND TRANSPORT ENGINEERING

Report Title: Ion Exchange – A Treatment Method for Acid Mine Drainage	Date: 06.06.2014 Number of pages (incl. appendices): 127			
	Master Thesis	X	Project Work	
Name: Amita Khan				
Professor in charge/supervisor: Cynthia Halle				
Other external professional contacts/supervisors: Stein Wold Østerhus				

Abstract: The sorption of heavy metals from Acid Mine Drainage (AMD) by using clinoptilolite, a natural zeolite, was studied in this thesis. The behavior of clinoptilolite, as an ion exchanger, was studied to see if the concentration of iron, copper, zinc, and manganese could be reduced to acceptable environmental standards. Folldal works, Løkken works, and Røros copper works were the mines investigated during this study. However, experiments were conducted on the AMD from Folldal and Løkken works.

From the kinetic experiments, the percent adsorption and distribution ratio (K_d) were determined as a function of heavy metal concentration. The percent adsorption showed that the ion exchange process followed three stages; *(1)* surface exchange with a high adsorption rate, *(2)* the inversion stage, and *(3)* moderate adsorption. Higher concentrations of clinoptilolite had a better treatment effect on iron, copper and zinc. The results also indicated competition between iron and manganese, where iron ions occupied the adsorption sites of manganese ions when all the surface sites are taken. The amount of manganese, unlike the other metals, increased with time during the experiment. The distribution ratio showed different results for each metal. In general for iron, copper, and zinc there was an increase in the distribution ratio as the heavy metal concentration decreased. This indicated that all the metals were to some extent exchanged with the cations of the clinoptilolite. The AMD from both areas contained large concentrations of total organic carbon (TOC), and it is assumed that fouling of the clinoptilolite could occur.

Equilibrium isotherms were determined and the results showed that neither the Langmuir nor the Freundlich isotherm have a good fit to the experimental data. The results showed that the adsorption capacity of clinoptilolite decreased as a result of surface coverage, and the selectivity sequence was determined to be $Fe^{3+} > Cu^{2+} > Zn^{2+} > Mn^{2+}$ for both Folldal and Løkken.

Ion exchange with clinoptilolite reduced the amount of heavy metals from the AMD, although the final concentrations were considerably higher than the set requirement of 10 µg Cu/L. Precipitation as an initial step before ion exchange was therefore tested. The results showed a better removal of iron, copper and zinc with 99.6, 97.3, and 37.7 % from Folldal, and 98.3, 98.7, and 59.9 % from Løkken, respectively. Even though the use of precipitation gave much better results, the final concentrations of the heavy metals were still above the acceptable environmental standard.

Keywords:

1. Acid Mine Drainage (AMD)
2. Clinoptilolite
3. Heavy metals

Acknowledgement

This report, under the name "Ion exchange – A Treatment Method for Acid Mine Drainage", is a result of the final thesis at the Department of Hydraulic and Environmental Engineering at the Norwegian University of Science and Technology (NTNU), spring 2014. The topic was selected because of its relevance to the Norwegian environment and my interest in water chemistry and laboratory work.

The master thesis is a continuation of the specialization project, which was conducted during the fall 2013. I have through this thesis worked on the different aspects of ion exchange, learned more about the metal pollution from decommissioned mine sites in Norway and gained more practical experience through work in the laboratory.

Throughout this process, many people helped me to achieve a product I am proud of. First, I would like to thank my supervisor, Associate Professor Cynthia Hallé at the Department of Hydraulic and Environmental Engineering at NTNU. Cynthia's help and support has been greatly appreciated through this semester.

Special thanks go to Senior Engineer Syverin Lierhagen at the Department of Chemistry at NTNU for analyzing the water samples. Gratitude is also given to the Staff Engineers Trine M. H. Ness and Gøril Thorvaldsen for helping me during my laboratory work.

I would like to thank John Arnt Holmen from Orkla industrial museum and Egil Eide the mayor of Folldal municipality for taking the time to show the sampling sites for the Acid Mine Drainage. The information they provided opened my eyes to the challenges that come with decommissioned mine sites.

Gratitude is extended to Richard and Donna Wiger for sharing their knowledge with me. Their valuable comments have been greatly appreciated and made my work easier.

Finally, special recognition goes to my family and friends for their support, encouragement and patience during this semester.

06. 06. 2014 NTNU, Trondheim

Amita Khan

Abstract

The sorption of heavy metals from Acid Mine Drainage (AMD) by using clinoptilolite, a natural zeolite, was studied in this thesis. The behavior of clinoptilolite, as an ion exchanger, was studied to see if the concentration of iron, copper, zinc, and manganese could be reduced to acceptable environmental standards. Folldal works, Løkken works, and Røros copper works were the mines investigated during this study. However, experiments were conducted on the AMD from Folldal and Løkken works.

From the kinetic experiments, the percent adsorption and distribution ratio (K_d) were determined as a function of heavy metal concentration. The percent adsorption showed that the ion exchange process followed three stages; *(1)* surface exchange with a high adsorption rate, *(2)* the inversion stage, and *(3)* moderate adsorption. Higher concentrations of clinoptilolite had a better treatment effect on iron, copper and zinc. The results also indicated competition between iron and manganese, where iron ions occupied the adsorption sites of manganese ions when all the surface sites are taken. The amount of manganese, unlike the other metals, increased with time during the experiment. The distribution ratio showed different results for each metal. In general for iron, copper, and zinc there was an increase in the distribution ratio as the heavy metal concentration decreased. This indicated that all the metals were to some extent exchanged with the cations of the clinoptilolite. The AMD from both areas contained large concentrations of total organic carbon (TOC), and it is assumed that fouling of the clinoptilolite could occur.

Equilibrium isotherms were determined and the results showed that neither the Langmuir nor the Freundlich isotherm have a good fit to the experimental data. The results showed that the adsorption capacity of clinoptilolite decreased as a result of surface coverage, and the selectivity sequence was determined to be $Fe^{3+} > Cu^{2+} > Zn^{2+} > Mn^{2+}$ for both Folldal and Løkken.

Ion exchange with clinoptilolite reduced the amount of heavy metals from the AMD, although the final concentrations were considerably higher than the set requirement of 10 µg Cu/L. Precipitation as an initial step before ion exchange was therefore tested. The results showed a better removal of iron, copper and zinc with 99.6, 97.3, and 37.7 % from Folldal, and 98.3, 98.7, and 59.9 % from Løkken, respectively. Even though the use of precipitation gave much better results, the final concentrations of the heavy metals were still above the acceptable environmental standard.

Sammendrag

Sorpsjon av tungmetaller fra surt gruvevann (AMD) ved bruk av clinoptilolite, en naturlig zeolitt, har blitt undersøkt i denne oppgaven. Oppførselen til clinoptilolite har blitt undersøkt for å se om konsentrasjonen av jern, kobber, sink og mangan ble redusert til pålagte krav. Gruvene ved Folldal verk, Løkken verk og Røros kobberverk har blitt undersøkt. Det er kun gruvevannet fra Folldal og Løkken det har blitt utført forsøk på.

De kinetiske forsøkene viste at den prosentvise adsorpsjonen og fordelingsforholdet (K_d) var avhengige av tungmetallkonsentrasjonen. Den prosentvise adsorpsjonen viste at ionebytteprosessen fulgte tre ulike stadier; *(1)* overflatereaksjoner med høy adsorpsjonsrate, *(2)* inversjonssteg, og *(3)* moderat adsorpsjon. Det har vist seg at større mengde clinoptilolite gir bedre renseeffekt av jern, kobber og sink. Resultatene indikerer også at det er konkurranse mellom jern og mangan. Jernionene overtar adsorpsjonsområdene til mangan når alle tilgjengelige plasser er tatt. I motsetning til de andre metallene øker konsentrasjonen av mangan i løpet av forsøket. Fordelingsforholdet viser ulike resultater for de forskjellige metallene. Felles for jern, kobber og sink, er at fordelingsforholdet øker samtidig som metallkonsentrasjonen minker. Dette indikerer at noe av metallet utveksles med kationene fra clinoptilolite. AMD fra begge områdene inneholder store mengder organisk materiale (TOC), og det antas at det vil forekomme gjentetting av clinoptilolite.

Likevekts-isotermer ble bestemt og resultatene viste at verken Langmuir eller Freundlich isotermet var tilpasset de eksperimentelle data. Resultatene viste at adsorpsjonskapasiteten for clinoptilolite ble redusert som et resultat av overflatedekning. Clinoptilolites selektivitetsserie ble bestemt til å være $Fe^{3+} > Cu^{2+} > Zn^{2+} > Mn^{2+}$ for både Folldal og Løkken.

Det har vist seg at ionebytting med clinoptilolite reduserer noe av tungmetallinnholdet i gruvevann. Likevel er endelig metallinnhold langt fra å oppfylle kravet om 10 µg Cu/L. Utfelling som behandlingstrinn i forkant av ionebytting, har derfor blitt testet. Resultatene viste bedre fjerning av jern, kobber og sink med henholdsvis 99.6, 97.3 og 37.7 % reduksjon fra Folldal, og 98.3, 98.7 og 59.9 % reduksjon fra Løkken. Selv om utfelling i forkant av ionebytte gav bedre resultat, ble sluttkonsentrasjonene fortsatt høyere enn de aksepterte kravene.

Table of Contents

List of Figures

List of Tables

1. Background

1.1 Introduction

The Norwegian mining industry has a long history dating back approximately 1000 years to the Akersberg silver mine in Oslo. In the early 1600s large-scale mining for copper and sulfur became common (Segalstad et al., 2006). The mining industry remained active until the late 1900s but then closed down due to low profitability. The mining industry on Svalbard, however, is still active, producing sand, gravel, stone, industrial minerals, iron ore and coal (Skei, 2010).

The many years of mining activities in Norway has resulted in the pollution of many ecosystems near these mines, since few measures were taken during the production period. Even though the activity around the mines ended many years ago, there are still a number of different problems related to these sites. Many of the decommissioned sulfide mines have led to acid drainage problems (Skei, 2010). Acid drainage problems can lead to polluted waterways and have severe consequences for the biodiversity. In the literature this problem is called Acid Mine Drainage (AMD), and it is caused when sulfide-bearing materials come into contact with oxygen and water.

Three of the previous sulfide mine districts in Norway, Folldal, Løkken, and Røros, have problems with polluted discharge water. The main concern with AMD is the amount of heavy metals found in the mine water. Large quantities of heavy metals have a negative effect on the environment since these metals are not degradable. Despite the fact that the sulfide mines have been closed down for many years, AMD poses major threats to the ecosystems nearby the mines. Fish and other organisms living in the nearby rivers are especially affected.

Today there are many possible ways to manage AMD. The treatment options are numerous and can be optimized to treat a specific water composition. The treatment option will vary from one site to another due to different needs that must be taken into account. One option is ion exchange. This method is not commonly used in Norway, but with the proper choice of material, ion exchange can be a cost effective and an environmental friendly choice. To see if ion exchange is a valid choice for treatment of AMD, different laboratory tests have to be conducted and evaluated.

1.2 Research goal and objectives

AMD is a potential threat to the environment and must therefore be treated before it is discharged into a nearby river. The problem description is as follows:

This master thesis will investigate the three decommissioned mine sites, Folldal, Løkken, and Røros. Furthermore, ion exchange as an active treatment option for the AMD from Folldal and Løkken will be examined in the laboratory. Natural zeolite as the ion exchanger will be tested. The thesis will study how natural zeolite preforms with respect to:

- *Kinetic studies*
- *Effect of solution pH*
- *Adsorption isotherms (equilibrium studies)*
- *Effect of competing substances such as other metals and total organic carbon (TOC)*

The aim of the master thesis is to determine whether or not ion exchange is a valid choice for the three locations.

2. Acid Mine Drainage

AMD is often associated with both working and decommissioned sulfide mines. The problems related to AMD are widespread and have large impacts on the environment, especially since AMD has a high content of heavy metals. The water quality of nearby recipients tends to be poor and the combination of acid water and high metal concentration has adverse effects on the ecosystem.

2.1 General background information about acid mine drainage

Drainage from underground mines or backfilling from mines can cause acid or alkaline water. AMD is acidic water produced due to the presence of sulfides. It has a pH below 5.0 and it tends to contain significant quantities of iron, sulfate and other metals. Alkaline drainage water has a pH above 6.0 and occurs because of carbonate material, however it may still contain metals and become acidic due to oxidation and hydrolysis (Skousen, 2011).

Oxidation of minerals is usually a slow process since the minerals are not in direct contact with oxygen. However, mining expose minerals in their reduced form to come in contact with oxygen which results in oxidation. This can occur in the depths of the mines or when the minerals are brought up to the surface. Sulfides in the form MS_2 (M stands for metal) will lead to the production of protons (H^+) that form acidic water. The most common sulfide mineral is pyrite (FeS_2) and in contact with water, the result is often formation of AMD. Sulfides can react with a variety of other metals such as As, Bi, Cd, Co, Cu, Fe, Ga, In, Hg, Mo, Pb, Re, Sb, Se, Sn, Te and Zn (Banks et al., 1997). Other common sulfide minerals that occur, are chalcopyrite ($CuFeS_2$), covellite (CuS), and arsenopyrite (FeAsS) (Skousen, 2011). AMD often occurs from a reaction with pyrite, but other metals will dissolve as a result of the acid water, causing the water to have a high metal content.

The formation of AMD is related to three primary conditions: (1) sulfide minerals, (2) water or humid atmosphere and (3) an oxidant, generally oxygen from the atmosphere (Akai & Koldas, 2009). Since pyrite is one of the most common sulfide minerals, it will be examined further.

The oxidation of pyrite can be viewed as a complex cycle of reactions, as seen in Figure 1, and from Equations (1) to (5).

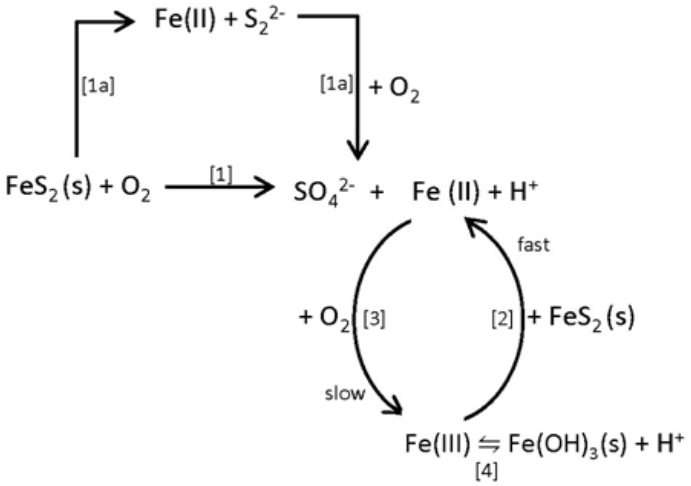

Figure 1: Model for the oxidation of pyrite (The International Network for Acid Prevention, 2012)

Equation (1) describes the dissolution of pyrite into ferrous iron (Fe^{2+}), sulfate (SO_4^{2-}) and protons (H^+):

$$FeS_2 + \frac{7}{2}O_2 + H_2O \rightarrow Fe^{2+} + 2SO_4^{2-} + 2H^+ \qquad (1)$$

The amount of ferrous iron and sulfate represents an increase in the total amount of dissolved solids. The increasing level of protons will lead to acid water and therefore a reduction in pH. The pH, amount of available oxygen, and bacterial activity will determine whether further oxidation will take place. If all the criteria are met, ferrous iron will oxidize to ferric iron (Fe^{3+}) (Akai & Koldas, 2009). The rate of reaction (2) will according to Benjamin (2002) increase by a factor of 100 for every unit increase in solution pH. In addition to helping control the conversion rate of ferrous iron to ferric iron, the pH affects the ultimate solubility of the iron once the system equilibrates:

$$Fe^{2+} + \frac{1}{4}O_2 + H^+ \rightarrow Fe^{3+} + \frac{1}{2}H_2O \qquad (2)$$

At a pH between 2.3 and 3.5, precipitation of ferric hydroxide ($Fe(OH)_3$) will occur. The presence of ferric hydroxide in the water can cause the water to have a maroon color:

$$Fe^{3+} + 3H_2O \rightarrow Fe(OH)_3(s) + 3H^+ \qquad (3)$$

As seen in Figure 1, ferric iron can also oxidize more of the pyrite. This applies mainly to the ferric iron that is not converted to ferric hydroxide. The reaction is shown in Equation (4):

$$FeS_2 + 14Fe^{3+} + 8H_2O \rightarrow 15Fe^{2+} + 2SO_4^{2-} + 16H^+ \qquad (4)$$

The total oxidation reaction, with oxygen as the oxidant, is shown in Equation (5) which is a combination of Equation (1) – (3):

$$FeS_2 + \frac{15}{4}O_2 + \frac{7}{2}H_2O \rightarrow Fe(OH)_3 + 2SO_4^{2-} + 4H^+ \qquad (5)$$

The majority of the equations above are specific for pyrite. As mentioned before, sulfide can react with many different ions and form other minerals. Each of these minerals has different pathways, stoichiometries and reaction rates, and can thus produce different compositions of AMD. However, this study focuses on pyrite because it is the most common sulfide mineral and the research on other sulfide minerals is limited.

2.1.1 Physical and biological factors

To ensure that the rates of the chemical reactions described in Equation (1) to (5) are optimal, the different physical and biological factors that the AMD process is depended on needs to be standardized. Some of the reactions described are too slow to contribute to the process if the specific factors are not satisfactory.

Physical factors of importance are pH, temperature, availability of oxygen and the surface area of the minerals. In addition to these factors the permeability of the waste rock dumps is very important. Higher permeability leads to higher diffusion of oxygen, and thus the rate of the oxidation increase. An increase in the chemical oxidation rate can result in higher temperature and more oxygen ingress because of convection (Akai & Koldas, 2009).

Equation (2) describes the oxidation of ferrous iron to ferric iron with oxygen as the oxidizing agent. This reaction is the rate-limiting step in the oxidation process of pyrite. Stumm and Morgan (1996) describe the oxygenation kinetics for Equation (2), which follows the rate law as seen in Equation (6):

$$\frac{-d[Fe(II)]}{dt} = k[Fe(II)][OH^-]^2 p_{O_2} \qquad (6)$$

Where k is the oxidation rate constant [$min^{-1}atm^{-1}mol^{-2}liter^{2}$] and p_{O_2} is the partial pressure of oxygen [atm]. From Equation (6) it is possible to see that the oxidation rate is first order with respect to ferrous iron and the partial pressure, and that the equation is second order for hydroxide (OH^-). The relationship between the oxidation rate and pH described in Equation (6) is shown in Figure 2.

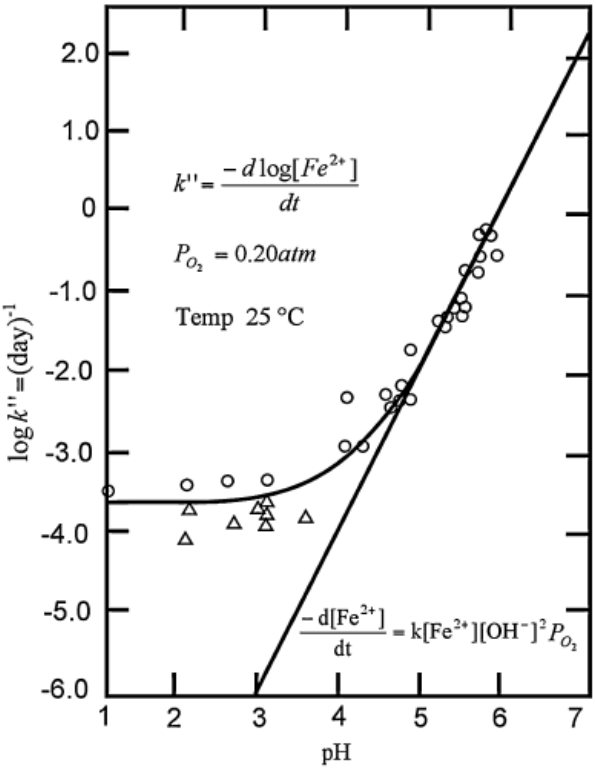

Figure 2: Oxidation rate of ferrous iron species as a function of pH (Morgan & Lahav, 2007)

From Figure 2, it is possible to see that when the pH is low, the oxidation rate is independent of pH. Whereas, for pH values above 4.0, the oxidation rate is dependent on pH, this is because of the second order dependency on hydroxide (Stumm & Morgan, 1996). When studying the relationship between the oxidation rate and pH, it is possible to see that for high pH values the rate would be independent of the pH. However, this has limited relevance since AMD remains on the acidic side of the pH scale. The oxidation rate will also increase with an increase in temperature for a given pH. Available surface area is also of relevance to the oxidation rate since a larger surface area can cause a greater portion of pyrite to oxidize.

Since decommissioned mine water tends to be acidic, the oxidation rate of ferrous iron to ferric iron is not dependent on pH. The oxidation reaction is, however, dependent on microbial activity since microorganisms can accelerate the reaction rate. For the oxidation process described in Equation (2) to take place, it is necessary that the chemoautotroph bacterias *Thiobacillus ferroxidans* and *Leptospirillum ferrooxidans* are present. *T. ferroxidans* are most efficient in the pH range between 1.5 and 3.0, whereas *L. ferrooxidans* are functional for a wider pH range (Schrenk et al., 1998). The energy for their metabolic process comes from the oxidation of reduced sulfur and iron, and carbon dioxide is used as the carbon source (Banks et al., 1997). Studies done by Boon et al. (1999) show that *L. ferrooxidans* are more important for the oxidation of pyrite, and in addition they dissolve pyrite more extensively than *T. ferroxidans.* However, one or both types of bacteria need to be present to generate AMD.

2.2 Heavy metals

The large amount of heavy metals found in AMD is one of the main reasons for being concerned about AMD. Heavy metals are harmful for the environment since the metals are not biodegradable and therefore accumulate in living organisms (Motsi et al., 2009). Metals defined as heavy metals have a density above 5 g/cm^3, and approximately 60 of the naturally occurring elements are heavy metals (Store Norske Leksikon, 2009). The most common heavy metals in Norwegian mine drainage are copper, zinc, cadmium, lead, and iron (Miljødirektoratet, 2013a). Copper is usually the metal of greatest importance in a pollution context, since copper has a greater toxic effect on the ecosystem than any other heavy metal (Banks et al., 1997). The acceptable environmental concentration has therefore been set to 10 µg Cu/L (Miljødirektoratet, 2013a). It is assumed that if the copper concentration is below this limit, the concentration of the other heavy metals will also be satisfactory.

The level of heavy metals in the water from decommissioned mine sites varies for the different mines, and from year to year. The released amounts of heavy metals vary with rainfall and temperature. Heavy rainfalls result in higher concentration of heavy metals in the river systems, since the storm water runoff carries the pollutants. This is particularly visible during the spring flooding, that contributes to a great part of the yearly heavy metal contamination (Miljødirektoratet, 2013a).

3. Problem areas

For many years mining was a vital part of the Norwegian economy. The Caledonian mountain chain, especially Trøndelag County is rich in sulfide-bearing minerals of iron, copper, sulfur, and zinc (Banks et al., 1997). The mining activity in the 19th century resulted in an increase of polluted waterways. In the 1960s and 1970s, a contamination peak was reached due to acid drainage that polluted several important river systems (Iversen & Arnesen, 2003). The main problems with AMD in Norwegian mines have been from both underground mines and waste deposits. The problems are related to old mines and mining methods that are no longer in used.

AMD has been an important source for the problems related to water quality in many Norwegian lakes and rivers. This has resulted in a negative influence on the ecosystem, especially the accumulation of heavy metals in fish. The problems related to AMD have been known for many years. In the 1980s the Norwegian Environment Agency (Klif) established guidelines for the permissible concentrations of heavy metals in aquatic environments. The requirement, as mentioned earlier, should not exceed 10 µg Cu/L. This requirement will, in most cases, result in an almost normal situation with regards to heavy metal accumulation in fish, drinking water supply and water for other practical uses.

The mines chosen for this study are three of Norway's largest pyrite mines, Folldal works, Løkken works and Røros copper works. Løkken works and Røros copper works are located in Trøndelag County, while Folldal works is in Hedmark, as shown in Figure 3.

Figure 3: Map of Norway, showing selected sulfide mines (Banks et al., 1997)

All three locations have had problems with AMD. Even though all of the mines are now closed down, and despite the fact that measures have been taken, the pollution potential is still high at the three locations. At all of these sites, heavy metals are leaking into the different recipient waters. To get a better picture of the situation, it is necessary to look at each case separately.

3.1 Folldal works

Folldal works consists of five mines around the area of Folldal, the main mine is Folldal center. In addition there are the Northern mine, Southern mine, Nygruva and Grimsdal mines (Rui, 2009). Folldal works was established in 1748 for the extraction of copper, zinc, and sulfur. The main mine in Folldal center was closed in 1941 and the others in1968. An exception is the mine in Hjerkinn at Tverrfjellet, which was in operation from 1968 to 1993 (Eide, 2013).

3.1.1 The pollution situation in Folldal center

The most important problems concerning Folldal works have been associated with the main mine in Folldal center, since this is the mine that releases most heavy metals. The amount of heavy metals from the other mines at Folldal works are so small in comparison to the contribution from Folldal center, that they have been disregarded in this study (Iversen & Arnesen, 2003). The two main sources for the AMD are the mine water from inside of the mine and drainage from mine tailings. In the 1980s, high concentrations of copper were discovered in the river Folla. As seen in Figure 4, the copper runoff from the main mine into Folla, was calculated to be 16 tons in 1985. During the period 1992 to 1994 drainage measures were implemented. Unfortunately, these measures did not have a positive effects on the heavy metal concentrations in the river Folla (Miljødirektoratet, 2013b). The amount of heavy metals being released varies from year to year. This is mainly associated with variations in rainfall and temperature fluctuations. The weather variations have direct impacts on the oxidation process and consequently the amounts of metals leaking into the river (G. Braastad, personal communication, 7th March 2014). High intensity rainfall events will to a greater extent lead to increased levels of heavy metals in the runoff, which in turn leads to the increase of heavy metals entering the recipient (Miljødirektoratet, 2013a)

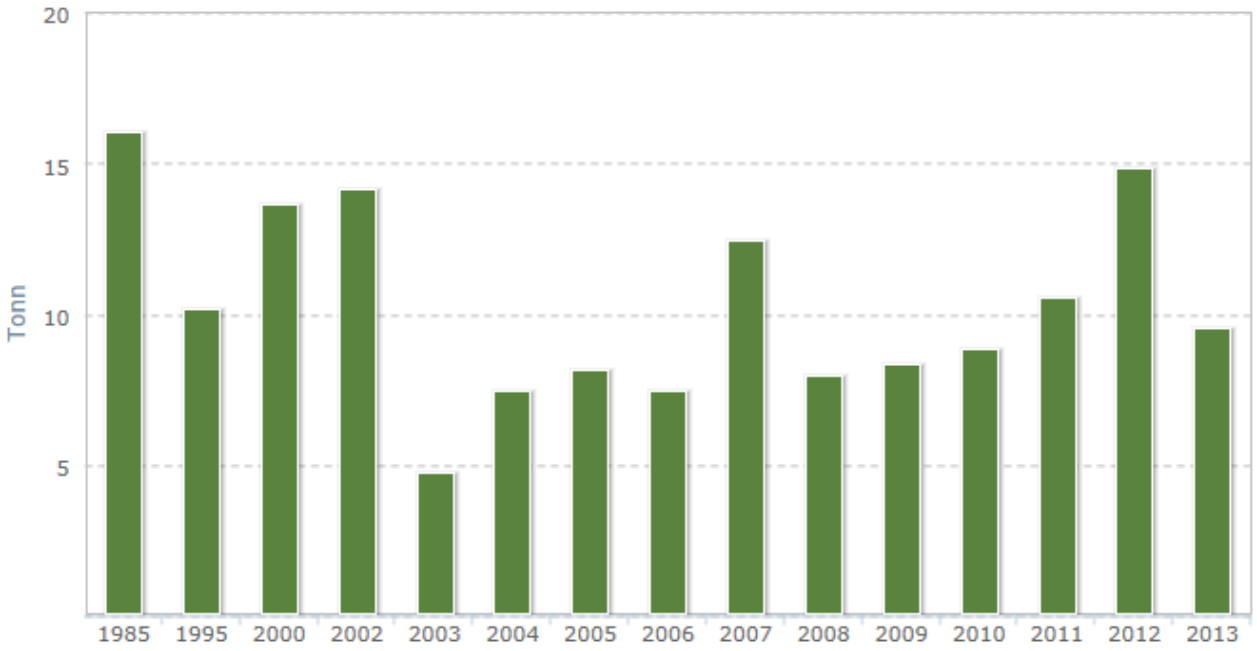

Figure 4: Copper runoff from Folldal center (Miljødirektoratet, 2013b)

Folldal center is protected by the Directorate for Cultural Heritage as a national cultural monument. This complicates the situation since it is not permitted to remove minerals, cover the tailings, or to fill up the mine. This protection makes it difficult to prevent AMD and the only option remaining is drainage treatment, which was previously attempted without success (Skei, 2010). Both the Norwegian Ministry of Trade and Industry (NHD) and the Norwegian Directorate of Mining has proposed different treatment options for the area (Miljødirektoratet, 2013b). There is currently no treatment plant for the runoff from Folla center but there is an ongoing project that is considering several alternatives (E. Eide & G. O. Slåen, Personal communication, 20th March 2014). The plan is to implement a lime-precipitation plant by 2015.

3.1.2 Folla

The main recipient of runoff from Folldal center is the river Folla that is a tributary stream of the large river Glomma. This river stretches from the mountains at Dovre, through Hjerkinn, proceeding down to Folldal and then to Alvdal. The total length of the river from Vålåsjøen at Dovre to Alvdal, where it joins Glomma, is 108 km and the catchment area is 2170 km^2 (Iversen & Arnesen, 2003). Figure 5 shows a map over lower Folla and the part where it meets Glomma.

During the time when the mines were in operation, the pollution from Folldal center was led directly into Folla. After the mine was closed in 1941, some of the drainage was collected into a

pond. The pond was not covered, and this led to the precipitation of different hydroxides causing even greater pollution of the water. In 1993, when Hjerkinn mine was closed, some of the contaminated soil was collected and dumped into the pond. Although some of the contaminated soil was removed from the pond, most of it remained. Despite the fact that drainage measures were carried out early in the 1990s, there is still a problem with polluted water going into Folla today. For many years the Norwegian Institute for Water research (NIVA) monitored the water in Folla. Their studies have shown that the AMD consist of mostly copper, iron and zinc, and the main source of these contaminants is drainage from tailings and from inside the mine (Iversen & Arnesen, 2003). Studies show that the copper concentration of the AMD from the mine is 79.6 mg Cu/L, which entails that the copper concentration in Folla is so high that there is no biological life for about 20 km downstream the river (E. Eide & G. O Slåen, Personal communication, 20th March 2014). The runoff also affects Glomma, which has a copper concentration above 10 µg Cu/L (Miljødirektoratet, 2013b). In Figure 5, the area marked in red shows the sections of the river with a copper concentration exceeding 10 µg Cu/L.

Figure 5: Map of the lower part of the river Folla and the river Glomma (Iversen & Arnesen, 2003)

3.2 Løkken works

Løkken works is located in Meldal in Sør-Trøndelag County. There was mining in this area from 1654 until 1987. The mining area consisted of four main shafts and the system was about four kilometer long (Banks et al., 1997). Production has varied over a large timeframe. During the period 1654 to 1844 the production consisted mainly of copper. From 1851, mining of pyrite minerals was dominating, mainly as raw material for the production of sulfuric acid. Between 1931 and 1962 the mining was based on copper and sulfur. From 1974 until 1987 mining of copper and zinc dominated (Miljødirektoratet, 2013c). According to J.A. Holmen the mines at Løkken contain the largest amount of copper containing sulfur ores in Norway. (Personal communication, 20th March 2014)

3.2.1 The pollution situation in Løkken

Throughout the years the pollution situation at Løkken works has been complex, and it is the mining area in Norway that has the greatest pollution potential. Periodically there have been considerable levels of heavy metals in the discharge sources in the mine water, leachate from overturn, effluent from concentration plant, and runoff from landfills (Miljødirektoratet, 2013c).

All the different mineral withdrawals and discharge sources have led to a very complex pollution situation in the area. In the period between the early 1970s and 1990s, the mine water was the main pollution source into the river Orkla. Studies done by NIVA in the 1990s, showed that around 48 tons of copper and 70 tons of zinc entered the river Orkla yearly (Miljødirektoratet, 2013c). To minimize the discharge of heavy metals, Løkken works stored the mine water inside the mine and then used Wallenberg mine as a small "treatment plant" for the incoming mine water and waste drainage (J. A. Holmen, Personal communication, 20th March 2014). How the water is stored can be seen from Figure 6. The idea to use Wallenberg mine as a "treatment plant", was proposed because the copper content in the incoming water was high, whereas the outgoing water had a lower content. The reason for this is, that copper adheres to pyrite and alkaline rock, which the mine consisted of. This measure was implemented from 1991 to 1992. As a result of this, the main source of runoff is from the various landfills, which are characterized as the rocks that have the highest sulfide content in Norway (Skei, 2010).

Figure 6: Sketch of the AMD stored inside Løkken works

As a result of using the Wallenberg mine as a "treatment plant", the copper concentration was reduced to around 7 µg Cu/L as an annual mean. In 2004, the supply of copper into the river Orkla was reduced by 70 % compared to the 1985 level. However, since 2004 there has been an increase in the metal discharge into the river Orkla. The reason was the limitation of the alkaline rock that was used for treatment, and this has resulted in a higher copper concentration entering the river Orkla in recent years. Figure 7 shows the yearly copper input in the runoff from Løkken works (Miljødirektoratet, 2013c). The concentration varies from year to year, as for Folldal works, the variations are mainly due to weather changes (G. Braastad, Personal communication, 7th March 2014).

After 2005, it became clear that the measures implemented in 1992 were not adequate, and it became necessary to implement new initiatives to ensure that the metal concentration leaking into the river Orkla was kept at a minimum. Increased monitoring in the area has been implemented and will continue until new measures are applied (Miljødirektoratet, 2013c).

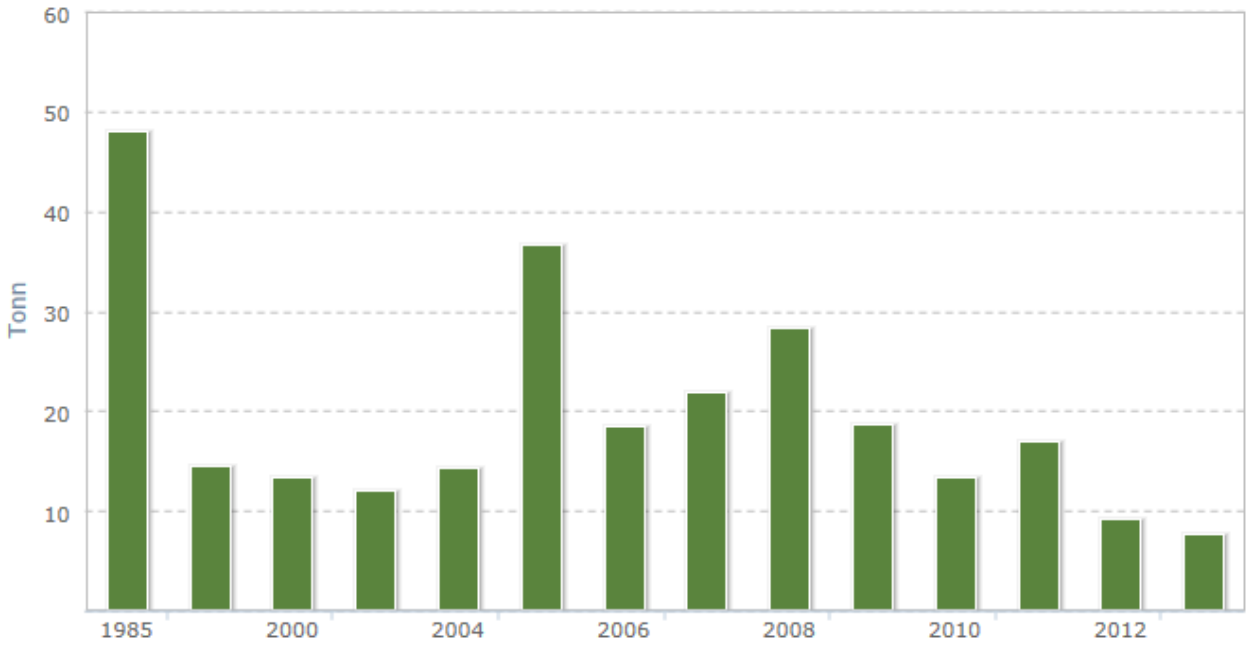

Figure 7: Copper runoff from Løkken works (Miljødirektoratet, 2013c)

3.2.2 Orkla

The main recipient for the pollution from Løkken works is Orkla. The river flows from the lake Store Orkelsjøen to Orkanger at Orkdalsfjorden and the distance is 172 km (Iversen & Arnesen, 2003). The runoff from Løkken works ends up in Orkla through two different pathways. From Løkken the runoff goes through Raubekken stream before it ends up in Orkla. From the Wallenberg area the water runs through lake Fagerlivatn on its way to Orkla (Miljødirektoratet, 2013c).

The heavy metal runoff from Løkken works has been the greatest pollution problem associated with Norwegian sulfide mines. Although implemented measures have reduced the copper content leaking into Orkla, the runoff from Løkken works still pollutes the river. It is important to protect Orkla from pollution because Orkla is one of Norway's most important salmon rivers. Contaminants that have negative effects on aquatic organisms and fish can thus lead to serious consequences affecting fish development, the sports fishing industry in the area and food quality (Miljødirektoratet, 2013c).

Since 1973, NIVA has monitored the water coming from Løkken works into Orkla. The measurements conducted by NIVA are taken at Vormstad, which also gets water from Dragset works and Høydalsgruva. The samples show that there is pollution from these two areas as well

as a the contribution from Løkken works. The area marked in red in Figure 8 shows which parts of Orkla river with a copper concentration above10 µg Cu/L.

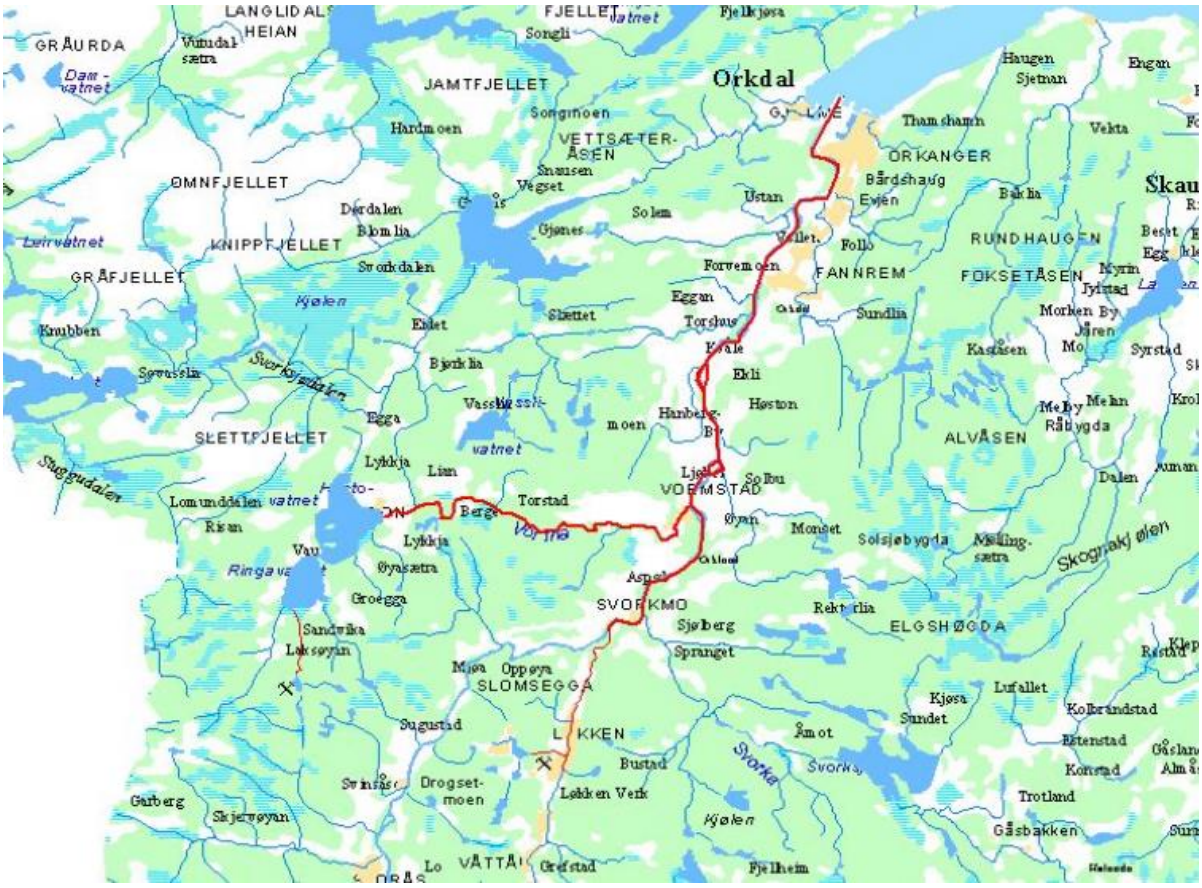

Figure 8: Map of lower rivers Orkla. Raubekken (Løkken works) and Bjøråa (Dragset plants) is highlighted (Iversen & Arnesen, 2003)

3.3 Røros copper works

The Røros mining district covers a large area and it can be divided into two main mine districts, Østgruvefeltet and Nordgruvefeltet. Both areas count 13 mines in total (Gvein, 2009). Røros copper works operated for 334 years, in the period from 1644 to 1978 (Miljødirektoratet, 2013d). The main environmental problem has been AMD from waste rock disposal and landfills. Røros has been a part of the World Heritage since 1980, and in 2010 there was an expansion of the circumference of the area (Riksantikvaren, 2012). The treatment options are limited because the area is a part of the cultural heritage.

3.3.1 The pollution situation at Storwartz

The Storwartz area was the largest mine field in Røros and most of the heavy metal contamination originates from this area. The production started in 1644 and ended in 1973. The main products from these mines are iron, copper, and zinc. The long and varied mining activities in Storwartz have resulted in large amounts of waste spread all over the area. This waste has led to a strong AMD through the watershed Hittervassdraget and all the way down to the river Glomma (Miljødirektoratet, 2013d).

Chemical analyses show that the drainage from the Storwartz area is the dominating contributor of heavy metals into the lake Djupsjøen, where the copper concentration is approximately 30 µg Cu/L. The concentration of heavy metals varies due to variations in the climate. For example, the spring floods can carry high concentrations of heavy metals into the recipient. The high content of heavy metals in the lake Djupsjøen and the river Hitterelva has resulted in a reduced biodiversity. There is a need for some type of treatment process. Unfortunately, no treatment methods have been implement partially due to the fact that the Røros mining area is a cultural heritage (Miljødirektoratet, 2013d).

3.3.2 Djupsjøen – Hitterelva - Glomma

The Hitterelva river starts in the lake Storhittersjøen east of Røros, flows through the lakes Grunnsjøen, Djupsjøen, Stikkillen and Hittersjøen, before it runs through the town Røros and then joins the river Håelva and ends up in the river Glomma. The total length of the river is 16 km down to Glomma. The pollution that is found in the water mainly comes from the Storwartz area (Iversen & Arnesen, 2003).

The runoff from Storwartz goes directly into the lake Djupsjøen. The AMD comes from a combination of mine water and waste deposits. The pollution from the mine water is relatively small compared to the pollution from the landfills. The runoff from the Storwartz mining area is divided into two pathways and both end up in Djupsjøen and then the river Hitterelva. The water can either flow from the streams Stormyrbekken or Prestbekken.

Glomma is also affected by the drainage that comes from the mines in Storwartz. There are two rivers that run into Glomma around the same point, Hitterelva and Håelva. Studies done by Iversen and Arnesen (2003) show that the pollutants found in Glomma originates from the mines

in Storwartz. Figure 9 shows a map of Glomma around Røros. The parts marked in red have a copper concentration above 10 µg Cu/L.

Figure 9: Map over the upper part of the river Glomma in the Røros area. Prestbekken from Storwartz is also shown (Iversen & Arnesen, 2003)

4. Ion exchange

Considering the number of mines with sulfide minerals in Norway, the formation of AMD is inevitable. Some of the effluents from these mines contain toxic substances such as heavy metals that in large quantities have negative effects on the surrounding environment. It would be preferable to prevent the formation of AMD. This is, however, difficult to achieve for all of the mines.

Treatment options for AMD are usually divided into either active or passive treatment. Both options include chemical and biological treatments to neutralize and remove metals from the solution. Active treatments generally include the traditional treatment processes such as neutralization, precipitation, aeration, adsorption, and ion exchange. Passive treatments are methods that take advantage of natural biological and geochemical processes. Typical passive treatment systems for AMD include anaerobic wetlands and anoxic limestone drains.

In this thesis, ion exchange as a treatment option will be examined further. Ion exchange is characterized by the replacement of one adsorbed ion with an exchangeable ion (Stumm & Morgan, 1996). When using ion exchange it is possible to replace the undesirable ions with other ions which will not contribute to contamination of the environment. Compared to other traditional treatment methods, ion exchange is, in some cases, a cheaper alternative. In comparison to ion exchange, precipitation is unfavorable when dealing with large volumes of AMD. The reason is that precipitation requires coagulation, flocculation and sedimentation which take up space. Furthermore, large amounts of sludge containing heavy metals will be produced and require proper handling.

4.1 Fundamentals of ion exchange

The use of natural materials as an ion exchanger for water treatment has been in use for thousands of years. However, it was not until 1854 that the first systematic study was conducted by Thomson and Way. They observed that ammonium ions adsorbed onto soils releasing calcium ions in equivalent amounts. Aluminum silicates present in the soil was responsible for the exchange, and the exchange of ions differed from true adsorption (Crittenden et al., 2005)

Ion exchange is a reversible process of ions between a liquid phase and a natural or artificial medium. The ion exchange resin can be designed to remove specific ions, but generally there will

be an exchange of more than one ion species (Droste, 1997). The ion exchange resin will eventually be saturated with the ions that should be removed from the water, and it is therefore necessary to regenerate the ion exchanger. The regeneration process is implemented by putting the ion exchanger in contact with a regeneration solution that can consist of various salt and acid solutions. The choice of regeneration solution depends on the particular application of the resin. (Crittenden et al., 2005). The reactions for normal operation and regeneration are shown in Equation (7) and (8):

$$nR^{-}A^{+} + B^{n+} \rightarrow R_n^{-}B^{n+} + nA^{+} \qquad (7)$$

$$R_n^{-}B^{n+} + nA^{+} \rightarrow nR^{-}A^{+} + B^{n+} \qquad (8)$$

Where *B* represents the metal that one wants to remove, *A* is the ion from the ion exchanger, n is the charge and R_n^{-} is the anionic group attached to the ion exchange resin. Figure 10 shows a schematic framework of the cation exchange resin described in Equation (7):

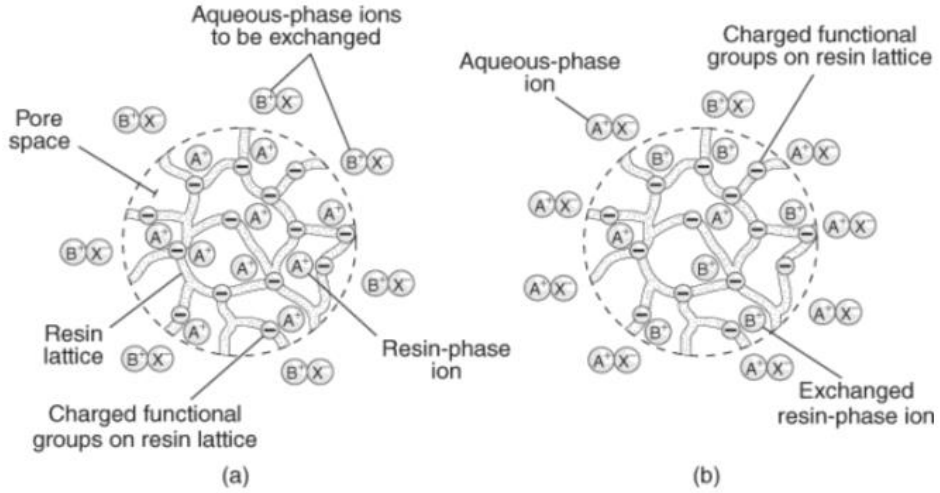

Figure 10: Cation exchange resin: "(a) resin initially immersed in an aqueous solution containing B+ cations and X- anions; (b) cation exchange resin in equilibrium with aqueous solution of B+ cations and X- anions" (Crittenden et al., 2005, p. 1362)

The equilibrium relation for Equation (7) is

$$K_{exch,A^{n+}\rightarrow B^{n+}} = \frac{[A^{+}]_S^n [R_n^{-}B^{n+}]_R}{[R^{-}A^{+}]_R^n [B^{n+}]_S} \qquad (9)$$

Where $K_{A^{+}\rightarrow B^{n+}}$ is the selectivity coefficient, $[A^{+}]_S^n$ and $[B^{n+}]_S$ is the concentration of *A* and *B* in the solution and $[R^{-}A^{+}]_R^n$ and $[R_n^{-}B^{n+}]_R$is the concentration of *A* and *B* on the exchange resin.

The selectivity coefficient is primarily dependent on the nature and valence of the ion, type of resin and its saturation, and the ion concentration in wastewater. It is typically valid over a narrow pH range (Metcalf et al., 2014a). However, the selectivity coefficient is rarely constant because the ion activity within the lattice structure of the ion exchanger is unknown. The coefficient is also dependent on the ion exchange phase, which keeps changing as the reaction described in Equation (7) takes place (Stumm & Morgan, 1996).

4.2 Adsorption Isotherms

When studying ion exchangers, it is common to look at the theory and design for adsorption, since this also applies to ion exchange. There is no common terminology when it comes to describing an adsorptive system. However, some terms are well-accepted, and the definitions are given below:

> **Adsorption** is the accumulation of a substance at or near an interface relative to its concentration in the bulk solution. **Desorption** is the reverse of an adsorption; i.e., it is the release of an adsorbed substance to the bulk solution. The substance that adsorbs is called the **adsorbate**, and the solid which it binds is called the **adsorbent** (Benjamin, 2002, p. 553).

The amount of adsorbate that an adsorbent can take up is determined by the characteristics, the concentration of the adsorbate, and water temperature. Important factors describing the adsorbant are solubility, saturation, the molecular structure, and weight. Generally, an adsorption isotherm describes the amount of material absorbed as a function of the concentration at a constant temperature (Metcalf et al., 2014a). Adsorption isotherms are typically derived empirically by collecting data for the adsorption density, q, as a function of the dissolved concentration of the adsorbate. The data is then attempted to fit simple equations. The isotherm can be used to predict the adsorbate behavior for systems with conditions that have not yet been examined experimentally. To accurately describe the adsorption that takes place over a wide range of conditions, the adsorption isotherms needs to consider the characteristics of the ion exchanger, the solution, and the interaction between these two components (Benjamin, 2002).

4.2.1The Langmuir isotherm

The Langmuir adsorption isotherm describes the equilibrium between the surface of the adsorbent and solution as a reverse chemical equilibrium between species. (Crittenden et al., 2005). To make use of the Langmuir isotherm three assumptions are required (Altig, 2010, p. 2):

- The surface of the adsorbant is in contact with a solution containing an adsorbate which is strongly attached to the surface.
- The surface has a specific number of sites where the solute molecules can be adsorbed.
- The adsorption involved the attachment of only one layer of molecules to the surface, i.e. monolayer adsorption.

Langmuir equation can be derived by using the application for mass law, and the reaction for monolayer adsorption is shown in Equation (10) (Stumm & Morgan, 1996):

$$S + A \leftrightarrow SA \qquad (10)$$

Where *S* is the surface site of the adsorbent, *A* is the adsorbate and *SA* is the adsorbate on the adsorbent. The equilibrium constant, K_{ads}, for the reaction is described in Equation (11). It is assumed that the Langmuir equation has a constant free-energy change, ΔG°_{ads} for all sites (Crittenden et al., 2005).

$$K_{ads} = \frac{[SA]}{[S] + [A]} = e^{-\Delta G^{\circ}_{ads}/RT} \qquad (11)$$

Both *[S]* and *[SA]* contribute to the maximum concentration of surface sites. A better way to express Equation (11) is by introducing S_T which is the total number of sites available on the adsorbent:

$$[S_T] = [S] + [SA] \qquad (12)$$

By inserting Equation (12) into Equation (11) and rewriting the equation one can obtain an expression for the concentration of the adsorbate on the adsorbent, *[SA]*:

$$[SA] = [S_T]\frac{K_{ads}[A]}{1 + K_{ads}[A]} \qquad (13)$$

From Equation (13) the surface concentration would be expressed in mmol/m^2 which is not desirable in mass balances. Instead, one would want to express the Langmuir equation in mass loading per mass of adsorbent. The surface concentration can be defined as shown in Equations (14) and (15), which give expressions for the equilibrium absorbent-phase concentration of an adsorbate (q) and the maximum adsorbent-phase concentration of adsorbate when the surface sites are saturated with adsorbate (q_{max}) (Crittenden et al., 2005):

$$q = \frac{[SA]}{m} \qquad (14)$$

$$q_{max} = \frac{[S_T]}{m} \qquad (15)$$

In both the equations, m, is the mass of the adsorbent. Equation (13) can then be written as:

$$q = q_{max} \frac{K_{ads}[A]}{1 + K_{ads}[A]} \qquad (16)$$

From Equation (16) it is possible to see that the isotherms incorporate two constants, q_{max}, which is the maximum adsorption density and K_{ads}. When $K_{ads}[A]$ is smaller than one, the denominator in Equation (16) is approximately equal to one and the isotherm becomes linear (Benjamin, 2002):

$$q \approx q_{max} K_{ads}[A] \qquad (16a)$$

On the other hand, if $K_{ads}[A]$ is bigger than one, the fraction in Equation (16) will be approximately one, which will result in (Benjamin, 2002):

$$q \approx q_{max} \qquad (16b)$$

To get a better understanding of whether or not the material tested fits the Langmuir isotherm, it is common to rearrange Equation (16) to a linear form (Crittenden et al., 2005):

$$\frac{[A]}{q} = \frac{1}{K_{ads} q_{max}} + \frac{[A]}{q_{max}} \qquad (17)$$

Often when conducting experiments with ion exchange, there will be more than one adsorbant present. The equation for competitive Langmuir adsorption is given as a generalization of Equation (16) (Benjamin, 2002):

$$q_i = q_{max} \frac{K_{ads,i}[A]_i}{1 + \sum_{all\ j} K_{ads,j}[A]_j} \qquad (18)$$

Where *j* is the adsorbates that compete for the surface sites for any species *i*. When working with competitive Langmuir adsorption it is important to include another assumption, there are no interactions between the adsorbate species on the adsorbent (Stumm & Morgan, 1996).

4.2.2 The Freundlich isotherm

The Freundlich isotherm is used to describe heterogeneous adsorbents. The isotherm was derived empirically in 1912 (Metcalf et al., 2014a). The Freundlich equation can be derived from the Langmuir equation in combination with the thermodynamics for heterogeneous adsorption. Deriving the Freundlich isotherm is complex and it will not be detailed. The Freundlich isotherm is defined as shown in Equation (19):

$$q = K_f[A]^{1/n} \qquad (19)$$

Where *q* describes the quantity of adsorbate associated with the adsorbent, K_f is referred to as the Freundlich capacity factor, *[A]* is the equilibrium concentration of the adsorbate in solution and *1/n* is the Freundlich intensity parameter.

Like the Langmuir isotherm, the Freundlich isotherm is defined by two constants; K_f and *n*. K_f describes the adsorption density under standard conditions, and *n* indicates how the binding strength can change as a result of changes in the adsorption density (Benjamin, 2002).

The Freundlich isotherm on a linear form is described in Equation (20):

$$\log(q) = \log(K_f) + \left(\frac{1}{n}\right)\log([A]) \qquad (20)$$

The difference between the two isotherms is that the Langmuir isotherms look at the density at each adsorption site individually, whereas the total adsorption density represents the summation of the adsorption densities onto a variety of sites for the Freundlich isotherm (Benjamin, 2002). When looking at competitive adsorption, the competitive effect can be of importance for even small fractions of the surface that are being occupied by another adsorbant. If there are only a few strong binding sites on an adsorbent, the strongest adsorbant will occupy these areas. Even though there might be plenty of other sites available, the competitive effect will be significant. A description of the competitive Freundlich isotherm is given in Equation (21):

$$q_A = K_{f,A}[A](\sum_{j=A,B,C} a_{Aj}[A])^{\frac{1}{n_A}-1} \qquad (21)$$

A,B and *C* are the various adsorbates competing for the adsorbent surface (Benjamin, 2002).

4.3 Natural zeolite - clinoptilolite

In the subsequent experiments, natural zeolite will be used as the ion exchange resin. Natural zeolites are among the most common inorganic cation exchangers. They are known for their selectivity abilities, temperature resistance, and ionizing radiations. They are also environmental friendly (Colella, 1996). The natural zeolites are hydrated aluminosilicate minerals and belong to the mineral group of tectosilicates, and they are commonly made from glass-rich volcanic rocks (tuff). The general structure of zeolites is a three-dimensional framework of a SiO_4 and AlO_4 tetrahedral. The aluminum ions are so small that they are able to position themselves in the center of the tetrahedron, between four oxygen atoms. There will be a negative charge in the lattice of the zeolite because the aluminum ions (Al^{3+}) will replace the silicon ions (Si^{4+}). The negative charge of zeolite is balanced with cations, such as sodium, potassium, calcium or magnesium, which are exchangeable with other cations such as heavy metals (Erdem et al., 2004).

Clinoptilolite is the most common form of natural zeolite. Since clinoptilolites are naturally formed, the chemical composition will vary for each specific location. However, the typical physiochemical properties for natural clinoptilolites such as, chemical stability, thermo stability, and the high rate of sorption equilibrium are generally similar. The pore diameters of clinoptilolite vary from around 0.45 to 0.6 nm. The pore size determines the size of ions that can enter the clinoptilolite pores and undergo ion exchange (Bogdanov et al., 2009).

4.3.1 Selectivity

Ion exchange resins have a certain preference for ions in aqueous solution, this is called selectivity (Crittenden et al., 2005). Generally there are certain chemical and physical rules that apply to the selectivity of an ion exchange resin. The most important chemical properties are the atomic number and magnitude of valance of the ion that should be removed. Overall an ion exchange resin will prefer a counterion of higher valence, as seen from the example below:

Cations: $Th^{4+} > Al^{3+} > Ca^{2+} > Na^{+}$ (Crittenden et al., 2005)

Physical factors of importance include pore size distribution, type of functional groups on the polymer chains and the hydration radius which leads to swelling or pressure within the resin. The hydration radius is the water molecules surrounding an ion in an aqueous solution. The radius of hydration tends to become larger as the size of the ion decreases. When it comes to selectivity, ions with smaller hydrated radius are preferred since the swelling pressure in the resin is reduced and the ions are more tightly bound to the resin. A small hydrated radius implies that ions with an increasing ionic number are preferred since the hydrated radius is inversely proportional to the ionic radius. The resin selectivity for ions, therefore increases with increasing atomic number, increasing ionic radius, and decreasing hydrated radius (Crittenden et al., 2005).

5. Materials and methods

5.1 Zeolite source and conditioning

The samples of natural zeolite used in this study were provided by the Norwegian distributor Alfsen & Gundersen in collaboration with the Italian distributor Carbonplant Srl. The samples of clinoptilolite were from the Leidi Angelo Srl Company in Zandobbio in the Northern part of Italy. The clinoptilolite was used in its natural state, without any modifications. Information about the product was provided by Carbonplant Srl and can be seen in Appendix 2.

The empirical chemical formula of the clinoptilolite used is $(Ca,K_2,Na_2,Mg)_4Al_8Si_{40}O_{96} \cdot 24H_2O$. The particle size range used in this study was 1 to 5 mm. Table 1 shows the mineralogical composition of the material. The clinoptilolite mainly consist of silica (SiO_2), alumina (Al_2O_3), quicklime (CaO), and potassium oxide (K_2O). Table 2 shows the physical properties of the clinoptilolite.

Table 1: Chemical composition and physical properties of natural zeolite

Chemical composition	[%]
SiO_2	68,7
Al_2O_3	10,2
CaO	4,2
K_2O	2,1

Table 2: Physical properties of natural zeolite

Physical properties	Values
Density	900-950 kg/m^3
Specific surface area	500-600 m^3/g
Average capacity of cation exchange	1.13 meq/g
Humidity packaging	4 %

For an alkaline solution the relative scale of cation exchange on the clinoptilolite is determined to (Appendix 2):

$$Cs^+ > NH^{4+} > Pb^{2+} > K^+ > Na^+ > Ca^{2+} > Mg^{2+} > Ba^{2+} > Cu^{2+} > Ni^{2+} > Cd^{2+} > Zn^{2+} > Fe^{3+} > Mn^{2+}$$

5.2 Water samples

Water samples were collected from Løkken works and Folldal center on March 20th, 2014. 40 liters samples of polluted mine water were collected from each of the study sites and transported back to the water laboratory at NTNU. To ensure minimal changes in the AMD composition, the water samples were placed in a cold and dark storage room until analysis. A sample from Røros was not collected for practical reasons.

5.2.1 Folldal Center

In Folldal, Major E. Eide (Personal communication, 20th March 2014) showed the discharge area for the collection of the AMD. Figure 11 shows the sampling site in Folldal. During the sampling it was cloudy, otherwise the weather was stable.

Figure 11: *(a)* Sampling site at Folldal center; *(b)* collecting the water

The brown-red color of the water indicates high concentration of dissolved metals. According to E. Eide, the water mainly consists of dissolved iron, copper, zinc, and sulfur.

5.2.2 Løkken works

J. A Holmen (Personal communication, 20th March 2014), from Orkla industrial museum, helped to collect the water from Gammelgruva at Løkken works. The sampling site was inside the mine and pictures of the site are shown in Figure 12.

Figure 12: ***(a)*** **Sampling site at Løkken works;** ***(b)*** **collecting the water**

The ore previously taken out of the mine was mainly copper and zinc. There is still a lot of iron ore in the mine, however, the iron was never utilized because the ore also contains large amounts of zinc, which has a negative effect on the iron ore. The AMD mainly contains dissolved sulfur, iron, copper, and zinc. It is, however, possible to find traces of manganese, arsenic, lead and cobalt since these, and other metals, has also been found in the extracted ore (Holmen, 2012).

5.3 Analysis of metal composition

The definition of heavy metals is not a firmly defined term. In toxicology the definition of heavy metals includes cadmium, mercury, and lead. All of these metals can bioaccumulate and have a toxic effect on living organisms (Life Extension, 1995 - 2014). However, during this thesis, heavy metals are, as mentioned in chapter 2.2, defined as metals with a density above 5 g/cm^3. The metals examined in this study are iron, copper, zinc, and manganese.

The analysis of the metal composition of the initial AMD and the treated solutions was measured using a high resolution inductive coupled plasma instrument (HR-ICP-MS) by Syverin Lierhagen at The Department of Chemistry at NTNU. The water samples were preserved with 0.1 M HNO_3 and analyzed directly without any further dilution.

5.4 Batch adsorption studies

A batch method was used to examine the exchange of heavy metals on clinoptilolite. The experiments were conducted using different quantities of natural zeolite; 5, 10 and 30 g, with initially 100 mL of AMD. At specific time intervals (0, 15, 30, 60, 120 and 180 min) a 5 mL

sample of the treated water was taken out and put into sampling tube. Between each sample the glass pipettes was rinsed with distilled water. The concentration of the different metals was determined by HR-ICP-MS.

To determine the amount of heavy metals adsorbed from the solution on to the ion exchanger, the mass balance expression was used:

$$q_e = \frac{V}{M} \times (C_i - C_e) \qquad (22)$$

Where q_e is the equilibrium adsorbent-phase concentration of the adsorbate [mg adsorbate/g adsorbent], V is the volume of solution added to the beaker [L], m is the mass of adsorbent [g], C_i is the initial concentration of the adsorbate [mg/L] and C_e is the equilibrium concentration of adsorbate [mg/L] (Crittenden et al., 2005).

The percentage adsorption [%] and the distribution ratio, K_d [mL/g] were calculated by using Equation (23) and (24):

$$\%\ adsorption = \frac{C_i - C_f}{C_i} \times 100 \qquad (23)$$

Where C_f is the final concentration of heavy metals in the solution (mg/L).

$$K_d = \frac{amount\ of\ metal\ in\ adsorbent}{amount\ of\ metal\ in\ solution} \times \frac{V}{m} = \frac{q_e}{C_e} \qquad (24)$$

If Equation (23) and (24) are put together the relationship between them will be as shown in Equation (25):

$$\%\ adsorption = \frac{100K_d}{K_d + \frac{V}{m}} \qquad (25)$$

5.4.1 Kinetic studies

The experiment was conducted for the AMD from Folldal and Løkken. Figure 13 shows how the kinetic experiment was set up. The weights of the natural zeolite that were used in the kinetic studies were 5, 10 and 30 g. The natural zeolite was tested with an initial AMD volume of 100 mL. To ensure that all the water came in contact with the natural zeolite a magnet stirrer was used. Samples of 5 mL were taken periodically at 0, 15, 30, 60, 120 and 180 min. In the end the metal composition of the treated AMD was determined.

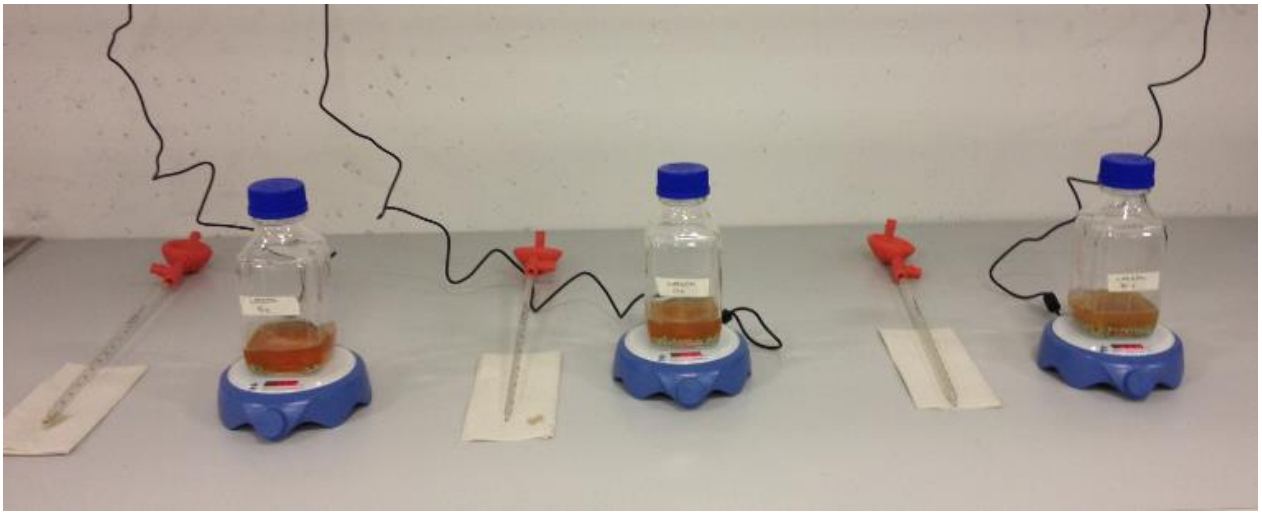

Figure 13: Kinetic experiment with AMD from Løkken

5.4.2 Adsorption isotherms (equilibrium studies)

For the equilibrium studies, the measurements obtained from the kinetic studies were used as a basis to develop and describe the adsorption isotherm relationships for the two different solutions. The two isotherm models which were used are the Langmuir and Freundlich models. A description of the models can be found in chapter 4.2.

5.4.3 Effect of competing ions

The composition of AMD contains more than one metal and in this thesis iron, copper, zinc, and manganese were studied. During the batch experiments the different metals were analyzed separately. However, the selectivity of a specific metal on the clinoptilolite can be influenced by other metals and content of organic matter in the AMD.

5.4.4 Effect of solution pH

The effect of solution pH on the adsorption capacity was investigated by comparing the adsorption at the initial pH of 2.6 and 2.4, for Folldal and Løkken, with the adsorption capacity at pH 7.0. For each test 100 mL of AMD and 30 g of natural zeolite was used. To increase the solutions pH to 7.0, 2 M sodium hydroxide (NaOH) was added.

5.5 Ion exchange in combination with precipitation

A combination of precipitation and ion exchange was tested to see if the two treatment methods could achieve the set requirements. Precipitation is often conducted by the addition of hydroxides

or sulfides (Strakis, 2013). In this experiment, the addition of sodium hydroxide was chosen because hydroxide formation is the most common precipitation method.

The first step of the experiment was to add 2 M sodium hydroxide (NaOH) to the AMD to cause precipitation of metal hydroxides and to reach pH 6.0. Figure 14 shows the addition of sodium hydroxide to the AMD from Løkken. When the desirable pH was attained, the solution was allowed to sediment in order to remove most of the particles before the ion exchange took place. The sedimented solution (100 mL) was added to glass bottles with 30 g of clinoptilolite. At specific time intervals of 0, 7.5, 15, 30 and 60 min, samples of the treated AMD was taken and analyzed for metal concentration.

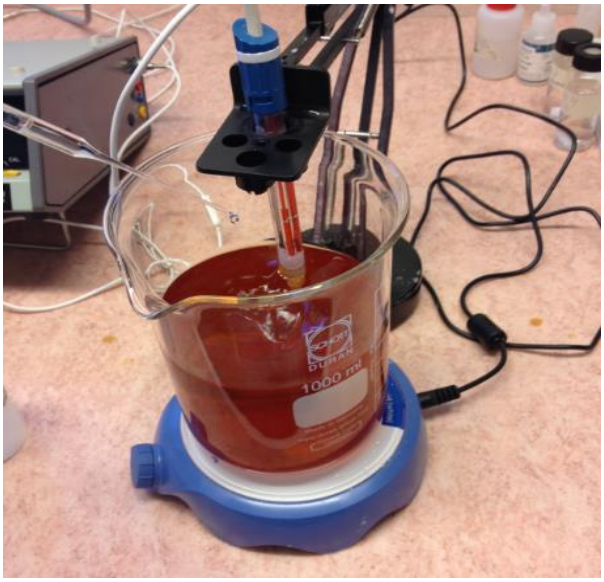

Figure 14: Addition of sodium hydroxide to AMD from Løkken

5.5.1 The relationship between theory and practice

To see if the precipitation consists mainly of metal hydroxides, the relationship between theory and practice was studied. This was done by filtering 100 mL of AMD through a 0.45 µm filter. Sodium hydroxide was then added to the AMD until it reached pH 6.0. The solution was placed in a heating cabinet, which held a temperature of 105^{o}C, for 24 hours before the dry matter was weighed. The practical value was compared to the theoretical value calculated from the metals log C – pH diagrams.

5.6 Sources of error

Upon conducting laboratory experiments there may be numerous sources of error. During the experiments some errors may be human imprecision, equipment imprecision, unaccounted for outside influences such as temperature, logic errors and calculation errors.

The vision is a source of uncertainty and there may therefore be errors connected to the measurements of the volume of AMD. The equipment that was used had not been washed with acid and may therefore have influenced the metal analysis since residues from previous experiments may have been present. It was assumed that the temperature in the laboratory was stable, but since this was not controlled the temperature is a source of uncertainty. The analysis of the heavy metal concentration was conducted by the Department of Chemistry. When several people are involved in the same project misunderstandings can arise and thus affect the end result.

6. Results and discussion

6.1 Analysis of the metal composition

The AMD from Folldal and Løkken have an orange brown color and a low pH. This indicates that there are high levels of dissolved metal in the water. Table 3 shows the initial metal concentration for the selected metals. To give an indication of the metal concentration in the AMDs from Folldal and Løkken, the values are compared to the heavy metal concentration in the AMD from the Wheal Jane Mine in Cornwall, UK. The initial metal concentration from Wheal Jane Mine is 200, 12, 85 and 15 mg/L for iron, copper, zinc, and manganese, respectively (Motsi et al., 2009). When comparing the metal concentration in the AMDs the differences are large, especially for iron and copper. The difference is larger between the AMD from Løkken and the Wheal Jane Mine.

Table 3: Initial concentrations of Fe, Cu, Zn and Mn and methodological uncertainties in the samples from Folldal center and Løkken works

	Folldal center		Løkken works	
Metal	**Initial concentration [mg/L]**	**Initial concentration [mmol/L]**	**Initial concentration [mg/L]**	**Initial concentration [mmol/L]**
Fe^{3+}	869.12 ± 26.9	15.56	2834.47 ± 405.3	50.75
Cu^{2+}	79.63 ± 3.7	1.25	174.38 ± 14.3	2.74
Zn^{2+}	56.19 ± 3.8	0.86	141.71 ± 4.7	2.17
Mn^{2+}	7.70 ± 0.4	0.14	18.33 ± 0.8	0.33

Dissolved iron can be found in two oxidation states, ferrous (Fe^{2+}) and ferric (Fe^{3+}) iron. The determination of whether the AMD contains ferrous or ferric iron was not possible to implement. Further in this thesis it is assumed that the iron in the AMD is in the form of ferric iron. This assumption is made based on the fact that oxygen was present at the collection site for AMD at Folldal and Løkken.

6.2 Kinetic studies

The results of the kinetic studies can be seen in Figures 15 and 16, where the adsorption of metals from the AMD onto the natural zeolite is shown. The calculations used to create the graphs are available in Appendix 4. The adsorption rate can be divided into three different stages. The

various stages are more evident for the results from Løkken than the results from Folldal. During the first stage (0 – 15 minutes) the adsorption rate is rapid for all metals. The rapid change in metal concentration is observed for all metals from both Folldal and Løkken. The small decrease in the graphs characterizes the second stage (15 – 30 minutes) of the adsorption rate. This inversion phenomenon describes the desorption process which occurs during some periods of the ion exchange process (Sprynskyy et al., 2006).

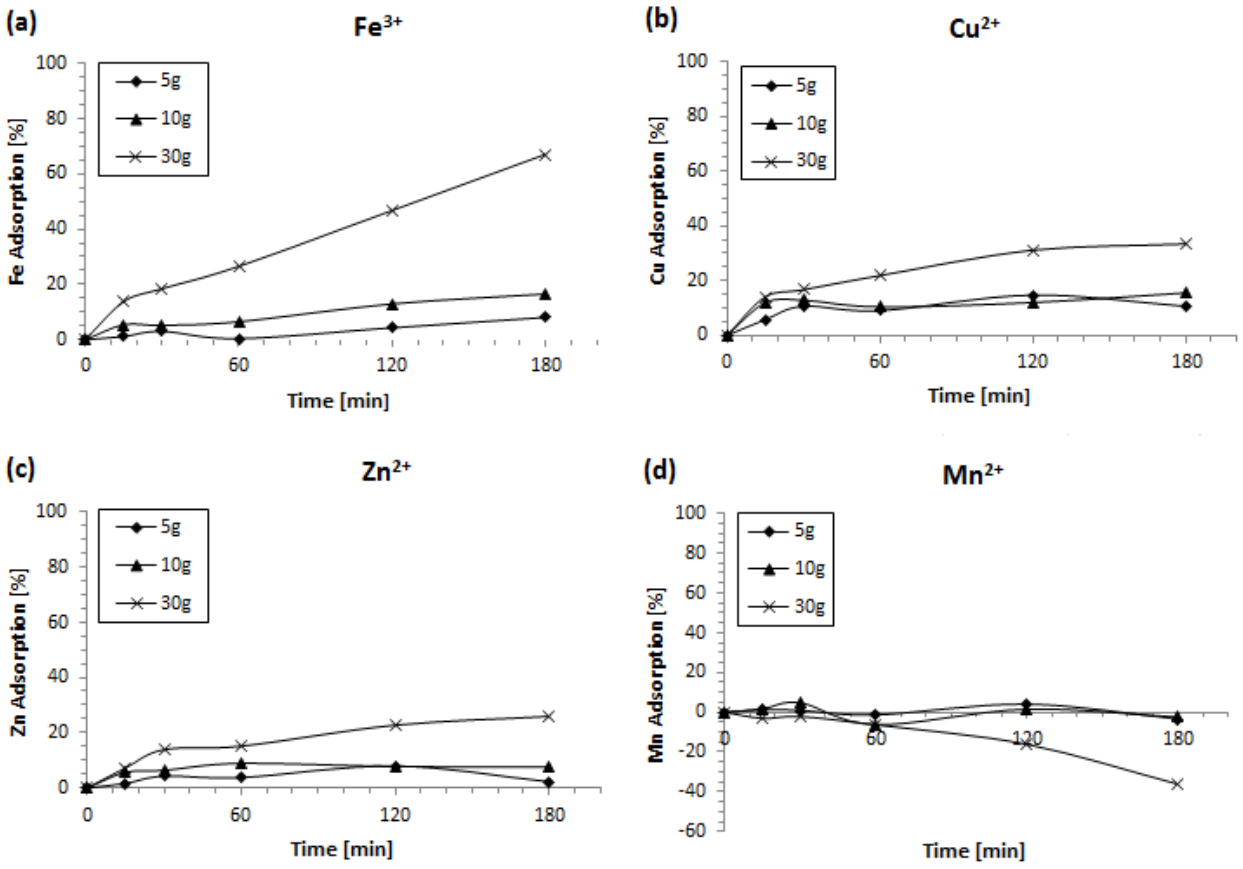

Figure 15: Kinetics of heavy metal ion adsorption with 5, 10 and 30 g of clinoptilolite, Folldal center; *(a)* iron (Fe^{3+}); *(b)* copper (Cu^{2+}); *(c)* zinc (Zn^{2+}); *(d)* manganese (Mn^{2+})

In the third stage (30 – 180 minutes) the adsorption rate is lower compared to the first stage, as seen from the figures. The exception is the adsorption rate of iron in solution with 30 g of clinoptilolite, which has a slope quite similar to the slope in the first stage. The level of metal removed during the different stages varies between the different metals. Unlike the other metals, the adsorption rate for manganese decreases for all amounts of clinoptilolite.

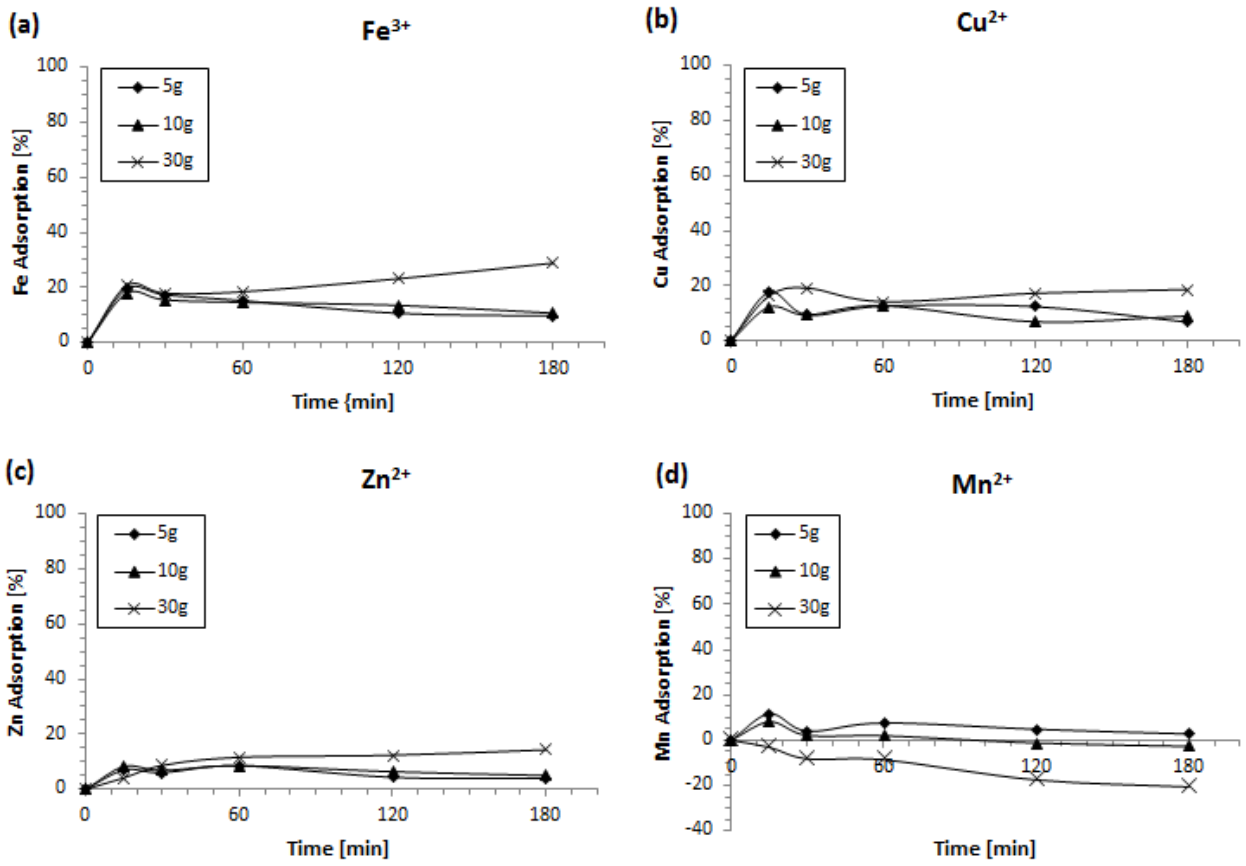

Figure 16: Kinetics of heavy metal ion adsorption with 5, 10 and 30 g of clinoptilolite, Løkken works; *(a)* iron (Fe^{3+}); *(b)* copper (Cu^{2+}); *(c)* zinc (Zn^{2+}); *(d)* manganese (Mn^{2+})

The difference in adsorption rate is due to the specific crystalline structure of the clinoptilolite. During the first stage, the exchange of heavy metals takes place in the micropores on the surface of the clinoptilolite grains (Sprynskyy et al., 2006). In this stage most of the pores in the clinoptilolite are available for diffusion of metals and this availability leads to the high adsorption rate. The desorption in the second stage is probably a counter-diffusion of exchangeable cations from the deeper layers of the clinoptilolite (Sprynskyy et al., 2006). During the third stage, the easily available exchange sites on the clinoptilolite are occupied. The remaining available sites are difficult to reach which implies that the exchange of heavy metals is reduced compared to the exchange rate during the first stage. For iron, copper, and zinc, the AMD solutions with 5 and 10 g of clinoptilolite show either a decrease or stabilization of the adsorption rate after 180 minutes. From the development of the adsorption rate it is assumed that the exchange of metals primarily occur on the clinoptilolites surface, since the rate appears to stabilize or decrease during the third stage. The situation is different for AMD solutions with 30 g of clinoptilolite because the

adsorption rate keeps increasing. This is especially visible for iron. This development suggests that there are still available exchange sites on the clinoptilolite.

The effect of the adsorbent dose on the uptake of the heavy metals is also shown in Figures 15 and 16, as well as Tables 4 and 5.

Table 4: Concentration, metal concentration per g of clinoptilolite and percentage reduction of heavy metals in AMD, after 3h of contact with clinoptilolite, Folldal center

	5g				10g			30g		
	Initial conc. [mg/L]	Metal conc. [mg/L]	Metal conc. [mg/gL]	Percentage removed [%]	Metal conc. [mg/L]	Metal conc. [mg/gL]	Percentage removed [%]	Metal conc. [mg/L]	Metal conc. [mg/gL]	Percentage removed [%]
Fe^{3+}	869.1	798.9	159.2	8.1	725.5	72.4	16.5	286.2	9.5	67.1
Cu^{2+}	79.6	71.2	14.2	10.6	67.3	6.7	15.5	53.0	1.8	33.4
Zn^{2+}	56.2	54.9	10.9	2.3	51.9	5.2	7.5	41.6	1.4	25.9
Mn^{2+}	7.7	8	1.6	-3.4	7.9	0.8	-2.5	10.5	0.3	-36.2

Table 5: Concentration, metal concentration per g of clinoptilolite and percentage reduction of heavy metals in AMD, after 3h of contact with clinoptilolite, Løkken works

	5g				10g			30g		
	Initial conc. [mg/L]	Metal conc. [mg/L]	Metal conc. [mg/gL]	Percentage removed [%]	Metal conc. [mg/L]	Metal conc. [mg/gL]	Percentage removed [%]	Metal conc. [mg/L]	Metal conc. [mg/gL]	Percentage removed [%]
Fe^{3+}	2834.5	2559.3	505.9	9.7	2531.9	252.8	10.7	2015.9	67.2	28.9
Cu^{2+}	174.4	162.5	32.1	6.8	158.6	15.8	9.0	141.8	4.7	18.7
Zn^{2+}	141.7	136.1	26.9	3.9	134.6	13.4	5.0	121.4	4.0	14.3
Mn^{2+}	18.3	17.8	3.5	2.8	18.8	1.9	-2.7	22.1	0.7	-20.6

It was observed that an increase in the amount of clinoptilolite had a positive effect on the reduction of iron, copper, and zinc. A reason for this is that an increase in the amount of clinoptilolite corresponds to more available adsorption sites for the ion exchanger. It is apparent that the available adsorption sites in solutions with 5 and 10 g of clinoptilolite are limited compared to solutions with 30 g. This relationship is clearly displayed for the adsorption of iron from the AMD from Folldal. Over the three hours the experiment was conducted, the adsorption rate for the solutions with 5 and 10 g had a lower slope than the solution with 30 g of clinoptilolite. Since the slope of the adsorption rate for 30 g of clinoptilolite does not stabilize, in contrast to solutions 5 and 10 g clinoptilolite, it suggests that there are still available adsorption sites on the natural zeolite

The treatment effect from ion exchange with clinoptilolite is far from satisfactory, since the metal concentrations in the samples were still high after three hours of treatment. The requirement to reduce the concentration of copper to less than 10 µg/L, is far from fulfilled. Clinoptilolite's effect on the AMD from Folldal and Løkken differ. The treatment effect of the heavy metals is better for the AMD from Folldal. One possible reason for the differences is related to the original concentrations of metals in the AMD from the two areas. The AMD from Løkken has an higher metal concentration which may have influenced the ion exchange process. Despite the differences between the two solutions, the ion exchange of the AMD from both areas has a negative effect on the amount of manganese. A cause for this might be the effect of competing ions. This will be discussed further in section 6.4.

Distribution ratio

The distribution ratio, K_d, indicates the selectivity, capacity, and affinity of an ion for ion exchange (Motsi et al., 2009). Figures 17 and 18 illustrate the distribution ratio as a function of the metal concentration over time. The complete set of data used to perform the calculations of the distribution ratio is presented in Appendix 4.

The graphs for iron, copper, and zinc from Folldal indicate that the distribution ratio increases with a decrease in the metal concentration (Erdem et al., 2004). The graphs for iron, copper, and zinc from Løkken have a different development. The distribution ratio initially increases with a decrease in the metal concentration, and at a certain point the distribution ratio starts to decrease as the metal concentration increases before returning to the original behavior (distribution ratio increases as the metal concentration decreases).

The distribution ratio of manganese for the AMD from both Folldal and Løkken, has a reverse development compared to the other metals. The manganese concentration increases while the distribution ratio decreases. This development corresponds well to the kinetic results for manganese. One possible reason for the development of manganese might be, as previously mentioned, the effect of competing ions which will be further discussed in chapter 6.4.

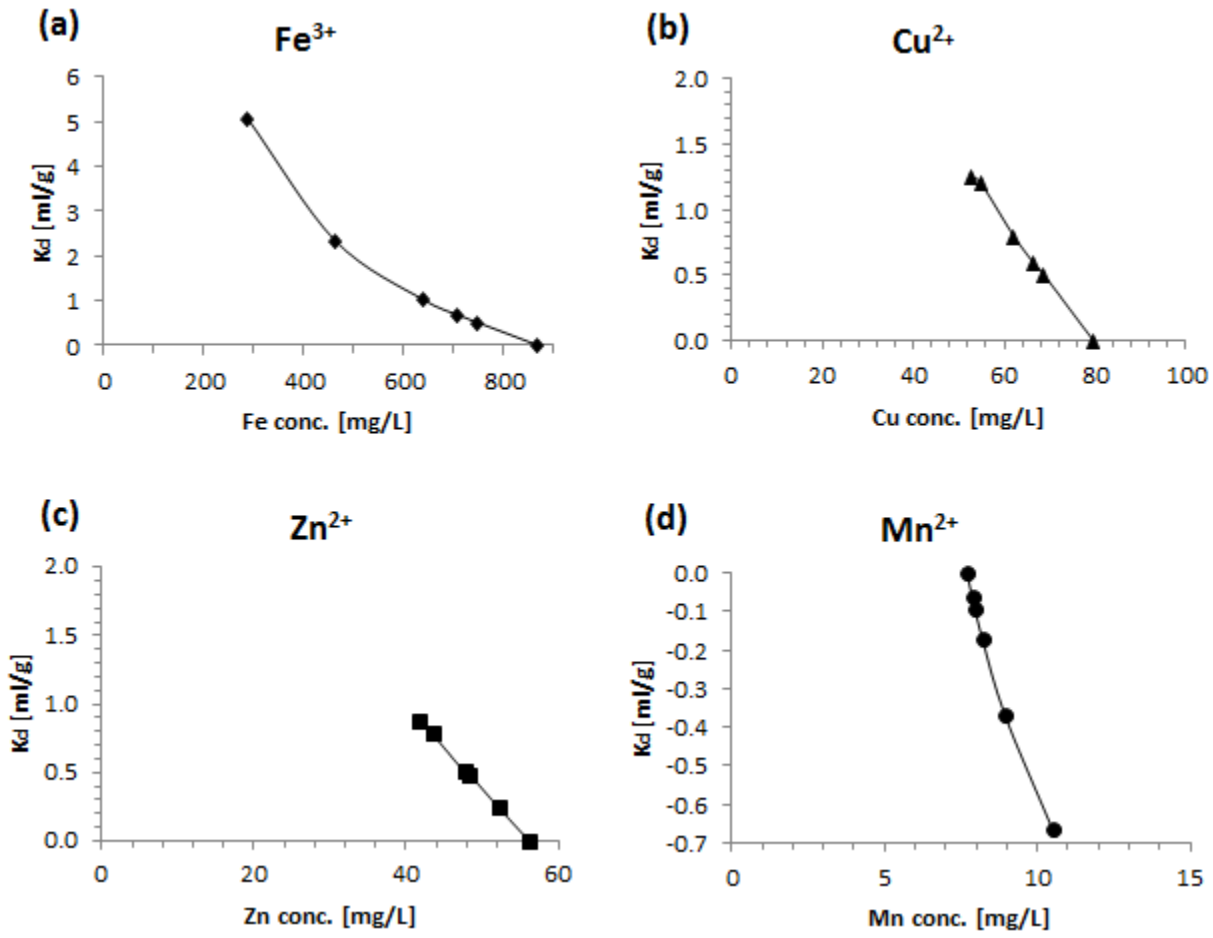

Figure 17: Variation of metal ions on clinoptilolite as a function of initial concentration, Folldal center: m = 30,007g, V = 100 -75 mL, time 15-180 min

A large distribution ratio indicates that the ions are distributed more onto the resin and therefore fewer ions remain in solution, and vice versa. (Davies, 2012). As seen for the graphs for iron, copper, and zinc from Folldal and Løkken, the distribution ratio increases between the initial high metal concentration and the lower final metal concentration. This means that the metals to some degree are exchanged with the cations from the clinoptilolite. The results from Folldal and Løkken suggest that iron is best adsorbed, followed by copper and zinc. However, the development of the distribution ratio for the metals from Løkken are lower that the values from Folldal. As mentioned previously, this may be a cause of the initial concentration of heavy metals in the AMD which was higher for the solution from Løkken.

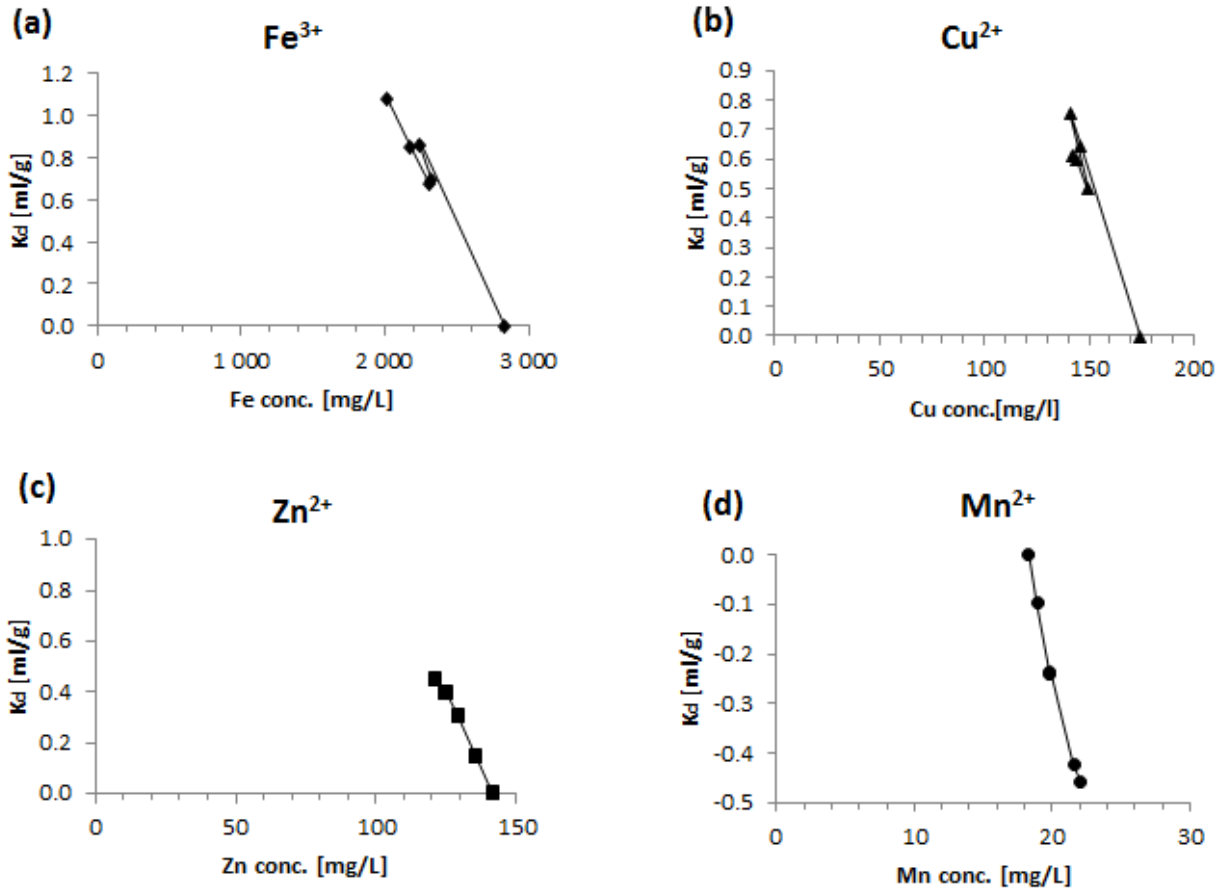

Figure 18: Variation of metal ions on clinoptilolite as a function of initial concentration, Løkken works: m = 30,013g, V = 100 - 75mL, time 15-180 min

Exchangable cations

The role of the exchangable cations of the clinoptilolite is shown in Figure 19. The graphs show that the increase of exchangable cations is inversley proportional with the removal of heavy metal ions. For both solutions the dominating exchangable cations are calcium and magnesium, and the order of exchange after three hours is $Ca^{2+} > Mg^{2+} > K^{+} > Na^{+}$. The results from Folldal show that the amount of exchangable calcium ions exceed the heavy metal concentration during the experiment. This is not the case for the results from Løkken, where the concentration of iron ions is far greather than the concentation of exchangable ions. The amount of exchangeble ions in solution is larger for the AMD from Løkken. An explanation can be that there are more heavy metals, especially iron, in the AMD from Løkken.

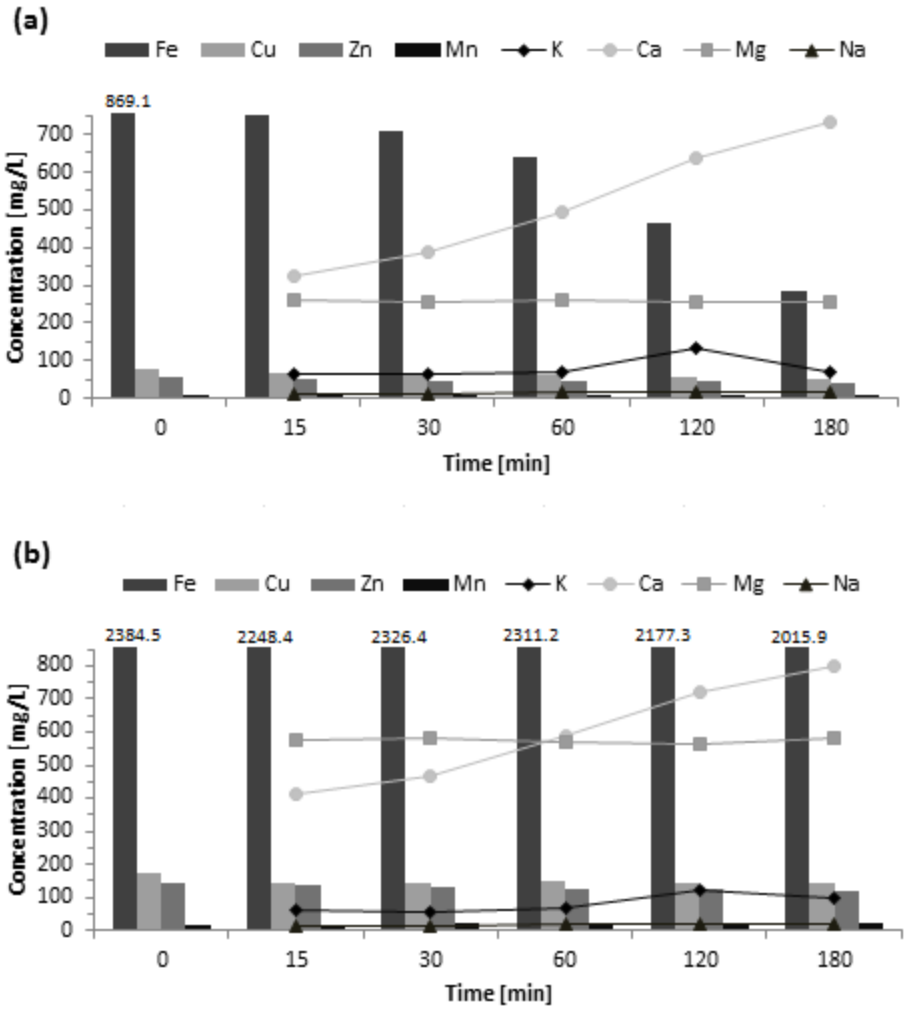

Figure 19: Dynamics of ion exchange of heavy metals with the clinoptilolite; *(a)* Folldal center, *m* = 30,007g; *(b)* Løkken works, *m* = 30,013g

6.3 Adsorption isotherms (equilibrium studies)

The adsorption of heavy metals of AMD from Folldal and Løkken, in solution with 30 g of clinoptilolite, was fitted to the Langmuir and Freundlich isotherms. To find the Langmuir and Freundlich isotherms Equation (16) and (19) were used:

Langmuir:

$$q = q_{max}\frac{K_{ads}[A]}{1 + K_{ads}[A]} \qquad (16)$$

Freundlich:

$$q = K_f[A]^{1/n} \qquad (19)$$

To use Equation (16) and (19) the isotherm parameters had to be determined. This was done by rearranging the Langmuir and Freundlich isotherms to a linear form, as seen from Equation (17) and (20):

Langmuir:

$$\frac{[A]}{q} = \frac{1}{K_{ads} q_{max}} + \frac{[A]}{q_{max}} \qquad (17)$$

Freundlich:

$$\log(q) = \log(K_f) + \left(\frac{1}{n}\right)\log([A]) \qquad (20)$$

The equation for the linear regression was applied to find the isotherm parameters. Figure 20 shows the linear regression to find the Langmuir and Freundlich isotherm parameters for iron for the AMD from Folldal. The linear regressions for the other metals are available in Appendix 5.

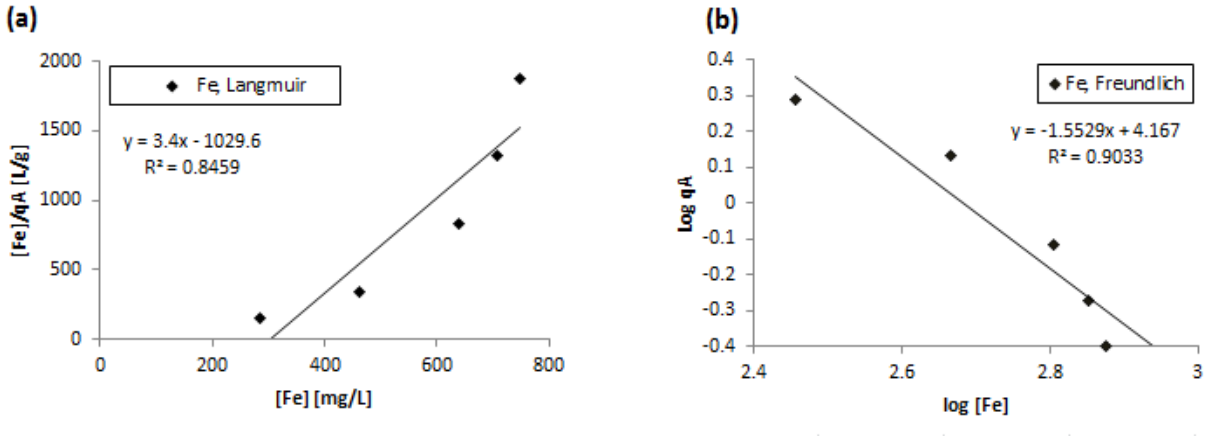

Figure 20: Linear regression to find the isotherm parameters for iron, for the AMD from Folldal center: *(a)* Langmuir; *(b)* Freundlich

Table 6 show the Langmuir and Freundlich isotherm parameters for adsorption of heavy metal ions in solution with 30 g clinoptilolite.

Table 6: Langmuir and Freundlich adsorption isotherm model parameters for heavy metal ion adsorption from solution by clinoptilolite

	Folldal center				Løkken works			
	Langmuir		Freundlich		Langmuir		Freundlich	
	q_{max}	K_{ads}	1/n	K_f	q_{max}	K_{ads}	1/n	K_f
Fe^{3+}	0.294	-0.003	-1.553	$1.47 \cdot 10^{4}$	0.492	-0.001	-3.314	$2.48 \cdot 10^{11}$
Cu^{2+}	0.013	-0.022	-3.312	$4.71 \cdot 10^{4}$	0.016	-0.008	-5.011	$6.57 \cdot 10^{9}$
Zn^{2+}	0.004	-0.025	-4.844	$4.63 \cdot 10^{6}$	0.003	-0.008	-11.125	$1.14 \cdot 10^{22}$
Mn^{2+}	0.000	0.097	n/a*	n/a*	0.000	-0.045	n/a*	n/a*

*not available

Figure 21 show that neither the Langmuir or Freundlich isotherms reveal any particular good correlation to the experimental data from Folldal. Figure 22 show that the Langmuir and Freundlich isotherms follow the tendency of the experimental data from Løkken. The experimental isotherm for manganese, for the AMD from both areas, is reverse due to the fact that the manganese concentration increased during the experiment. It was not possible to develop the Freundlich isotherm for the manganese.

Langmuir isotherm

According to the maximum adsorbent-phase concentration of adsorbate, q_{max}, the sorption on the clinoptilolite follow the same selectivity sequence for the AMD from both Folldal and Løkken:

$$Fe^{3+} > Cu^{2+} > Zn^{2+} > Mn^{2+}$$

The clinoptilolite prefers iron over the other metals and is thus in agreement with the rules of selectivity which says the ion exchange resin tends to assimilate ions of higher valence. When it comes to copper, zinc, and manganese which all have the same valence, the selectivity of the ion exchange resin follows different rules. According to Crittenden et al. (2005) ion exchange resins prefer ions with small hydration radius. The hydration radius for copper, zinc, and manganese are 4.19, 4.30 4.38 Å, respectively (Motsi et al., 2009). Copper has the smallest hydration radius and is therefore preferred over zinc and manganese. Manganese, with its largest hydration radius, is clinoptilolite's least favored metal.

As seen from Figures 21 and 22, the Langmuir isotherm deviates from the experimental data. An assumption made when developing the Langmuir isotherm is that the adsorptive surface is uniformly flat and infinite in extent. This is, however, not the case, since some adsorption sites are in the middle of the crystalline structure whereas other can be on the edges. These differences

cause the different sites to have various affinities for the adsorbate molecules. The model also assumes that each adsorption site is independent of each other. This assumption does not correspond to reality since a reaction on one site can affect other areas of the material (Benjamin, 2002).

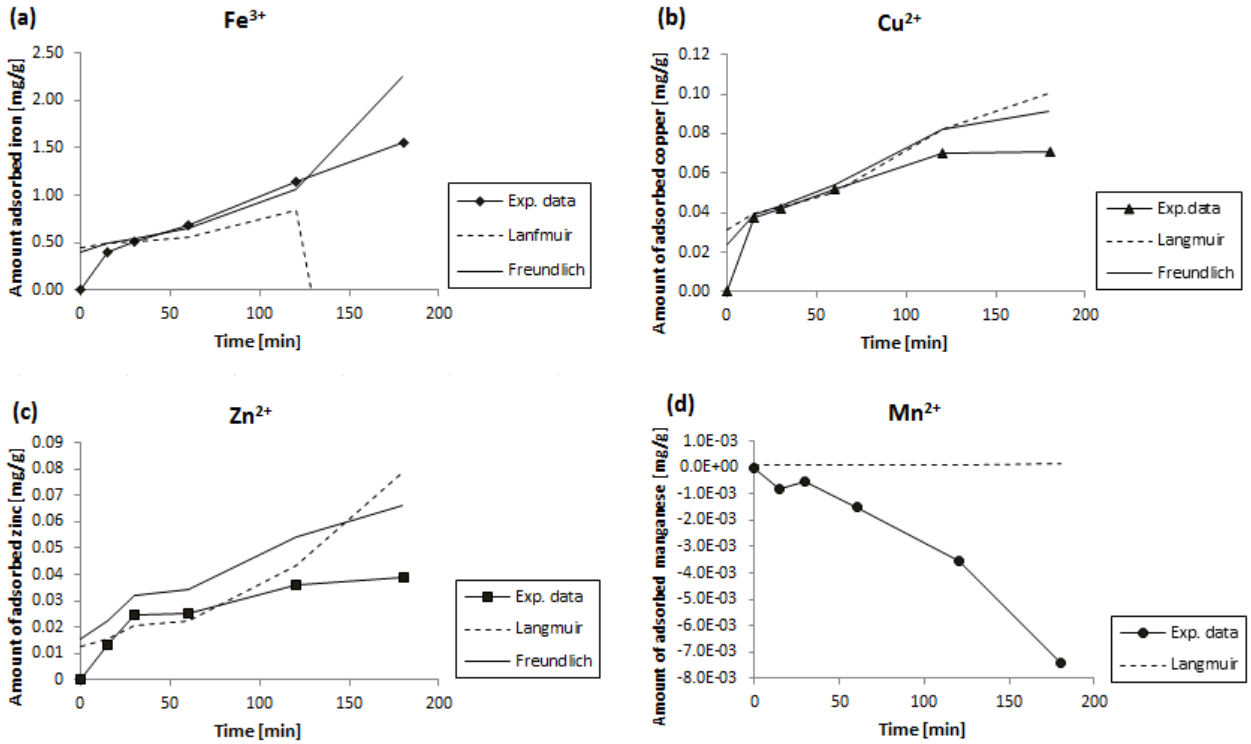

Figure 21: Adsorption isotherms of heavy metal ions (Fe^{3+}, Cu^{2+}, Zn^{2+} and Mn^{2+}) described by Langmuir and Freundlich models, Folldal center

Freundlich isotherm

The capacity factor, K_f, from the Freundlich isotherm, shows the same selectivity sequence as the Langmuir isotherm. Just as the Langmuir isotherm, the Freundlich isotherm also deviates from the experimental data.

The intensity parameter, *1/n*, indicates the adsorption capacity of the clinoptilolite for the different metals. The results in Table 6 show that the intensity parameter is below one for the AMD from Folldal and Løkken. This indicates that the average binding strength will decrease as a result of an increase in the surface coverage (Benjamin, 2002). Consequently, the adsorption of metals subsides as the metal concentration decreases. This is consistent with the results for copper and zinc, from the kinetic studies where the adsorption rate eventually stabilizes.

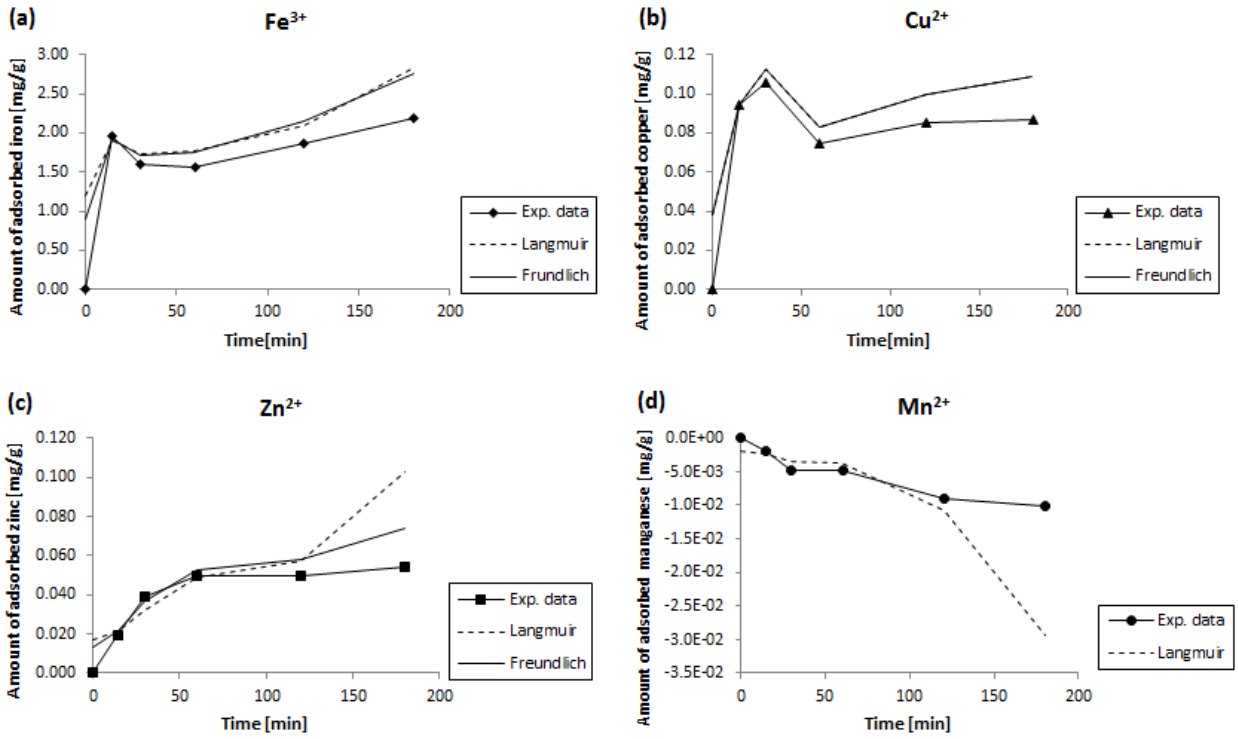

Figure 22: Adsorption isotherms of heavy metal ions (Fe^{3+}, Cu^{2+}, Zn^{2+} and Mn^{2+}) described by Langmuir and Freundlich models, Løkken works

6.4 Effect of competing ions

The AMD from Folldal and Løkken both consist of various heavy metals with different concentrations. As a result of the concentration difference between the heavy metals, it is assumed that there will be competition between the cations. This assumption is further confirmed when comparing the iron concentration with the other metal concentrations. The large difference in metal concentration can lead to clinoptilolite selecting iron over the other metals.

On the basis of the kinetic results shown in Figures 15 and 16 there is a connection between the iron and manganese ions. The adsorption of iron increases whereas the adsorption of manganese decreases. This development shows that the iron ions can displace some of the manganese ions on the clinoptilolite. The clinoptilolite selectivity of iron over manganese is in agreement with the selectivity sequence found in the adsorption isotherm study.

A possible reason for the clinoptilolites preference of iron ions could be that the ion exchange resin is attracted to ions with a higher valence. Another possibility for the competitiveness between iron and manganese may be the concentration difference, which is larger compared to the other metal ions.

Figures 15 and 16 clearly show that the concentration of manganese ions increases above the initial concentration during the three hours the experiment lasted. This is especially visible for the solutions containing 30 g clinoptilolite. This phenomenon is not only a result of the competitiveness between the iron and manganese ions. When comparing the different amounts of clinoptilolite used, it is evident that the amount of manganese increases with the amount of clinoptilolite. One possible explanation is that the clinoptilolite consists of a substance which the HR-ICP-MS registers as manganese. It has not been possible to follow up this assumption due to the time limit of this thesis. Upon further research of the AMD from Folldal and Løkken with clinoptilolite, the development of the manganese concentration should be studied.

In addition to competition between the different heavy metal ions, there is a possibility that the amount of organic matter in the AMD affects the clinoptilolites uptake of heavy metals. The amounts of total organic carbon (TOC) in the AMD for Folldal and Løkken are given in Table 7.

Table 7: Amount of TOC in the AMD from Folldal center and Løkken works

	TOC [mgC/L]
Folldal center	17.9
Løkken works	34.8

Large quantities of TOC can result in fouling of the clinoptilolites pores. Fouling is most commonly associated with accumulation of substances on the surface and within the pores of a structure (Lu et al., 2010). Since the amount of TOC in the AMD from Folldal and Løkken are high, there is reason to believe that there is fouling of the clinoptilolite, which possibly can have led to a lower exchange of the heavy metals.

6.5 Effect of solution pH

The initial pH for the samples from Folldal center and Løkken works was 2.6 and 2.4, respectively. During the three hours the batch experiment was conducted, there were no changes in the pH and no precipitation was observed. The metal content in the AMD is high, especially the amount of iron, as seen from Table 3. When the pH is increased to 7.0, by adding sodium hydroxide, there will be precipitation of metal hydroxides which typically follows Equation (26):

$$Me^{n+} + nOH^{-} \leftrightarrow Me(OH)_n \qquad (26)$$

As mentioned in chapter two, ferric hydroxide will precipitate when the pH is between 2.3 to 3.5. When sodium hydroxide was added and the pH was around 3.0, there was heavy precipitation. Because of the high iron content, it is assumed that most of the precipitate was ferric hydroxide. Due to the large amount of precipitation it was not, at that time, viewed feasible to complete the experiment. This decision was based on the assumption that most of the metal was removed during precipitation and ion exchange would therefore have limited treatment efficiency.

6.6 Ion exchange in combination with precipitation

The AMDs from Folldal and Løkken have high metal levels and the previous batch studies were not satisfactory with respect to the remaining concentrations of heavy metals. Precipitation was included as a treatment step to see if a larger proportion of heavy metals would be removed. This was done because adding precipitation is one of the most common ways to remove heavy metals from wastewater.

6.6.1 Precipitation

Sodium hydroxide was added to the AMD solutions until pH 6.0 was reached. Between pH 2.0 and 3.0 visible signs of precipitation occurred. Stabilization of the pH was not possible before a given amount of the metal ions had reacted with the added hydroxides. When the desired pH was reached, the samples were set aside so that the particles could sediment. The water had a visible change in color after sedimentation. Figure 23 shows the solution after precipitation and sedimentation:

Figure 23: AMD after precipitation and sedimentation

Tables 8 and 9 show the amount of metal that was removed from the AMD after precipitation:

Table 8: Heavy metal concentration before and after precipitation, and the percentage removal of metals by precipitation, Folldal center

Metal	Initial concentration [mg/L]	Concentration after precipitation [mg/L]	Amount of metals removed by precipitation [%]
Fe^{3+}	869.1	5.1	99.4
Cu^{2+}	79.6	4.3	94.5
Zn^{2+}	56.2	44.0	21.2
Mn^{2+}	7.7	n.a.	n.a.

n.a.: data not available

Table 9: Heavy metal concentration before and after precipitation, and the percentage removal of metals by precipitation, Løkken works

Metal	Initial concentration [mg/L]	Concentration after precipitation [mg/L]	Amount of metals removed by precipitation [%]
Fe^{3+}	2834.5	48.1	98.3
Cu^{2+}	174.4	2.2	98.7
Zn^{2+}	141.7	56.8	59.9
Mn^{2+}	18.3	n.a.	n.a.

n.a.: data not available

The AMDs from Folldal and Løkken show a reduction of the iron, copper, and zinc concentrations. Precipitation for the AMD from Folldal had the largest reduction of iron, whereas the AMD from Løkken had approximately the same percentage reduction of iron and copper. The reduction of zinc was not quite as great as the reduction of the other two metals.

The amount of metals removed after precipitation is due to the selected pH of 6.0 and the difference in metal solubility. Many heavy metals are amphoteric, which means that they can exist in strong acids and strong bases. In other words they are capable of donating or accepting a proton (Metcalf et al., 2014b). Since iron, copper, zinc, and manganese are amphoteric metals their corresponding hydroxides will only precipitate for specific pH values. Precipitation will reach its peak when the different metals reach their solubility minimum (Strakis, 2013). The solubility minimum for iron, copper, zinc, and manganese is around pH 8, 9, 10 and 11, respectively. The solubility minimum can be read from Figure 24, which shows the log C – pH diagrams for the various metals from Folldal. The log C – pH diagrams for the heavy metals from Løkken can be seen in Appendix 6. The log C – pH diagrams can tell how much of the different complexes a solution contains at a certain pH. For the AMD from Folldal and Løkken at pH 6.0, the dominating precipitate are iron(III)hydroxide ($Fe(OH)_3$) and copper(II)hydroxide

($Cu(OH)_2$). At pH 6.0 the log C – pH diagram from zinc shows that most of the zinc will be present as zinc ions.

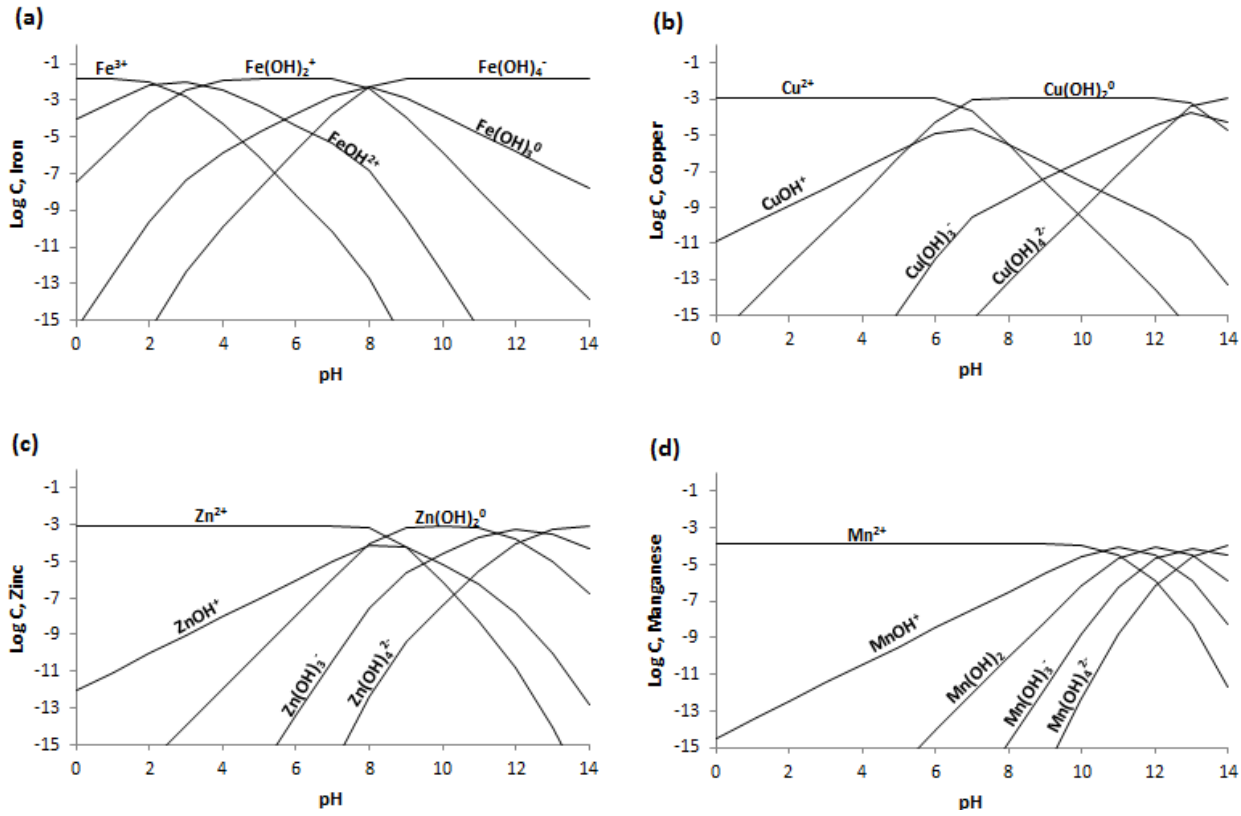

Figure 24: Log C - pH diagram for iron (Fe^{3+}), copper (Cu^{2+}), zinc (Zn^{2+}) and manganese (Mn^{2+}) for the AMD from Folldal center

To see if there is a connection between theory and practice the amount of dry matter from 100 mL AMD from both Folldal and Løkken was compared to the amount calculated by the help of the log C – pH diagrams. Table 10 shows the theoretical and practical amounts of dry matter for the AMD from Folldal and Løkken. The calculations can be seen in Appendix 6.

Table 10: Theoretical and practical amounts of dry matter for AMD from Folldal center and Løkken works

	Folldal center	Løkken works
Theoretical amount [mg/100mL]	185.9	586.2
Practical amount [mg/100mL]	899.6	2337.9
Difference [mg]	713.7	1751.7

The difference is large between the theoretical and practical amount. One possibility is that other metal hydroxides form when adding sodium hydroxide. Another possibility is that the TOC molecules attach to the metal hydroxides as they precipitate.

6.6.2 Ion exchange

Precipitation and sedimentation were followed by ion exchange. Tables 11 and 12 show the reduction of the heavy metal ions over a time period of 60 minutes. For both solutions the concentrations of iron, copper, and zinc are reduced, with the largest reduction being in the copper concentration. Since the amount of iron was so greatly reduced during precipitation, this might have had an effect on the selectivity of the clinoptilolite.

Table 11: Ion exchange of heavy metal concentration in AMD in contact with 30 g clinoptilolite after precipitation, Folldal center

Time [min]	$[Fe^{3+}]$ [mg/L]	$[Cu^{2+}]$ [mg/L]	$[Zn^{2+}]$ [mg/L]	$[Mn^{2+}]$ [mg/L]
0	5.1	4.3	44.3	n.a.
7,5	7.8	3.2	39.5	n.a.
15	8.3	3.0	37.9	n.a.
30	7.4	2.4	35.4	n.a.
60	3.3	2.2	35.0	n.a.
% adsorption,$_{ion\ exchange}$	*35.6*	*49.9*	*21.0*	n.a.

n.a.: data not available

Table 12: Ion exchange of heavy metal concentration in AMD in contact with 30 g clinoptilolite after precipitation, Løkken works

Time [min]	$[Fe^{3+}]$ [mg/L]	$[Cu^{2+}]$ [mg/L]	$[Zn^{2+}]$ [mg/L]	$[Mn^{2+}]$ [mg/L]
0	48.1	2.2	56.8	n.a.
7,5	23.0	1.6	45.8	n.a.
15	20.3	1.4	44.1	n.a.
30	17.7	1.3	44.3	n.a.
60	16.0	1.2	42.5	n.a.
% adsorption,$_{ion\ exchange}$	*32.1*	*44.9*	*14.3*	n.a.

n.a.: data not available

Tables 13 and 14 show the total amount of heavy metals removed when combining precipitation and ion exchange. When comparing the amount of heavy metals removed during precipitation and the amount during ion exchange, the majority of metals are removed during the precipitation step.

Table 13: Total amount and percentage of heavy metal removed by combining precipitation and ion exchange in the AMD from Folldal center

Metal	Initial concentration [mg/L]	Final concentration [mg/L]	Amount of metal removed [%]
Fe^{3+}	869.1	3.3	99.6
Cu^{2+}	79.7	2.2	97.3
Zn^{2+}	56.2	35.0	37.7
Mn^{2+}	7.7	n.a.	n.a.

n.a.: data not available

Table 14: Total amount and percentage of heavy metal removed by combining precipitation and ion exchange in the AMD from Løkken works

Metal	Initial concentration [mg/L]	Final concentration [mg/L]	Amount of metal removed [%]
Fe^{3+}	2834.5	16.0	99.4
Cu^{2+}	174.4	1.2	99.3
Zn^{2+}	141.7	42.5	70.0
Mn^{2+}	18.3	n.a.	n.a.

n.a.: data not available

Table 15 shows the percentage of removed heavy metals during ion exchange, precipitation and a combination of precipitation and ion exchange. The combination of precipitation and ion exchange gives the best treatment effect of the heavy metals. Precipitation is responsible for the largest reduction of iron and copper. According to the log C – pH diagrams, the amount of metals removed during precipitation would increase with an increase of the pH. Since the majority of heavy metals are removed during precipitation it may be profitable to study treatment of AMD with precipitation further.

Table 15: Comparing the amount of removed heavy metals from ion exchange alone and the combination of precipitation and ion exchange: m = 30g

	Folldal center			Løkken works		
Metal	Ion exchange [%]	Precipitation [%]	Precipitation and ion exchange [%]	Ion exchange [%]	Precipitation [%]	Precipitation and ion exchange [%]
Fe^{3+}	67.1	99.4	99.6	28.9	98.3	99.4
Cu^{2+}	33.4	94.5	97.3	18.7	98.7	99.3
Zn^{2+}	25.9	21.2	37.7	14.3	59.9	70
Mn^{2+}	-36.2	n.a.	n.a.	-20.6	n.a.	n.a.

n.a.: data not available

6.7 Differences between the AMDs from Folldal center and Løkken works

The main difference between the AMDs from Folldal and Løkken is the initial concentrations of heavy metals, which were greater for the AMD from Løkken. A cause of this disparity is the treatment effect the ion exchange had on the different solutions. The AMD from Folldal in solution with clinoptilolite had a larger proportion of the heavy metals removed. Despite the large difference in heavy metal content, the experiments showed similarities between the AMD from the two locations. Ion exchange with clinoptilolite gave the best reduction of iron, followed by copper and zinc. For these three metals the adsorption rate increased with the amount of clinoptilolite in solution. The experiments also showed similar results regarding the concentration of manganese, which increased during the course of the experiment and increased with higher amounts of clinoptilolite. Treatment with precipitation combined with ion exchange gave similar results for the AMD from both areas.

The various experiments show that treatment of AMD with clinoptilolite, behaves differently depending on the initial level of heavy metals. The composition of AMD is site specific, which means that the treatment of AMD should be evaluated for each location.

7. Conclusion

Norway has a rich mining history and many of the mines contain sulfur-bearing minerals, which contributes to the problems with AMD. AMD is mainly formed by the oxidation of pyrite, and the chemical reactions that take place makes the water acid and leads to the dissolution of other metals. The consequences of AMD are severe since large amounts of heavy metals are added to recipient waters, which lead to bioaccumulation of heavy metals in living organisms.

The decommissioned mines in Folldal, Løkken, and Røros all have problems with AMD. Ion exchange with clinoptilolite was tested as a treatment option for the AMD from Folldal and Løkken. Both AMD solutions had a large content of heavy metals and the metals studied were iron, copper, zinc, and manganese.

7.1 Kinetic studies

The kinetic experiment showed similarities between the AMD from Folldal and Løkken. The percentage removal of iron, copper, zinc, and manganese was 67.1, 33.4, 25.9 and -36.2 % from Folldal, and 28.9, 18.7, 14.3 and -20.6 % from Løkken, respectively. As seen from the results, ion exchange had the best treatment effect on iron, followed by copper and zinc. The experiments showed that the adsorption rate can be divided into three different stages. The development of the adsorption rate suggests that the exchange of heavy metals primarily takes place on the surface of the clinoptilolite. During the experiment it was observed that the amount of clinoptilolite corresponds to the amount of heavy metals removed. The solutions with 30 g of clinoptilolite had a better treatment effect for iron, copper, and zinc than the solutions containing 5 and 10 g clinoptilolite. The distribution ratio after 180 minutes for iron, copper, zinc, and manganese was 5.1, 1.3, 0.9 and -0.7 mL/g from Folldal, and 1.1, 0.6, 0.4 and -0.5 mL/g from Løkken, respectively. The development of the distribution ratio showed that there was some degree of exchange between the iron, copper, and zinc ions and the exchangeable cations. This coincides well with the study done on exchangeable ions, where it is visible that the concentrations of calcium and magnesium increase. The removal of manganese ions was unsuccessful for the AMD from both areas.

Despite the similarities, the experiment showed differences between the samples from the two sites. The treatment effect was better for the AMD from Folldal. This difference is related to the

different concentrations of heavy metal between the AMDs from the two areas. Regardless of the differences, the treatment effect from ion exchange with clinoptilolite is far from satisfactory for either of the samples.

7.2 Adsorption isotherms

The fit between the experimental data and the theoretical isotherms was different for the two solutions of AMD. The results for Folldal showed that neither the Langmuir nor the Freundlich isotherm had any good correlation with the experimental data. Even though the theoretical isotherms did not fit the experimental data from Løkken, the tendency between the Langmuir and Freundlich isotherms were similar to the experimental data. The selectivity series was deducted from the equilibrium isotherms to $Fe^{3+} > Cu^{2+} > Zn^{2+} > Mn^{2+}$ and it was similar for the AMD from both Folldal and Løkken. The intensity parameter for the Freundlich isotherm was below one for each of the metals which suggests that the binding strength decreases with the increase of surface coverage.

7.3 Effect of competing ions

Since the concentration difference between iron and manganese is so large it is assumed that there is a competing effect between the two metals. The clinoptilolite prefers iron over manganese resulting in the displacement of manganese ions so that the iron ions can attach to the adsorption sites. The increase of manganese concentration can not only be a result of the effect of competing ions. Since the concentration of manganese exceeds the initial value, there must be other factors to consider. A possible explanation could be that the clinoptilolite consists of a substance that the HR-ICP-MS registers as manganese.

Analysis of the AMD shows that both solutions consist of large amounts of TOC. TOC does not contribute to the effect of competing ions, but the TOC molecules can lead to fouling of the pores of the clinoptilolite, resulting in a smaller reduction of the heavy metals.

7.4 Precipitation in combination with ion exchange

The combination of precipitation and ion exchange gave a better removal of the heavy metals than ion exchange alone. The percentage removal of iron, copper, and zinc was 99.6, 97.3 and 37.7 % from Folldal and 99.4, 99.3 and 70.0 % from Løkken, respectively. The precipitation step

was primarily responsible for the removal of iron and copper ions from the solutions. Even though the reduction of heavy metals was significantly improved when combining precipitation and ion exchange, the final heavy metal concentrations are still above the acceptable environmental standards.

The precipitate formed during the addition of sodium hydroxide did not only consist of the metals studied in this thesis, since there were significant differences between theoretical and practical amount of dry matter. The log C – pH diagrams show that a greater proportion of the heavy metals would be removed if the pH was increased further.

7.6 Further work

The levels of heavy metals discharged from decommissioned mine sites to nearby rivers has large consequences for the ecosystem. It is therefore important to treat the AMD before it is discharged. It is evident from the experiments that ion exchange with clinoptilolite is capable of removing heavy metals. However, the treatment effect is far from satisfactory. The reason for this is probably the high amount of heavy metals. Even though clinoptilolite is not suitable for the treatment of AMD, other ion exchange resins might give other results and should therefore not be excluded from further research.

The experiments showed that ion exchange in combination with precipitation gave a good treatment effect of the heavy metals. The requirement to reach 10 µg Cu/L was, however, not fulfilled. Since precipitation removed most of the heavy metals it may be profitable to study the treatment of AMD with precipitation further. As neither of the methods studied in this thesis gave the desired results, consideration should be given to research other treatment methods.

This thesis has only touched base on AMD, the problems connected to it and some treatment possibilities. The challenges connected to AMD are not only found in Norway but also in many other countries where mining has taken place or is still ongoing. In order to prevent further damage to the environment, it is important to find good and inexpensive treatment methods for AMD.

References

Akai, A., & Koldas, S. (2009). Acid Mine Drainage (AMD): causes, treatment and case studies. *Elsevier, 14 (2006)*, 1139-1145. doi: http://dx.doi.org/10.1016/j.jclepro.2004.09.006

Altig, J. (2010). The Langmuir Adsorption Isotherm. *Physical Chemistry Laboratory*(2), 1-7.

Banks, D., Younger, P. L., Arnesen, R. T., Iversen, E. R., & Banks, S. B. (1997). Mine-water chemistry: the good, the bad and the ugly. *Springer-Verlag, 32 (2)*, 157 - 174.

Benjamin, M. M. (2002). *Water Chemistry* (1st ed. Vol. 1). Washington, USA: McGraw Hill.

Bogdanov, B., Georgiev, D., Angelova, K., & Yaneva, K. (2009). Natural zeolites: clinoptilolite review. *Internationa Science conference*, 1-6.

Boon, M., Brasser, H. J., Hansford, G. S., & Heijnen, J. J. (1999). Comparison of the oxidation kinetics of different pyrites in the presence of Thiobacillus ferrooxidans or Leptospirillum ferrooxidans. *Hydrometallurgy, 53*(1), 57-72.

Colella, C. (1996). Ion exchange equilibria in zeolite minerals. *Mineralium Deposita, 31*(6), 554-562. doi: http://dx.doi.org/10.1007/BF00196136

Crittenden, J. C., Trussell, R. R., Hand, D. W., Howe, K. J., & Tchobanoglous, G. (2005). *Water Treatment: Principles and Design* (2nd ed.). New Jersey, USA: John Wiley & Sons, Inc.

Davies, C. M. (2012). Determination of distribution coefficients for cation exchange resin and optimalisation of ion exchange chromatography for chromium separation for geological materials. *The University of Manchester, Faculty of Engineering and Physical Sciences*, 1 - 102. doi: https://www.escholar.manchester.ac.uk/uk-ac-man-scw:181065

Droste, R. L. (1997). *Theory and practice of water and wastewater treatment* (1st ed.). United States: John Wiley & sons, Inc.

Eide, E. (2013). *Avrenning fra nedlagt Folldal verk til Folla*. Unpublished internal document. Folldal kommune.

Erdem, E., Karapinar, N., & Donat, R. (2004). The removal of heavy metal cations by natural zeolites. *Journal of Colloid and Interface Science, 280*(2), 309-314. doi: http://dx.doi.org/10.1016/j.jcis.2004.08.028

Gvein, Ø. (2009, 09.11.2011). Røros Kobberverk. Retrieved March 6, 2014, from http://snl.no/R%C3%B8ros_Kobberverk

Holmen, J. A. (2012, 09.07.2012). Det var en gang..... Retrieved 16th May, 2014, from http://www.oi.no/utstillingstekster/1-bergverk/

Iversen, E. R., & Arnesen, R. T. (2003). Elvestrekninger påvirket av gruveforurensning. *Norsk institutt for Vannforskning (NIVA), 1986/2003*, 1-81.

Life Extension. (1995 - 2014). Heavy Metal Detoxification. Retrieved 16th May, 2014, from http://www.lef.org/protocols/health_concerns/heavy_metal_detoxification_01.htm

Lu, J., Liu, N., Li, L., & Lee, R. (2010). Organic fouling and regeneration of zeolite membrane in wastewater treatment. *Separation and Purification Technology*, *72*(2), 203-207. doi: http://dx.doi.org/10.1016/j.seppur.2010.02.010

Metcalf, L., Eddy, H. P., Tchobanoglous, G., Stensel, H. D., Tsuchihashi, R., & Burton, F. (2014a). *Wastewater Engineering Treatment and Resource Recovery* (5 ed. Vol. 2). Singapore: McGraw-Hill Education.

Metcalf, L., Eddy, H. P., Tchobanoglous, G., Stensel, H. D., Tsuchihashi, R., & Burton, F. (2014b). *Wastewater Engineering Treatment and Resource Recovery* (5 ed. Vol. 1). Singapore: McGraw-Hill Education.

Miljødirektoratet. (2013a, 02.12.2013). Avrenning av tungmetaller fra nedlagte kisgruver. Retrieved February 17, 2014, from http://www.miljostatus.no/Tema/Ferskvann/Miljogifter_ferskvann/Avrenning-fra-gruver/

Miljødirektoratet. (2013b, 02.12.2013). Folldal Verk. Retrieved February 27, 2014, from http://www.miljostatus.no/Tema/Ferskvann/Miljogifter_ferskvann/Avrenning-fra-gruver/Folldal-Verk/

Miljødirektoratet. (2013c, 03.03.2014). Løkken Gruber. Retrieved March 3, 2014, from http://www.miljostatus.no/Tema/Ferskvann/Miljogifter_ferskvann/Avrenning-fra-gruver/Lokken-Gruber/

Miljødirektoratet. (2013d, 20.11.2013). Storwartzområdet, Røros. Retrieved November 30, 2013, from http://www.miljostatus.no/Storwartzomradet/

Morgan, B., & Lahav, O. (2007). The effect of pH on the kinetics of spontaneous Fe(II) oxidation by O2 in aqueous solution – basic principles and a simple heuristic description. *Chemosphere, 68* (11), 2080-2084. doi: http://dx.doi.org/10.1016/j.chemosphere.2007.02.015

Motsi, T., Rowson, N. A., & Simmons, M. J. H. (2009). Adsorption of heavy metals from acid mine drainage by natural zeolite. *International Journal of Mineral Processing, 92*(1–2), 42-48. doi: http://dx.doi.org/10.1016/j.minpro.2009.02.005

Riksantikvaren. (2012, 05.12.2012). Røros bergstad og Circumferensen. Retrieved November 30, 2012, from http://www.miljostatus.no/Tema/Kulturminner/Verdensarven/Roros-Bergstad/

Rui, I. J. (2009, 13.08.2011). Folldal Verk A/S. Retrieved November 28, 2013, from http://snl.no/Folldal_Verk_A/S

Schrenk, M. O., Edwards, K. J., Goodman, R. M., Hamers, R. J., & Banfield, J. F. (1998). Distribution of Thiobacillus ferrooxidans and Leptospirillum ferrooxidans: Implications for Generation of Acid Mine Drainage. Retrieved January 29, 2014, from http://www.sciencemag.org/content/279/5356/1519.short

Segalstad, T. V., Walder, I. F., & Nilssen, S. (2006). Mining mitigation in Norway and future improvement possibilities. *America Society of Mining and Reclamation (ASMR)*, 1952 - 1960.

Skei, J. (2010). Bergverk og avfallsdeponering - Status, miljøutfordringer og kunnskapsbehov. *Klima- og forurensningsdirektoratet (Klif)*, 1 - 108.

Skousen, J. (2011). Acid Drainage Technology Initiative. Retrieved November 27, 2013, from http://www.aciddrainage.com/amd.cfm

Sprynskyy, M., Buszewski, B., Terzyk, A. P., & Namieśnik, J. (2006). Study of the selection mechanism of heavy metal (Pb2+, Cu2+, Ni2+, and Cd2+) adsorption on clinoptilolite. *Journal of Colloid and Interface Science, 304*(1), 21-28. doi: http://dx.doi.org/10.1016/j.jcis.2006.07.068

Store Norske Leksikon. (2009, 15.02.2009). Tungmetaller. Retrieved February 17, 2014, from http://snl.no/tungmetaller

Strakis, K. (2013, 31.10.2013). Metal Hydroxide Precipitation. Retrieved March 27, 2014, from http://asterionstc.com/2013/10/metal-hydroxide-precipitation/

Stumm, W., & Morgan, J. J. (1996). *Aquatic chemistry - Chemical Equilibria and Rates in Natural Waters* (3 ed. Vol. 3). United States: John Wiley & sons inc.

The International Network for Acid Prevention. (2012, 09.05.2012). Chapter 2. Retrieved November 26, 2013, from http://www.gardguide.com/index.php/Chapter_2

Appendix 1: E- mail correspondence with Grethe Braastad from Miljødirektoratet

Fra: Amita Khan

Sendt: 7. mars 2014 14:19

Til: miljostatus@miljodir.no

Kopi: Miljøstatus

Emne: SV: Folldal Verk - Løkken Verk

Hei,

Mitt navn er Amita og for øyeblikket studerer jeg vann- og miljøteknikk på NTNU. Dette er mitt siste semester ved NTNU og nå skriver jeg masteroppgave om forurenset gruvevann ved gruvene i Folldal, Løkken og Røros. I forbindelse med dette har jeg noen spørsmål.

Jeg har sett på nettsidene deres for hvert av de aktuelle områdene;

Folldal verk (http://www.miljostatus.no/Tema/Ferskvann/Miljogifter_ferskvann/Avrenning-fra-gruver/Folldal-Verk/)

- Figuren "Kobberavrenning fra Folldal sentrum" viser variasjonene i kobbermengden, er det en spesiell grunn til at det var så lavt innhold i 2003? Hvorfor har den etter dette økt?

- Dere skriver også at et renseanlegg ble satt i drift høsten 2013. Hva slags type anlegg er dette?

Løkke Gruber

(http://www.miljostatus.no/Tema/Ferskvann/Miljogifter_ferskvann/Avrenning-fra-gruver/Lokken-Gruber/)

- Fra "Kobberavrenning fr Løkken Gruber" er det en minkning i kobberkonsentrasjonen de siste åra. Hva skyldes dette?

Mvh

Amita Khan
Tlf.: 928 38 731

Fra: Grethe Braastad
Sendt: 7. mars 2014 14:19
Til: amita.khan90@gmail.com
Kopi: Miljøstatus
Emne: SV: Folldal Verk - Løkken Verk

Hei Amita

Det var en spenstig oppgave.

Folldal er delt inn i to adskilte (mhp forurensning) gruveområder. Det gamle området i Folldal sentrum og det nye gruveområdet på Hjerkinn (Tverrfjellet gruve). Disse to områdene har ingenting annet felles enn Folla, som er resipienten for avrenningen.

Renseanlegget du nevner er installert ved Tverrfjellet gruve på Hjerkinn, og et er naturbasert anlegg (se vedlegg).

Når det gjelder avrenning av tungmetaller fra nedlagte gamle gruver så vil disse kunne variere ganske mye fra år til år, både mhp konsentrasjon og mengde. Dette har flere årsaker, men spesielt værforhold spiller en viktig rolle for oksydasjonsprosesser som fører til syredannelse og derav utlekking av metaller. Hvis du klikker deg rundt på gruvesidene på Miljøstatus vil du finne en del generell informasjon.

Riktig lykke til med prosjektet ditt.

Med hilsen

Grethe Baarstad
Seniorrådgiver, industriseksjon 2 (IN2)
Miljødirektoratet
Telefon: 03400 / 73 58 05 00
Mobil: 452 52 394
E-post: grethe.braastad@miljodir.no
www.miljødirektoratet.no- www.miljøstatus.no

CARBOPLANT Srl
Trattamento Acque

Sistema Certificato
UNI EN ISO 9001
CC 12 3172/EA 28

SCHEDA DI SICUREZZA

(93/113/CEE)

1. IDENTIFICAZIONE DEL PRODOTTO E DELLA SOCIETA':

- IDENTIFICAZIONE PRODOTTO: **CLINO FEED CLINOPTILOLITE**
- DISTRIBUITO DA : **LEIDI ANGELO SRL – ZANDOBBIO (BG)**
  VIA MADONNA DELLA NEVE 1

2. IDENTIFICAZIONE DEI PERICOLI :

- RISCHI PER LA SALUTE: **NESSUNO**
- RISCHI PER L'AMBIENTE: **NESSUNO**

3. COMPOSIZIONE / INFORMAZIONE SUGLI INGREDIENTI:

- SOSTANZA : **MINERALE ATOSSICO**
- COMPOSIZIONE : **FORMULA EMPIRICA ($Ca,K_2,Na_2,Mg)_4Al_8Si_{40}O_{96}.24H_20$)**
- N° C.A.S :
- COSTITUENTI PERICOLOSI : **NESSUNO**

4. MISURE DI PRIMO SOCCORSO :

- INDICAZIONI GENERALI: **PRODOTTO NATURALE ATOSSICO**
- IN CASO INALAZIONE: **NON NECESSARIE**
- IN CASO DI CONTATTO ACCIDENTALE CON GLI OCCHI: **LAVARE CON ACQUA**
- IN CASO DI CONTATTO ACCIDENTALE CON LA PELLE: **LAVARE CON ACQUA**
- IN CASO DI INGESTIONE: **NON NECESSARIO**
- CONSULTAZIONE DEL MEDICO: **NON NECESSARIO**

CARBOPLANT Srl – Sede Legale ed Officina: Via Carlo Gazzo, 20 - 27029 Vigevano (PV) Italy
Tel. 0381.692434 – Fax 0381.693210 – C. Fisc e P.IVA 02093820187 – E-mail: info@carboplantsrl.it
Website: www.carboplantsrl.it

5. MISURE ANTINCENDIO :

- INDICAZIONI GENERALI: **PROD. NON COMBUSTIBILE E NON INFIAMMABILE**
- MEZZI E PROCEDURE DI ESTINZIONE APPROPRIATI: **NESSUNO**
- MEZZI E PROCEDURE DI ESTINZIONE SCONSIGLIATI: **NESSUNO**
- COMPONENTI DI COMBUSTIONE PERICOLOSI: **NESSUNO**
- PERICOLI SPECIFICI: **NESSUNO**
- METODI SPECIFICI: **NESSUNO**
- MEZZI DI PROTEZIONE SPECIALI: **NESSUNO**

6. MISURE IN CASO DI FUORIUSCITA ACCIDENTALE :

- PROTEZIONI INDIVIDUALI: **PRODOTTO NATURALE E INERTE, CHE NON RICHIEDE MISURE DI SICUREZZA SPECIFICHE. QUANDO SI IMPIEGA IL PRODOTTO A GRANULOMETRIA FINE, SI CONSIGLIA L'USO DI MASCHERE E OCCHIALI IDONEI PER IL MANEGGIO DI PRODOTTI PULVERULENTI**

- PROTEZIONI PER L'AMBIENTE: **PRODOTTO NATURALE E INERTE, CHE NON RICHIEDE MISURE DI SICUREZZA SPECIFICHE**

- PROCEDURE PER IL CONTENIMENTO: **NON RICHIEDE MISURE DI SICUREZZA SPECIFICHE.**

7. MANIPOLAZIONE E STOCCAGGIO :

- MANIPOLAZIONE: **NON SONO NECESSARIE MISURE SPECIFICHE PER LA MANIPOLAZIONE. SI CONSIGLIA L'USO DI MASCHERE E OCCHIALI ADATTI ALLA MANIPOLOAZIONE DEI PRODOTTI PULVERULENTI IN CASO DI IMPIEGO DEL PRODOTTO A GRANULOMETRIA FINE**

- STOCCAGGIO: **PER IL PRODOTTO A GRANULOMETRIA FINE E/O TALCATA SI CONSIGLIA DI STOCCARLO IN AMBIENTE NON TROPPO UMIDO ALFINE DI EVITARE L'IMPACCAMENTO**

8. CONTROLLO DELL'ESPOSIZIONE / PROTEZIONE INDIVIDUALE :

- PRECAUZIONI GENERALI DA ADOTTARE: **PRODOTTO MINERALE ATOSSICO**
- PROTEZIONE DELL'APPARATO RESPIRATORIO: **LA MANIPOLAZIONE DI GRANDI QUANTITA' PUO' GENERARE UN AMBIENTE POLVEROSO, PERTANTO SI CONSIGLIA L'USO DELLA MASCHERA.**
- PROTEZIONE DELLE MANI: **NON NECESSARIA.**
- PROTEZIONE DEGLI OCCHI: **LA MANIPOLAZIONE DI GRANDI QUANTITA' PUO' GENERARE UN AMBIENTE POLVEROSO, PERTANTO SI CONSIGLIA L'USO DEGLI OCCHIALI.**
- PROTEZIONE DELLA PELLE: **NON NECESSARIA.**

CARBOPLANT Srl
Trattamento Acque

9. PROPRIETA' FISICHE E CHIMICHE :

- STATO FISICO: **SOLIDO**
- COLORE: **GRIGIO-VERDE**
- ODORE: **INODORE**
- pH: **6.9 – 7.6**
- PUNTO DI FUSIONE: **1 340 °C**
- PUNTO DI INFIAMMABILITA': **NON INFIAMMABILE**
- PROPRIETA' ESPLOSIVE: **NESSUNA**
- PROPRIETA' COMBURENTI: **NON COMBUSTIBILE**
- DUREZZA: **Mohs hardness 1,5 - 2,5**
- RESISTENZA ALLA COMPRESSIONE: **33 MPa**
- SUPERFICIE SPECIFICA: **VARIABILE IN FUNZIONE DELLA GRANULOMETRIA**
- SOLUBILITA': **NESSUNA**
- SCALA DI ASSORBIMENTO: ***> NH4+ > Pb2+ >K+ > Na+ > Ca2+ > Mg2+ > Ba2+ > Cu2+ > Zn2+***
- CAPACITA' DI SCAMBIO: **8 500 mg NH / 1 kg**

10. STABILITA' E REATTIVITA' :

- INDICAZIONI GENERALI: **PRODOTTO NATURALE INERTE**
- CONDIZIONI DA EVITARE: **NESSUNA**
- MATERIE DA EVITARE: **NESSUNA**

11. INFORMAZIONI TOSSICOLOGICHE :

- TOSSICITA': **PRODOTTO NATURALE ATOSSICO**
- EFFETTI IMMEDIATI/RITARDATI PER BREVE/PROLUNGATA ESPOSIZIONE: **NON CONOSCIUTI**

12. INFORMAZIONI ECOLOGICHE :

- INFORMAZIONI GENERALI': **PRODOTTO NATURALE INERTE**
- MOBILITA': -------
- DEGRADABILITA': **NON DEGRADABILE**
- EFFETTI A BREVE / LUNGO TERMINE: **NESSUNO**

13. INFORMAZIONI ECOLOGICHE :

- SMALTIMENTO DEL PRODOTTO': **ELIMINARE I RESIDUI IN CONFORMITA' ALLE DISPOSIZIONI LEGISLATIVE LOCALI. NON SONO NECESSARIE PRECAUZIONI PARTICOLARI.**

CARBOPLANT Srl
Trattamento Acque

14. INFORMAZIONI SUL TRASPORTO :

- PRECAUZIONI: **NESSUNA**
- NUMERO O.N.U: ----------
- TRASPORTO STRADALE: ----------
- TRASPORTO FERROVIARIO: ----------
- TRASPORTO MARITTIMO: ----------
- TRASPORTO AEREO: ----------

15. INFORMAZIONI SULLA REGOLAMENTAZIONE :

- CLASSIFICAZIONECEE: **EC L 651, 09/07/2013**
- IMBALLAGGIO: ----------
- ETICHETTATURA: **TENORE MAX1% NEI MANGIMI**
- SPECIFICHE DISPOSIZIONI COMUNITARIE: **TENORE MAX.1% NEI MANGIMI**
- LEGISLAZIONE: **TENORE MAX.1% NEI MANGIMI**

16. ALTRE INFORMAZIONI:

- **QUESTA SCHEDA DI SICUREZZA COMPLETA LE INFORMAZIONI RIPORTATE NELLA SCHEDA DEL PRODOTTO, TUTTAVIA NON LA SOSTITUISCE.**

- **I DATI RIPORTATI NELLA PRESENTE SCHEDA DEI DATI DI SICUREZZA SONO BASATI SULLE NOSTRE ATTUALI CONOSCENZE, AVENDO COME UNICO SCOPO QUELLO DI INFORMARE SUGLI ASPETTI DI SICUREZZA.**

CARBOPLANT Srl
Trattamento Acque

Sistema Certificato
UNI EN ISO 9001
SC 12-3172/EA 28

Scheda Tecnica ***ZEOCLINOPTLOLITE*** ZPE
caratteristiche tecniche e chimiche

ORIGINE

La Zeolite attiva si ottiene da minerale naturale selezionato avente una buona resistenza meccanica e basso tenore di impurezze.

APPLICAZIONI

La ZPE è tra le più attive resine naturali a scambio cationico. Possiede una elevata capacità di scambio con lo ione ammonio ($NH4+$) che la rende particolarmente idonea alla rimozione di ammoniaca (NH_3).
La ZPE può essere impiegata, sia in filtri a gravità che in pressione, ha ottime caratteristiche meccaniche, che riducono al minimo le perdite per attrito durante il lavaggio.
La ZPE per la sua estesa superficie specifica e la spiccata capacità di scambio cationico, è largamente utilizzata per il trattamento di acque potabili e reflue.

Caratteristiche tecniche generali:

Granulometria:	polveri 1 – 2,5 mm – 2,5-5 mm.
Colore:	Bianco azzurro/marrone chiaro
pH sospensione acquosa:	alcalino
Densità apparente:	900-950 kg./m^3
Umidità all'imballo:	4%
Superfice specifica B.E.T.:	500-600 m^3/g
Capacità media di scambio cationico:	1,13 meq/g (trattamento con soluzione 1 M di MH_4C1)
Scala di scambio cationico:	Cs^{2-}-> NH_{4+} >Pb^{2} >K^{3+} >Na^{3+} >Ca^{3+} >Mg^{3+} >Ba^{3+} >Cu^{3+} >Ni^{3+} >Cd^{2-} >Zn^{3+} >Fe^{3+} >Mn^{3+}

Analisi chimica sul tal quale:

SiO^2	68,7 %
$A1^20^3$	10,2 %
CaO	4,2 %
K^2O	2,1 %

CARBOPLANT Srl – Sede Legale ed Officina: Via Carlo Gazzo, 20 - 27029 Vigevano (PV) Italy
Tel. 0381.692434 – Fax 0381.693210 – C. Fisc e P.IVA 02093820187 – E-mail: info@carboplantsrl.it
Website: www.carboplantsrl.it

Appendix 3: Heavy metal concentration

Resultater korrigert for 10x fortynning, dvs resultater i orginalprøvene levert av oppdragsgiver

Date of analyses: 03.04.14 sekvens 21

Counting digits = 3

	Sample received	Project-Inr	Tid	Remarks	Elements	Cu	Fe	Pb	Zn
Start formulas	1				Start formulas				
	31.01.2014	1	0		4	1	1	1	1
	31.01.2014	2	0		4	1	1	1	1
					0				
				Forbehanlding prøve 1-2, prøvene ble konservert med 0.1M HNO3 i orginal-røret, der	0				
Stop formulas					Stop formulas				
number		2	2		4	2	2	2	
Average					6				

Project-Inr shall be an continuous unique Inr from

Isotope	Y89(LR)		Cd114(LR)	
Parameteres	Conc.		Conc.	
Sample ID	µg/L	RSD, %	µg/L	RSD, %
Start statistical calculations				
Anita-Kahn-10x-1-2-1: Initial Folldal center	215.3	3.2	147.2	2.9
Anita-Kahn-10x-1-2-2: Initial Løkken works	336.9	5.4	413.8	2.0
Stop statistical calculations				
Average	276.106	4.3	280.514	2.5
Min	215.294	3.2	147.244	2.0
Max	336.918	5.4	413.784	2.9
Std	86.001	1.6	188.472	0.6
Rsd % <5, 5-10, >10	31.1		67.2	
Confidence interval 95%	172.002	3.1	376.945	1.3
Confidence interval 95% (%) <5, 5-10, >10	62.3		134.4	
Number	2	2	2	2

Mo98(MR)		Cs133(LR)		Ce140(LR)		Pr141(LR)		Nd146(LR)		Sm147(LR)		Tb159(LR)		Dy163(LR)		Ho165(LR)		Er166(LR)		Tm169(LR)		Yb172(LR)		Lu175(LR)		Hf178(LR)		W182(LR)		Tl205(LR)	
Conc.		Conc.		Conc.		Conc.		Conc.		Conc.		Conc.		Conc.		Conc.		Conc.		Conc.		Conc.		Conc.		Conc.		Conc.		Conc.	
µg/L	RSD, %	µg/L	RSD, %	µg/L	RSD, %	µg/L	RSD, %	µg/L	RSD, %	µg/L	RSD, %	µg/L	RSD, %	µg/L	RSD, %	µg/L	RSD, %	µg/L	RSD, %	µg/L	RSD, %	µg/L	RSD, %	µg/L	RSD, %	µg/L	RSD, %	µg/L	RSD, %	µg/L	RSD, %
0.02	33.8	0.357	3.4	16.0746	2.8	2.4800	4.9	12.121	0.8	3.280	3.3	0.6752	2.7	4.2449	8.2	0.7952	4.0	2.2708	1.8	0.3068	3.0	2.0164	4.0	0.3116	6.7	0.0084	10.8	0.012	20.9	0.004	9.6
0.38	11.1	0.931	6.5	21.0694	2.5	3.1707	7.6	14.846	5.4	4.431	2.4	0.9780	3.5	6.0378	4.4	1.2143	6.6	3.3844	2.1	0.4747	4.1	2.9113	2.3	0.4233	0.7	0.0295	7.4	0.009	8.9	0.027	4.4
0.20	22.5	0.644	5.0	18.5720	2.7	2.8254	6.3	13.484	3.1	3.856	2.9	0.8266	3.1	5.1413	6.3	1.0047	5.3	2.8276	2.0	0.3907	3.6	2.4639	3.2	0.3674	3.7	0.0189	9.1	0.010	14.9	0.015	7.0
0.02	11.1	0.357	3.4	16.0746	2.5	2.4800	4.9	12.121	0.8	3.280	2.4	0.6752	2.7	4.2449	4.4	0.7952	4.0	2.2708	1.8	0.3068	3.0	2.0164	2.3	0.3116	0.7	0.0084	7.4	0.009	8.9	0.004	4.4
0.38	33.8	0.931	6.5	21.0694	2.8	3.1707	7.6	14.846	5.4	4.431	3.3	0.9780	3.5	6.0378	8.2	1.2143	6.6	3.3844	2.1	0.4747	4.1	2.9113	4.0	0.4233	6.7	0.0295	10.8	0.012	20.9	0.027	9.6
0.26	16.1	0.406	2.2	3.5319	0.2	0.4884	1.9	1.927	3.3	0.814	0.6	0.2142	0.6	1.2677	2.7	0.2963	1.8	0.7874	0.2	0.1187	0.8	0.6328	1.2	0.0790	4.2	0.0149	2.4	0.002	8.5	0.017	3.7
127.2		63.1		19.0		17.3		14.3		21.1		25.9		24.7		29.5		27.8		30.4		25.7		21.5		78.8		22.1		107.9	
0.52	32.1	0.812	4.4	7.0638	0.4	0.9769	3.8	3.854	6.5	1.628	1.3	0.4283	1.1	2.5354	5.4	0.5927	3.7	1.5749	0.4	0.2375	1.6	1.2656	2.4	0.1579	8.5	0.0299	4.8	0.004	17.0	0.033	7.4
254.4		126.1		38.0		34.6		28.6		42.2		51.8		49.3		59.0		55.7		60.8		51.4		43.0		157.7		44.2		215.8	
2	2	2	2	2	2	2	2	2	2	2	2	2	2	2	2	2	2	2	2	2	2	2	2	2	2	2	2	2	2	2	2

Pb208(LR)		Bi209(LR)		Th232(LR)		U238(LR)		Li7(MR)	B11(MR)		Mg25(MR)		Al27(MR)		Si29(MR)		P31(MR)		S34(MR)		K39(MR)		Ca43(MR)		Sc45(MR)		Ti49(MR)		V51(MR)	
Conc. µg/L	RSD, %	Conc. µg/L	RSD, %	Conc. µg/L	RSD, %	Conc. µg/L	RSD, %	Conc. µg/L	Conc. µg/L	RSD, %	Conc. µg/L	RSD, %	Conc. µg/L	RSD, %	Conc. µg/L	RSD, %	Conc. µg/L	RSD, %	Conc. µg/L	RSD, %	Conc. µg/L	RSD, %	Conc. µg/L	RSD, %	Conc. µg/L	RSD, %	Conc. µg/L	RSD, %	Conc. µg/L	RSD, %
0.20	0.5	0.002	14.4	0.703	4.7	0.98	5.3	7.1	2	6.8	26 133	5.0	19 090.1	4.1	2 452	5.4	133.0	0.8	174 636	1.1	181	5.1	18 046	1.8	6.926	6.0	19.48	6.2	8.16	2.5
0.38	2.3	0.010	3.8	0.983	2.4	3.74	2.6	17.9	6	2.2	55 990	7.4	51 719.2	7.8	2 621	3.9	498.6	8.6	448 024	5.8	103	6.2	25 078	7.6	21.775	9.0	85.48	6.0	56.53	11.4
0.29	1.4	0.006	9.1	0.843	3.6	2.36	4.0	12.5	4	4.5	41 061	6.2	35 404.6	6.0	2 537	4.7	315.8	4.7	311 330	3.5	142	5.7	21 562	4.7	14.350	7.5	52.48	6.1	32.35	7.0
0.20	0.5	0.002	3.8	0.703	2.4	0.98	2.6	7.1	2	2.2	26 133	5.0	19 090.1	4.1	2 452	3.9	133.0	0.8	174 636	1.1	103	5.1	18 046	1.8	6.926	6.0	19.48	6.0	8.16	2.5
0.38	2.3	0.010	14.4	0.983	4.7	3.74	5.3	17.9	6	6.8	55 990	7.4	51 719.2	7.8	2 621	5.4	498.6	8.6	448 024	5.8	181	6.2	25 078	7.6	21.775	9.0	85.48	6.2	56.53	11.4
0.13	1.3	0.006	7.5	0.198	1.6	1.95	1.9	7.6	3	3.3	21 113	1.7	23 072.2	2.6	120	1.1	258.5	5.5	193 314	3.3	55	0.8	4 973	4.1	10.500	2.1	46.67	0.1	34.20	6.3
45.9		100.8		23.5		82.6		60.7	67.2		51.4		65.2		4.7		81.9		62.1		38.8		23.1		73.2		88.9		105.7	
0.27	2.5	0.012	15.0	0.396	3.3	3.90	3.8	15.2	5	6.5	42 225	3.4	46 144.5	5.2	239	2.1	517.0	11.0	386 628	6.6	110	1.6	9 946	8.2	21.001	4.2	93.34	0.3	68.41	12.6
91.8		201.5		46.9		165.2		121.4	134.4		102.8		130.3		9.4		163.7		124.2		77.7		46.1		146.3		177.8		211.5	
2	2	2	2	2	2	2	2	2	2	2	2	2	2	2	2	2	2	2	2	2	2	2	2	2	2	2	2	2	2	2

Cr52(MR)		Mn55(MR)		Fe56(MR)		Co59(MR)		Ni60(MR)		Cu63(MR)		Zn66(MR)		Ga69(MR)		Rb85(MR)		Sr88(MR)		Sb121(MR)		Ba137(MR)		La139(MR)		As75(HR)		Nb93(HR)	
Conc. µg/L	RSD, %	Conc. µg/L	RSD, %	Conc. µg/L	RSD, %	Conc. µg/L	RSD, %	Conc. µg/L	RSD, %	Conc. µg/L	RSD, %	Conc. µg/L	RSD, %	Conc. µg/L	RSD, %	Conc. µg/L	RSD, %	Conc. µg/L	RSD, %	Conc. µg/L	RSD, %	Conc. µg/L	RSD, %	Conc. µg/L	RSD, %	Conc. µg/L	RSD, %	Conc. µg/L	RSD, %
50.65	4.3	674.05	5.3	86 368.7	3.1	147.654	7.4	55.97	1.8	6 881.27	4.7	4 568.11	6.6	1.563	10.2	0.7	8.7	21	4.8	0.018	23.4	1.84	18.7	6.410	5.6	1.23	5.2	0.019	37.8
73.69	15.5	1 607.08	4.1	253 818.8	14.3	838.545	4.6	100.08	2.5	15 034.04	8.2	11 423.33	3.3	5.666	9.2	0.5	8.2	41	3.7	0.062	19.7	0.21	1.7	9.681	4.1	46.63	1.6	0.158	26.3
62.17	9.9	1 140.57	4.7	170 093.7	8.7	493.100	6.0	78.03	2.2	10 957.65	6.5	7 995.72	5.0	3.614	9.7	0.6	8.5	31	4.3	0.040	21.6	1.03	10.2	8.045	4.9	23.93	3.4	0.089	32.1
50.65	4.3	674.05	4.1	86 368.7	3.1	147.654	4.6	55.97	1.8	6 881.27	4.7	4 568.11	3.3	1.563	9.2	0.5	8.2	21	3.7	0.018	19.7	0.21	1.7	6.410	4.1	1.23	1.6	0.019	26.3
73.69	15.5	1 607.08	5.3	253 818.8	14.3	838.545	7.4	100.08	2.5	15 034.04	8.2	11 423.33	6.6	5.666	10.2	0.7	8.7	41	4.8	0.062	23.4	1.84	18.7	9.681	5.6	46.63	5.2	0.158	37.8
16.29	7.9	659.75	0.8	118 405.1	7.9	488.534	2.0	31.19	0.5	5 764.88	2.5	4 847.37	2.3	2.901	0.7	0.1	0.4	14	0.8	0.031	2.6	1.15	12.0	2.313	1.1	32.10	2.5	0.099	8.1
26.2		57.8		69.6		99.1		40.0		52.6		60.6		80.3		15.6		44.6		76.9		112.4		28.8		134.1		111.3	
32.59	15.8	1 319.50	1.7	236 810.2	15.8	977.068	4.0	62.37	1.0	11 529.76	4.9	9 694.74	4.7	5.802	1.4	0.2	0.7	28	1.6	0.062	5.2	2.31	24.0	4.627	2.1	64.21	5.1	0.197	16.3
52.4		115.7		139.2		198.1		79.9		105.2		121.2		160.5		31.3		89.1		153.9		224.8		57.5		268.3		222.6	
2	2	2	2	2	2	2	2	2	2	2	2	2	2	2	2	2	2	2	2	2	2	2	2	2	2	2	2	2	2	2

Resultater korrigert for 50x fortynning, dvs resultater i orginalprøvene levert av oppdragsgiver

Date of analyses: 09.04.14 sekvens 23

Counting digits = 3

	Sample received	Localities	Tid	Elements	Cu	Fe	Pb	Zn	Project-Inr	Sample ID	Y89(LR) Conc. µg/L	Y89(LR) RSD, %	Cd114(LR) Conc. µg/L	Cd114(LR) RSD, %	Mo98(MR) Conc. µg/L	Mo98(MR) RSD, %
Start formulas	1			Start formulas						Start statistical calculations						
	07.04.2014	Løkken verk (5g)	15	4	1	1	1	1	3	Løkken verk (5g), 15 min	353	3.1	525	3.2	5.24	13.5
	07.04.2014	Løkken verk (10g)	15	4	1	1	1	1	4	Løkken verk (10g), 15min	348	1.0	553	10.5	6.17	3.3
	07.04.2014	Løkken verk (30g)	15	4	1	1	1	1	5	Løkken verk (30g), 15 min	368	6.5	540	5.0	5.68	1.7
	07.04.2014	Løkken verk (5g)	30	4	1	1	1	1	6	Løkken verk (5g), 30 min	350	0.9	534	3.1	4.36	1.9
	07.04.2014	Løkken verk (10g)	30	4	1	1	1	1	7	Løkken verk (10g), 30 min	371	5.6	541	1.9	5.42	8.6
	07.04.2014	Løkken verk (30g)	30	4	1	1	1	1	8	Løkken verk (30g), 30 min	377	4.2	551	2.1		
	07.04.2014	Løkken verk (5g)	60	4	1	1	1	1	9	Løkken verk (5g), 60 min	353	1.9	542	7.5	4.47	3.7
	07.04.2014	Løkken verk (10g)	60	4	1	1	1	1	10	Løkken verk (10g), 60 min	367	1.2	535	0.7	4.56	9.8
	07.04.2014	Løkken verk (30g)	60	4	1	1	1	1	11	Løkken verk (30g), 60 min	385	6.1	513	3.1	4.41	3.7
	07.04.2014	Løkken verk (5g)	120	4	1	1	1	1	12	Løkken verk (5g), 120 min	381	4.1	540	3.3	3.73	5.3
	07.04.2014	Løkken verk (10g)	120	4	1	1	1	1	13	Løkken verk (10g), 120 min	408	9.1	520	3.4	4.41	9.7
	07.04.2014	Løkken verk (30g)	120	4	1	1	1	1	14	Løkken verk (30g), 120 min	414	8.7	523	1.9	4.55	2.7
	07.04.2014	Løkken verk (5g)	180	4	1	1	1	1	15	Løkken verk (5g), 180 min	377	3.9	538	2.0	3.44	3.6
	07.04.2014	Løkken verk (10g)	180	4	1	1	1	1	16	Løkken verk (10g), 180 min	387	5.5	547	1.2	4.03	7.9
	07.04.2014	Løkken verk (30g)	180	4	1	1	1	1	17	Løkken verk (30g), 180 min	417	4.4	481	1.3	3.11	8.6
	07.04.2014	Folldal sentrum (5g)	15	4	1	1	1	1	18	Folldal sentrum (5g), 15 min	231	3.4	192	3.0	0.50	30.2
	07.04.2014	Folldal sentrum (10g)	15	4	1	1	1	1	19	Folldal sentrum (10g), 15 min	232	5.2	187	2.6	0.45	8.5
	07.04.2014	Folldal sentrum (30g)	15	4	1	1	1	1	20	Folldal sentrum (30g), 15 min	227	1.8	188	4.1	0.84	9.9
	07.04.2014	Folldal sentrum (5g)	30	4	1	1	1	1	21	Folldal sentrum (5g), 30 min	238	6.7	197	3.5	0.19	4.9
	07.04.2014	Folldal sentrum (10g)	30	4	1	1	1	1	22	Folldal sentrum (10g), 30 min	236	8.3	193	4.9	0.63	49.1
	07.04.2014	Folldal sentrum (30g)	30	4	1	1	1	1	23	Folldal sentrum (30g), 30 min	231	1.3	183	2.3	1.06	28.9
	07.04.2014	Folldal sentrum (5g)	60	4	1	1	1	1	24	Folldal sentrum (5g), 60 min	234	3.4	190	0.8	0.29	24.8
	07.04.2014	Folldal sentrum (10g)	60	4	1	1	1	1	25	Folldal sentrum (10g), 60 min	239	5.3	182	3.8	0.78	14.0
	07.04.2014	Folldal sentrum (30g)	60	4	1	1	1	1	26	Folldal sentrum (30g), 60 min	244	1.7	183	1.4	0.62	26.1
	07.04.2014	Folldal sentrum (5g)	120	4	1	1	1	1	27	Folldal sentrum (5g), 120 min	230	1.6	183	2.7	0.23	9.9
	07.04.2014	Folldal sentrum (10g)	120	4	1	1	1	1	28	Folldal sentrum (10g), 120 min	236	7.5	190	8.9	0.82	33.6
	07.04.2014	Folldal sentrum (30g)	120	4	1	1	1	1	29	Folldal sentrum (30g), 120 min	237	3.0	168	1.6	1.45	12.1
	07.04.2014	Folldal sentrum (5g)	180	4	1	1	1	1	30	Folldal sentrum (5g), 180 min	246	6.9	202	0.9	0.48	13.3
	07.04.2014	Folldal sentrum (10g)	180	4	1	1	1	1	31	Folldal sentrum (10g), 180 min	247	3.1	189	2.7	0.28	30.7
	07.04.2014	Folldal sentrum (30g)	180	4	1	1	1	1	32	Folldal sentrum (30g), 180 min	239	4.5	158	3.8	0.81	13.1
										Stop statistical calculations						
Forbehandling: Or										Average	306.808	4.3	358.894	3.2	2.52	13.6
	Ingen synlige partikler etter fortynning.									Min	226.871	0.9	158.347	0.7	0.19	1.7
										Max	417.238	9.1	552.967	10.5	6.17	49.1
Stop formulas				Stop formulas						Std	73.307	2.4	176.769	2.3	2.09	11.7
number		30	30	30	30	30	30		30	Rsd % <5, 5-10, >10	23.9		49.3		82.9	
Average				90						Confidence interval 95%	27.225	0.9	65.650	0.8	0.79	4.4
										Confidence interval 95% (%) <5, 5-10, >10	8.9		18.3		31.3	
										Number	30	30	30	30	29	29

Sn118(LR)		W182(LR)		Hg202(LR)		Pb208(LR)		U238(LR)		Li7(MR)		Na23(MR)		Mg25(MR)		Al27(MR)		Si29(MR)		P31(MR)		S34(MR)		K39(MR)	
Conc.		Conc.		Conc.		Conc.		Conc.		Conc.		Conc.		Conc.		Conc.		Conc.		Conc.		Conc.		Conc.	
µg/L	RSD, %	µg/L	RSD, %	µg/L	RSD, %	µg/L	RSD, %	µg/L	RSD, %	µg/L	RSD, %	µg/L	RSD, %	µg/L	RSD, %	µg/L	RSD, %	µg/L	RSD, %	µg/L	RSD, %	µg/L	RSD, %	µg/L	RSD, %
0.52	9.7	0.29	7.9	0.20	11.9	16.078	1.7	40.202	5.6	182.1	6.2	8 371	2.5	535 256	1.2	513 911	3.7	33 353	2.6	4 846	3.6	4 221 564	4.1	15 391	3.9
0.66	10.5	0.47	7.2	0.12	14.9	25.618	1.5	42.169	1.7	192.3	4.5	10 832	8.8	555 700	4.9	540 697	1.4	35 529	3.0	4 992	1.2	4 332 217	5.9	31 444	5.5
0.59	9.3	0.07	10.1	0.17	1.9	48.088	3.0	43.624	2.7	177.5	5.1	15 554	3.6	572 766	1.9	568 265	4.3	45 950	4.1	5 050	1.3	4 563 796	0.7	63 888	3.8
0.58	13.3	0.08	5.0	0.18	6.6	14.067	5.4	40.942	4.5	185.6	2.7	9 436	4.7	570 136	4.6	565 001	6.6	38 547	6.2	4 955	2.3	4 517 541	5.1	28 366	2.8
0.53	13.9	0.13	4.9	0.04	6.6	30.521	2.9	41.868	3.8	184.7	1.5	10 689	4.9	553 992	4.9	557 167	2.6	38 685	3.1	5 120	2.8	4 608 769	2.7	40 634	7.1
0.95	4.2	0.60	63.2	0.09	7.5	39.399	0.2	45.230	0.9	178.3	2.3	14 781	1.3	580 435	0.9	549 095	4.1	49 550	3.1	5 239	2.5	4 488 360	3.0	57 958	9.0
0.83	17.0	-0.07	6.0	0.11	2.7	12.645	3.3	39.741	1.7	187.0	4.2	9 238	1.5	529 659	3.9	542 442	2.4	40 171	1.0	4 967	2.1	4 542 483	4.9	32 737	1.6
0.74	6.6	0.03	18.6	0.09	12.0	25.215	3.1	40.788	2.7	178.7	2.7	10 999	3.5	536 384	2.3	563 398	0.9	45 725	7.5	5 005	0.6	4 611 065	3.1	41 525	4.2
0.65	5.6	0.07	14.1	0.07	9.9	42.758	2.7	49.168	9.3	170.3	2.0	17 397	3.3	567 151	3.5	551 036	2.0	53 930	6.6	5 063	1.9	4 707 777	2.2	67 219	3.9
0.78	3.7	0.03	4.7	0.08	6.2	18.090	55.7	40.196	0.9	190.4	3.0	10 492	4.0	572 132	2.4	578 247	6.7	52 351	8.0	5 106	2.0	4 807 936	1.9	39 059	5.7
0.93	7.1	0.04	9.0	0.13	14.3	31.481	5.1	43.296	0.2	180.4	3.2	12 356	5.3	558 876	1.8	570 211	0.3	53 339	3.7	5 141	2.3	4 800 422	4.0	56 432	3.6
0.66	4.9	0.14	25.3	0.12	2.3	59.835	4.1	52.990	6.1	162.5	2.3	19 681	2.6	560 532	2.9	601 631	2.1	77 485	6.3	5 172	1.5	4 834 800	2.7	123 898	5.6
1.93	7.0	0.12	26.7	0.01	10.9	10.155	3.9	43.142	7.1	189.8	1.7	11 038	3.1	610 184	4.1	553 181	2.6	55 959	13.1	5 132	1.1	4 889 041	0.2	43 519	0.9
0.78	9.4	-0.02	5.3	0.09	7.4	31.512	1.8	45.167	4.7	182.6	6.7	13 092	4.7	603 238	4.0	590 415	3.7	58 543	9.7	5 185	1.2	4 985 745	2.0	73 249	3.4
0.59	5.6	0.08	11.6	0.10	22.9	49.723	11.8	56.873	2.2	157.1	2.6	20 926	2.8	581 015	3.1	564 624	6.6	79 844	3.5	4 664	3.4	4 848 156	3.4	99 736	3.0
0.07	16.7	-0.06	14.2	0.07	15.9	7.212	3.9	11.235	2.3	75.9	5.8	5 600	7.4	267 060	6.4	202 710	1.4	31 178	1.6	1 309	2.3	1 892 379	2.8	15 532	2.3
0.14	3.0	-0.02	5.9	0.10	5.6	17.431	58.0	11.758	2.3	74.6	2.7	7 061	7.3	255 055	4.7	199 613	1.2	35 671	3.5	1 270	3.5	1 846 896	1.2	24 557	2.1
0.60	13.2	0.63	32.3	0.03	14.1	28.480	3.6	15.273	6.1	74.7	6.8	12 036	2.8	262 488	3.4	227 726	0.6	56 505	5.2	1 286	4.2	1 907 223	1.3	64 457	5.5
0.20	16.9	0.09	40.0	0.05	3.0	7.069	1.8	11.454	1.1	77.4	2.2	5 933	1.9	265 719	1.2	203 000	2.8	32 392	9.5	1 272	2.4	1 902 678	1.1	18 838	1.2
0.37	10.0	0.11	21.0	0.00	16.0	12.273	7.5	11.983	3.1	72.8	4.1	7 437	1.7	260 663	5.6	200 806	4.8	43 711	12.5	1 270	1.3	1 770 317	3.1	31 826	7.2
0.58	4.1	0.70	43.7	0.05	7.1	24.806	2.3	24.072	54.3	71.7	5.5	13 512	2.2	256 548	4.1	216 622	5.3	68 314	13.2	1 202	1.6	1 845 975	4.0	64 523	1.8
0.17	11.0	0.03	7.7	0.01	10.5	7.870	2.3	11.951	2.0	74.3	2.8	6 970	1.3	278 010	1.1	200 135	3.8	36 530	7.5	1 291	0.5	1 897 124	1.8	24 054	2.7
0.45	17.6	0.30	10.7	0.00	16.3	13.355	1.3	13.374	3.7	76.3	4.4	8 611	2.2	268 756	3.3	212 827	2.9	51 232	7.3	1 340	0.5	1 868 129	2.4	38 332	5.1
0.66	14.5	0.10	25.0	0.03	13.2	20.990	4.2	18.732	2.6	68.2	12.6	15 319	6.1	259 226	2.5	207 628	2.8	72 853	3.5	1 014	4.0	1 906 730	4.8	69 326	3.2
0.22	11.9	0.01	16.7	0.03	10.2	7.297	8.9	11.988	3.5	73.9	1.2	7 228	3.6	257 091	3.9	198 660	4.0	33 992	0.9	1 200	1.5	1 806 016	5.6	26 984	1.4
0.35	14.2	0.01	29.7	0.11	13.8	18.708	3.4	14.661	2.5	71.1	5.6	10 184	3.3	271 493	4.3	222 883	3.8	59 028	2.8	1 228	1.7	1 905 774	3.6	56 768	1.9
0.54	17.5	0.06	13.9	0.06	19.0	48.020	3.0	23.849	1.0	66.6	1.5	17 899	0.9	256 504	3.4	241 242	2.5	91 406	4.7	856	1.1	1 830 661	3.5	135 695	4.4
0.16	9.4	0.05	21.3	0.03	4.3	8.393	1.6	12.952	2.3	74.4	1.8	8 332	2.7	269 906	3.0	200 631	1.2	42 073	6.9	1 217	2.0	1 957 733	0.8	64 545	4.1
0.51	11.4	0.07	17.5	-0.01	11.0	14.917	5.9	15.830	1.7	73.3	2.3	10 973	2.1	274 163	4.9	209 352	6.4	67 676	6.9	1 065	2.4	1 875 493	3.6	54 092	5.5
0.67	16.4	0.17	24.6	0.02	11.8	23.870	3.8	26.181	3.3	61.2	2.9	17 947	3.8	254 761	1.7	197 763	1.2	88 543	12.0	426	15.2	1 833 855	1.0	72 377	1.5
0.580	10.5	0.143	18.1	0.072	10.3	23.862	7.3	30.023	4.9	126.19	3.8	11 664	3.5	414 830	3.3	385 030.6	3.2	52 336	6.0	3 096.1	2.5	3 260 222	2.9	52 565	3.8
0.069	3.0	-0.073	4.7	-0.015	1.9	7.069	0.2	11.235	0.2	61.19	1.2	5 600	0.9	254 761	0.9	197 762.5	0.3	31 178	0.9	426.1	0.5	1 770 317	0.2	15 391	0.9
1.930	17.6	0.699	63.2	0.196	22.9	59.835	58.0	56.873	54.3	192.33	12.6	20 926	8.8	610 184	6.4	601 631.2	6.7	91 406	13.2	5 239.2	15.2	4 985 745	5.9	135 695	9.0
0.346	4.6	0.201	13.6	0.055	5.2	14.566	13.7	15.404	9.6	55.21	2.3	4 171	1.9	154 492	1.4	179 415.3	1.9	17 025	3.6	1 989.1	2.6	1 422 418	1.5	29 296	2.0
59.6		140.5		75.8		61.0		51.3		43.7		35.8		37.2		46.6		32.5		64.2		43.6		55.7	
0.128	1.7	0.075	5.0	0.020	1.9	5.410	5.1	5.721	3.5	20.50	0.9	1 549	0.7	57 377	0.5	66 633.2	0.7	6 323	1.3	738.7	1.0	528 273	0.6	10 880	0.7
22.1		52.2		28.2		22.7		19.1		16.2		13.3		13.8		17.3		12.1		23.9		16.2		20.7	
30	30	30	30	30	30	30	30	30	30	30	30	30	30	30	30	30	30	30	30	30	30	30	30	30	30

Ca44(MR) Conc.		Cr52(MR) Conc.		Mn55(MR) Conc.		Fe57(MR) Conc.		Co59(MR) Conc.		Ni60(MR) Conc.		Cu63(MR) Conc.		Zn66(MR) Conc.		Sr88(MR) Conc.		Ag109(MR) Conc.		Sb121(MR) Conc.	
µg/L	RSD, %	µg/L	RSD, %	µg/L	RSD, %	µg/L	RSD, %	µg/L	RSD, %	µg/L	RSD, %	µg/L	RSD, %	µg/L	RSD, %	µg/L	RSD, %	µg/L	RSD, %	µg/L	RSD, %
280 726	1.8	756	2.8	16 180	1.9	2 282 323	3.7	9 078	4.4	1 051	0.6	143 643	3.9	131 732	7.2	505	2.4	0.17	37.1	0.88	27.5
315 884	4.1	783	6.3	16 831	3.4	2 329 081	1.7	8 461	4.7	1 086	3.0	152 953	3.5	129 951	3.3	665	4.0	0.44	18.0	0.75	24.9
409 708	2.6	817	8.2	18 896	2.0	2 248 374	1.8	9 323	3.6	1 128	2.1	145 962	4.6	135 803	3.6	1 145	3.3	0.11	26.1	0.76	26.2
302 717	3.9	759	1.5	17 598	3.7	2 342 684	1.0	8 935	1.9	1 129	2.1	157 981	3.0	133 182	1.5	621	3.5	0.17	24.5	0.72	22.7
341 490	4.7	791	3.8	17 943	2.3	2 395 385	4.2	8 801	3.6	1 126	3.1	157 958	3.7	132 093	6.1	790	5.9	0.19	13.3	0.66	10.5
464 593	4.7	779	4.6	19 840	1.5	2 326 420	1.3	8 875	4.6	1 150	4.1	140 917	2.9	129 446	2.1	1 195	5.1	0.12	25.0	0.77	30.0
307 518	2.1	783	3.3	16 917	1.9	2 402 618	5.7	8 826	2.0	1 154	2.4	152 266	5.6	129 585	4.8	710	1.0	0.19	11.5	0.60	5.4
355 710	3.9	780	1.5	17 958	5.3	2 420 259	2.8	9 115	3.4	1 117	5.5	152 083	4.0	129 601	1.1	913	2.8	0.24	39.9	0.78	8.1
585 834	1.0	759	3.4	19 909	4.7	2 311 225	3.6	8 572	2.4	1 150	1.9	149 576	1.4	125 262	0.7	1 644	1.3	0.20	48.1	0.68	37.4
341 610	4.0	808	2.6	17 436	2.6	2 532 701	3.0	9 376	2.8	1 178	2.7	152 714	0.6	135 600	3.3	824	0.6	0.21	47.0	0.67	26.7
404 338	4.5	788	1.7	18 549	2.8	2 450 890	1.5	9 280	0.7	1 118	1.4	162 313	2.9	132 691	2.2	1 196	2.5	0.16	25.8	0.91	4.7
718 658	2.8	771	3.6	21 540	3.6	2 177 304	3.8	8 657	4.8	1 128	2.2	144 214	1.7	124 167	2.9	2 631	3.5	0.19	12.4	0.77	19.9
359 113	4.2	803	6.9	17 817	3.9	2 559 327	4.1	9 002	4.7	1 170	4.6	162 518	4.2	136 136	0.8	933	2.4	0.16	31.9	0.64	17.4
452 554	5.5	780	1.3	18 819	1.9	2 531 681	5.3	9 195	0.8	1 192	1.3	158 620	2.5	134 632	2.2	1 475	2.0	0.25	24.2	0.65	29.8
801 938	6.1	745	3.2	22 106	2.9	2 015 883	1.7	8 751	1.5	1 143	6.0	141 840	1.8	121 441	3.1	2 725	1.7	0.17	22.9	0.71	22.7
200 417	3.1	494	3.9	7 609	4.6	859 100	3.8	1 691	3.3	633	2.1	75 059	3.5	55 263	2.5	326	4.5	0.09	36.1	0.42	25.2
232 211	3.5	480	1.0	7 571	2.9	822 268	1.7	1 702	0.2	647	1.0	70 177	4.9	53 001	3.8	433	2.3	0.10	31.1	0.23	4.9
325 385	3.4	476	3.8	7 941	3.3	749 498	3.7	1 632	3.4	643	3.9	68 469	2.3	52 103	1.0	1 005	2.2	0.18	11.2	0.44	64.4
213 951	1.8	493	1.2	7 629	0.6	842 967	3.3	1 724	3.5	650	1.0	71 157	3.5	53 771	2.1	364	4.6	0.04	32.8	0.20	64.4
250 954	3.4	485	1.8	7 336	2.6	823 916	3.6	1 615	1.1	640	3.5	69 392	2.6	52 597	3.5	529	0.9	0.02	67.3	0.44	7.9
387 827	3.7	469	3.7	7 869	0.7	708 867	1.6	1 623	3.8	598	1.8	66 369	1.6	48 387	3.2	1 169	1.0	54.24	171.9	0.37	22.7
237 652	1.4	511	1.8	7 803	3.3	865 783	6.6	1 714	4.1	661	2.0	72 440	2.5	54 056	1.6	413	3.4	0.07	50.9	0.36	60.1
275 104	3.3	488	0.8	8 183	2.2	812 628	0.7	1 696	3.0	645	4.1	71 338	2.5	51 180	3.8	656	3.6	0.19	33.0	0.34	31.1
493 305	4.3	447	3.0	8 193	2.7	638 521	5.4	1 572	3.5	608	2.6	62 238	7.8	47 689	4.6	1 458	1.9	0.21	46.7	0.70	7.5
245 051	5.2	466	5.1	7 387	1.7	831 667	4.7	1 607	0.9	635	2.5	67 912	0.8	51 714	1.1	464	1.6	0.07	48.4	0.35	35.9
329 378	4.1	477	2.1	7 585	2.1	756 584	1.8	1 649	2.5	660	4.2	70 072	4.3	51 831	2.9	956	1.9	0.16	48.0	0.32	6.2
635 465	4.9	394	4.3	8 945	0.4	462 650	7.3	1 437	2.9	586	2.2	54 852	1.5	43 423	2.9	2 456	0.9	0.13	57.1	0.44	6.8
268 094	0.8	497	3.1	7 965	0.5	798 865	1.8	1 750	4.6	663	1.1	71 159	1.7	54 915	3.0	513	1.8	15.12	3.3	0.19	57.0
357 158	2.9	470	4.2	7 891	1.7	725 545	5.1	1 726	2.1	629	2.8	67 251	1.4	51 945	4.1	957	2.2	0.17	26.3	0.48	28.9
730 031	6.8	362	2.7	10 487	2.6	286 157	1.3	1 443	2.3	580	1.9	53 046	2.9	41 625	1.2	1 957	1.2	0.08	22.3	0.50	43.5
387 479	3.6	623.68	3.2	13 291.1	2.5	1 543 705.7	3.3	5 294.26	2.9	883.35	2.7	109 549.61	3.0	90 827.4	2.9	1 054.23	2.5	2.461	36.5	0.557	26.0
200 417	0.8	362.23	0.8	7 335.6	0.4	286 156.7	0.7	1 436.86	0.2	580.36	0.6	53 045.81	0.6	41 624.7	0.7	325.58	0.6	0.016	3.3	0.188	4.7
801 938	6.8	816.96	8.2	22 105.7	5.3	2 559 326.7	7.3	9 375.68	4.8	1 192.10	6.0	162 517.59	7.8	136 135.7	7.2	2 724.91	5.9	54.241	171.9	0.906	64.4
160 124	1.4	162.15	1.8	5 509.1	1.2	838 796.3	1.8	3 723.68	1.3	257.51	1.3	43 382.63	1.5	40 819.1	1.5	659.85	1.4	10.154	29.7	0.206	17.7
41.3		26.0		41.4		54.3		70.3		29.2		39.6		44.9		62.6		412.6		36.9	
59 468	0.5	60.22	0.7	2 046.0	0.5	311 521.1	0.7	1 382.94	0.5	95.64	0.5	16 111.90	0.6	15 159.8	0.6	245.06	0.5	3.771	11.0	0.076	6.6
15.3		9.7		15.4		20.2		26.1		10.8		14.7		16.7		23.2		153.3		13.7	
30	30	30	30	30	30	30	30	30	30	30	30	30	30	30	30	30	30	30	30	30	30

Date of analyses: 25.04.14 sekvens 27														
Counting digits = 3														
Isotope	Pb208(LR)		U238(LR)		Fe56(MR)		Fe57(MR)		Ni60(MR)		Cu63(MR)		Zn66(MR)	
Parameteres	Conc.		Conc.		Conc.		Conc.		Conc.		Conc.		Conc.	
Sample ID	µg/L	RSD, %	µg/L	RSD, %	µg/L	RSD, %	µg/L	RSD, %	µg/L	RSD, %	µg/L	RSD, %	µg/L	RSD, %
Start statistical calculations														
Folldal sentrum (0min)	<0.05	17.1	0.169	7.7	4 393	2.5	5 129	2.5	610	1.8	4 347	5.7	44 294	1.9
Folldal sentrum (7,5min)	33.42	4.6	2.417	27.8	6 936	1.2	7 806	6.0	545	1.5	3 160	3.2	39 505	2.5
Folldal sentrum (15min)	33.09	4.6	2.265	6.2	7 570	1.0	8 303	5.7	509	2.2	2 955	1.8	37 877	0.7
Folldal sentrum (30min)	50.40	0.7	3.136	5.3	7 393	1.9	7 442	3.7	480	1.3	2 445	5.6	35 412	1.9
Folldal sentrum (60min)	14.18	3.0	1.043	17.1	2 801	6.0	3 302	8.1	499	2.9	2 178	2.3	35 006	4.0
Løkken verk (0min)	0.51	3.3	0.295	4.4	45 580	1.4	48 141	3.7	634	0.3	2 221	3.4	56 804	2.3
Løkken verk (7,5min)	21.35	4.5	1.416	5.5	19 763	2.5	22 959	6.8	531	1.3	1 587	2.8	45 792	0.8
Løkken verk (15min)	20.66	3.2	1.965	20.7	17 795	1.0	20 335	5.5	507	1.7	1 435	2.4	44 122	0.6
Løkken verk (30min)	10.91	6.3	1.498	25.7	16 083	1.9	17 717	4.3	515	0.7	1 329	6.2	44 291	3.3
Løkken verk (60min)	61.06	2.1	3.993	3.9	14 961	3.6	16 047	2.1	479	1.5	1 224	3.3	42 488	1.2
Stop statistical calculations														
Average	27.287	4.9	1.820	12.4	14 327.5	2.3	15 718.0	4.8	530.84	1.5	2 287.95	3.7	42 559.0	1.9
Min	0.511	0.7	0.169	3.9	2 800.5	1.0	3 302.0	2.1	478.67	0.3	1 223.85	1.8	35 005.7	0.6
Max	61.063	17.1	3.993	27.8	45 580.2	6.0	48 140.8	8.1	633.58	2.9	4 346.80	6.2	56 803.7	4.0
Std	19.309	4.5	1.200	9.4	12 480.0	1.5	13 255.9	1.9	52.41	0.7	986.40	1.6	6 335.1	1.1
Rsd % <5, 5-10, >10	70.8		65.9		87.1		84.3		9.9		43.1		14.9	
Confidence interval 95%	13.653	3.0	0.800	6.3	8 320.0	1.0	8 837.2	1.3	34.94	0.5	657.60	1.1	4 223.4	0.8
Confidence interval 95% (%) <5, 5-10, >10	50.0		43.9		58.1		56.2		6.6		28.7		9.9	
Number	9	10	10	10	10	10	10	10	10	10	10	10	10	10

Date of analyses: 22.05.14 sekvens 32

Counting digits = 3

Lokalitet	Preservation	Elements	Cu	Fe	Pb	Zn	Isotope / Parameteres / Sample ID	Cd111(LR) Conc. µg/L	Cd111(LR) RSD, %	Mo98(MR) Conc. µg/L	Mo98(MR) RSD, %	Sn118(LR) Conc. µg/L	Sn118(LR) RSD, %	W182(LR) Conc. µg/L	W182(LR) RSD, %	Pb208(LR) Conc. µg/L	Pb208(LR) RSD, %	U238(LR) Conc. µg/L	U238(LR) RSD, %	Mg25(MR) Conc. µg/L	Mg25(MR) RSD, %
		Start formulas					Start statistical calculations														
Folldal center (f. utfelling)	0.1M HNO3	4	1	1	1	1	Anita-Kahn-50x-43-48-43	192	1.0	0.299	41.1	0.170	8.4	0.102	13.8	2.80	4.2	10.70	1.7	276 389	4.8
Folldal center (e. utfelling)	0.1M HNO3	4	1	1	1	1	Anita-Kahn-50x-43-48-44	125	2.3	0.275	43.7	0.124	42.7	0.032	16.7	0.00	7.3	0.07	7.5	261 965	1.3
Løkken verk (f. utfelling)	0.1M HNO3	4	1	1	1	1	Anita-Kahn-50x-43-48-45	549	2.4	1.143	14.7	0.550	11.4	0.125	22.0	4.71	4.1	41.32	3.5	604 391	3.0
Løkken verk (e. utfelling)	0.1M HNO3	0					Anita-Kahn-50x-43-48-46	305	3.9	0.368	35.6	0.036	41.6	0.023	35.9	<0.05	4.1	0.12	9.5	535 897	3.9
Folldal center (Fe2+ or Fe3+)	0.1M HNO3	0					Anita-Kahn-50x-43-48-47	192	2.3	0.370	62.5	0.035	11.8	0.056	23.6	2.70	8.4	11.02	1.7	278 385	3.1
Løkken works (Fe2+ or Fe3+)	0.1M HNO3	0					Anita-Kahn-50x-43-48-48	578	1.7	1.251	14.0	0.523	2.6	0.124	21.6	4.71	1.5	41.64	0.6	615 807	2.5
		0					Stop statistical calculations														
fortynnet 50x og rekonservert med 0.12M HNO3.							Average	323.4788	2.3	0.618	35.3	0.240	19.8	0.0770	22.3	2.985	4.9	17.4780	4.1	428 806	3.1
							Min	124.7648	1.0	0.275	14.0	0.035	2.6	0.0233	13.8	0.004	1.5	0.0671	0.6	261 965	1.3
		Stop formulas					Max	578.1261	3.9	1.251	62.5	0.550	42.7	0.1248	35.9	4.711	8.4	41.6447	9.5	615 807	4.8
6	6	7	3	3	3		Std	195.1544	1.0	0.451	18.6	0.236	17.7	0.0460	7.6	1.933	2.5	19.2075	3.6	173 759	1.2
		9					Rsd % <5, 5-10, >10	60.3		73.1		98.4		59.7		64.8		109.9		40.5	
							Confidence interval 95%	174.5514	0.9	0.404	16.6	0.211	15.8	0.0411	6.8	1.933	2.2	17.1798	3.2	155 415	1.1
							Confidence interval 95% (%) <5, 5-10, >10	54.0		65.4		88.1		53.4		64.8		98.3		36.2	
							Number	6	6	6	6	6	6	6	6	5	6	6	6	6	6

Al27(MR) Conc. µg/L	Al27(MR) RSD, %	Si29(MR) Conc. µg/L	Si29(MR) RSD, %	S34(MR) Conc. µg/L	S34(MR) RSD, %	Cl35(MR) Conc. µg/L	Cl35(MR) RSD, %	Ca44(MR) Conc. µg/L	Ca44(MR) RSD, %	Mn55(MR) Conc. µg/L	Mn55(MR) RSD, %	Fe57(MR) Conc. µg/L	Fe57(MR) RSD, %	Cu63(MR) Conc. µg/L	Cu63(MR) RSD, %	Zn66(MR) Conc. µg/L	Zn66(MR) RSD, %	Sr88(MR) Conc. µg/L	Sr88(MR) RSD, %	Ag109(MR) Conc. µg/L	Ag109(MR) RSD, %
203 430	2.4	27 939	5.4	1 890 961	2.1	1 163	4.3	186 182	5.3	7 858	1.5	864 288	2.0	76 675	3.5	54 861	0.5	232	1.8	0.110	21.7
362	1.0	5 617	4.3	1 745 886	1.2	4 569	1.4	176 483	6.5	5 765	1.3	1 787	0.9	916	4.8	19 022	1.4	218	1.6	0.124	28.9
581 235	4.1	30 694	1.3	4 982 156	3.6	2 662	1.8	286 191	0.9	18 794	3.9	2 856 046	1.6	176 002	0.8	141 229	3.3	434	1.4	0.168	65.0
210	4.3	3 257	0.4	4 347 964	2.2	7 235	6.3	239 625	4.8	12 757	1.0	859	5.3	942	2.2	32 744	2.7	381	3.2	0.116	36.7
205 135	1.5	27 862	1.3	1 949 694	2.3	1 431	4.3	183 417	3.6	7 701	3.1	869 118	1.8	79 631	2.9	56 186	2.8	227	3.5	0.168	33.1
582 133	1.8	31 026	1.9	5 205 725	0.8	7 104	6.5	280 675	5.4	18 330	3.5	2 834 472	0.7	174 375	2.4	141 706	1.5	433	4.8	0.123	44.1
262 084.27	2.5	21 066	2.4	3 353 731	2.0	4 027	4.1	225 429	4.4	11 867.55	2.4	1 237 761.6	2.1	84 756.99	2.8	74 291.41	2.0	320.68	2.7	0.135	38.3
210.32	1.0	3 257	0.4	1 745 886	0.8	1 163	1.4	176 483	0.9	5 765.34	1.0	859.3	0.7	915.63	0.8	19 022.39	0.5	217.93	1.4	0.110	21.7
582 133.28	4.3	31 026	5.4	5 205 725	3.6	7 235	6.5	286 191	6.5	18 794.30	3.9	2 856 046.1	5.3	176 002.02	4.8	141 705.81	3.3	433.84	4.8	0.168	65.0
263 836.64	1.4	12 970	2.0	1 659 297	1.0	2 715	2.2	50 293	2.0	5 678.24	1.3	1 303 938.0	1.7	78 106.28	1.3	53 873.12	1.1	106.07	1.3	0.026	15.1
100.7		61.6		49.5		67.4		22.3		47.8		105.3		92.2		72.5		33.1		19.3	
235 982.66	1.2	11 601	1.8	1 484 120	0.9	2 429	1.9	44 983	1.8	5 078.77	1.1	1 166 277.6	1.5	69 860.38	1.2	48 185.58	1.0	94.87	1.2	0.023	13.5
90.0		55.1		44.3		60.3		20.0		42.8		94.2		82.4		64.9		29.6		17.3	
6	6	6	6	6	6	6	6	6	6	6	6	6	6	6	6	6	6	6	6	6	6

Appendix 4: Calculations for the kinetic studies

The results of the kinetic experiments were calculated by using Equation (23) from chapter 5.

$$\%\ adsorption = \frac{C_i - C_f}{C_i} \times 100 \qquad (23)$$

Folldal center

Tables 16, 17, 18 and 19 shows the calculations for the four different metals which dominated in the AMD from Folldal. Figure 15 shows the corresponding graphs for all the metals.

Table 16: Percentage adsorption of iron

Time [min]	Metalconc.,5g [mg/L]	adsorption [%]	Metalconc.,10g [mg/L]	adsorption [%]	Metalconc.,30g [mg/L]	adsorption [%]
0	869.1	0.0	869.1	0.0	869.1	0.0
15	859.1	1.2	822.3	5.4	749.5	13.8
30	843.0	3.0	823.9	5.2	708.9	18.4
60	865.8	0.4	812.6	6.5	638.5	26.5
120	831.7	4.3	756.6	12.9	462.6	46.8
180	798.9	8.1	725.5	16.5	286.2	67.1

Table 17: Percentage adsorption of copper

Time [min]	Metalconc.,5 g [mg/L]	adsorption [%]	Metalconc.,10 g [mg/L]	adsorption [%]	Metalconc.,30 g [mg/L]	adsorption [%]
0	79.6	0.0	79.6	0.0	79.6	0.0
15	75.1	5.7	70.2	11.9	68.5	14.0
30	71.2	10.6	69.4	12.9	66.4	16.7
60	72.4	9.0	71.3	10.4	62.2	21.8
120	67.9	14.7	70.1	12.0	54.9	31.1
180	71.2	10.6	67.3	15.5	53.0	33.4

Table 18: Percentage adsorption of zinc

Time [min]	Metalconc.,5 g [mg/L]	adsorption [%]	Metalconc.,10 g [mg/L]	adsorptio n [%]	Metalconc.,30 g [mg/L]	adsorption [%]
0	56.2	0.0	56.2	0.0	56.2	0.0
15	55.3	1.6	53.0	5.7	52.1	7.3
30	53.8	4.3	52.6	6.4	48.4	13.9
60	54.1	3.8	51.2	8.9	47.7	15.1
120	51.7	8.0	51.8	7.8	43.4	22.7
180	54.9	2.3	51.9	7.5	41.6	25.9

Table 19: Percentage adsorption of manganese

Time [min]	Metalconc.,5 g [mg/L]	adsorption [%]	Metalconc.,10 g [mg/L]	adsorption [%]	Metalconc.,30 g [mg/L]	adsorption [%]
0	7.7	0.0	7.7	0.0	7.7	0.0
15	7.6	1.2	7.6	1.7	7.9	-3.1
30	7.6	0.9	7.3	4.7	7.9	-2.2
60	7.8	-1.3	8.2	-6.3	8.2	-6.4
120	7.4	4.1	7.6	1.5	8.9	-16.2
180	8.0	-3.4	7.9	-2.5	10.5	-36.2

Løkken works

Tables 20, 21, 22 and 23 shows the calculations for the four different metals which dominated in the AMD from Løkken. Figure 16 shows the corresponding graphs for all the metals.

Table 20: Percentage adsorption of iron

Time [min]	Metalconc.,5 g [mg/L]	adsorption [%]	Metalconc.,10 g [mg/L]	adsorption [%]	Metalconc.,30 g [mg/L]	adsorption [%]
0	2 834.5	0.0	2 834.5	0.0	2 834.5	0.0
15	2 282.3	19.5	2 329.1	17.8	2 248.4	20.7
30	2 342.7	17.4	2 395.4	15.5	2 326.4	17.9
60	2 402.6	15.2	2 420.3	14.6	2 311.2	18.5
120	2 532.7	10.6	2 450.9	13.5	2 177.3	23.2
180	2 559.3	9.7	2 531.7	10.7	2 015.9	28.9

Table 21: Percentage adsorption of copper

Time [min]	Metalconc.,5 g [mg/L]	adsorption [%]	Metalconc.,10 g [mg/L]	adsorption [%]	Metalconc.,30 g [mg/L]	adsorption [%]
0	174.4	0.0	174.4	0.0	174.4	0.0
15	143.6	17.6	153.0	12.3	146.0	16.3
30	158.0	9.4	158.0	9.4	140.9	19.2
60	152.3	12.7	152.1	12.8	149.6	14.2
120	152.7	12.4	162.3	6.9	144.2	17.3
180	162.5	6.8	158.6	9.0	141.8	18.7

Table 22: Percentage adsorption of zinc

Time [min]	Metalconc.,5g [mg/L]	adsorption [%]	Metalconc.,10g [mg/L]	adsorption [%]	Metalconc.,30g [mg/L]	adsorption [%]
0	141.7	0.0	141.7	0.0	141.7	0.0
15	131.7	7.0	130.0	8.3	135.8	4.2
30	133.2	6.0	132.1	6.8	129.4	8.7
60	129.6	8.6	129.6	8.5	125.3	11.6
120	135.6	4.3	132.7	6.4	124.2	12.4
180	136.1	3.9	134.6	5.0	121.4	14.3

Table 23: Percentage adsorption of manganese

Time [min]	Metalconc.,5g [mg/L]	adsorption [%]	Metalconc.,10g [mg/L]	adsorption [%]	Metalconc.,30g [mg/L]	adsorption [%]
0	18.3	0.0	18.3	0.0	18.3	0.0
15	16.2	11.7	16.8	8.2	18.9	-3.1
30	17.6	4.0	17.9	2.1	19.8	-8.2
60	16.9	7.7	18.0	2.0	19.9	-8.6
120	17.4	4.9	18.5	-1.2	21.5	-17.5
180	17.8	2.8	18.8	-2.7	22.1	-20.6

Distribution ratio, K_d

The distribution ratio was calculated by using Equation (24):

$$K_d = \frac{amount\ of\ metal\ in\ adsorbent}{amount\ of\ metal\ in\ solution} \times \frac{V}{m} = \frac{q_e}{C_e} \qquad (24)$$

For both Folldal and Løkken the values for 30 g of clinoptilolite have been examined. The results can be seen from Tables 24 and 25, and Figures 17 and 18. Since there are large differences in the concentrations in the first 15 minutes, these values had been excluded in the figures.

Table 24: Variation of metal ions on clinoptilolite as a function of initial concentration, Folldal center: m = 30,007g, V = 100- 75 ml, time 0-180 min

Time [min]	Volume [mL]	Fe^{3+} [mg/L]	$K_{d,Fe}$ [mL/g]	Cu^{2+} [mg/L]	$K_{d,Cu}$ [mL/g]	Zn^{2+} [mg/L]	$K_{d,Zn}$ [mL/g]	Mn^{2+} [mg/L]	$K_{d,Mn}$ [mL/g]
0	100	869.1	0.0	79.6	0.0	56.2	0.0	7.7	0.0
15	100	749.5	0.5	68.5	0.5	52.1	0.2	7.9	-0.1
30	95	708.9	0.7	66.4	0.6	48.4	0.5	7.9	-0.1
60	90	638.5	1.0	62.2	0.8	47.7	0.5	8.2	-0.2
120	85	462.6	2.3	54.9	1.2	43.4	0.8	8.9	-0.4
180	80	286.2	5.1	53.0	1.3	41.6	0.9	10.5	-0.7

Table 25: Variation of metal ions on clinoptilolite as a function of initial concentration, Løkken works: m = 30,013g, V = 100 - 75ml, time 0-180 min

Time [min]	Volume [mL]	Fe^{3+} [mg/L]	$K_{d,Fe}$ [mL/g]	Cu^{2+} [mg/L]	$K_{d,Cu}$ [mL/g]	Zn^{2+} [mg/L]	$K_{d,Zn}$ [mL/g]	Mn^{2+} [mg/L]	$K_{d,Mn}$ [mL/g]
0	100	2 834.5	0.0	174.4	0.0	141.7	0.0	18.3	0.0
15	100	2 248.4	0.9	146.0	0.6	135.8	0.1	18.9	-0.1
30	95	2 326.4	0.7	140.9	0.8	129.4	0.3	19.8	-0.2
60	90	2 311.2	0.7	149.6	0.5	125.3	0.4	19.9	-0.2
120	85	2 177.3	0.9	144.2	0.6	124.2	0.4	21.5	-0.4
180	80	2 015.9	1.1	141.8	0.6	121.4	0.4	22.1	-0.5

Analysis of the role of different exchangeable cations

The concentration reduction of the heavy metals was compared to the exchanged cations from the clinoptilolite, as seen from Tables 26 and 27, and Figure 19. The analysis was based on the values when 30 g of clinoptilolite was added to AMD.

Table 26: Dynamics of ion exchange of heavy metals with the clinoptilolite, Folldal center

Time [min]	Fe^{3+} [mg/L]	Cu^{2+} [mg/L]	Zn^{2+} [mg/L]	Mn^{2+} [mg/L]	K^{+} [mg/L]	Ca^{2+} [mg/L]	Mg^{2+} [mg/L]	Na^{+} [mg/L]
0	869.1	79.6	56.2	7.7	n.a.	n.a.	n.a.	n.a.
15	749.5	68.5	52.1	7.9	64.5	325.4	262.5	12.0
30	708.9	66.4	48.4	7.9	64.5	387.8	256.5	13.5
60	638.5	62.2	47.7	8.2	69.3	493.3	259.2	15.3
120	462.6	54.9	43.4	8.9	135.7	635.5	256.5	17.9
180	286.2	53.0	41.6	10.5	72.4	730.0	254.8	17.9

n.a.: data not available

Table 27: Dynamics of ion exchange of heavy metals with the clinoptilolite, Løkken works

Time [min]	Fe^{3+} [mg/L]	Cu^{2+} [mg/L]	Zn^{2+} [mg/L]	Mn^{2+} [mg/L]	K^{+} [mg/L]	Ca^{2+} [mg/L]	Mg^{2+} [mg/L]	Na^{+} [mg/L]
0	2 834.5	174.4	141.7	18.3	n.a.	n.a.	n.a.	n.a.
15	2 248.4	146.0	135.8	18.9	63.9	409.7	572.8	15.6
30	2 326.4	140.9	129.4	19.8	58.0	464.6	580.4	14.8
60	2 311.2	149.6	125.3	19.9	67.2	585.8	567.2	17.4
120	2 177.3	144.2	124.2	21.5	123.9	718.7	560.5	19.7
180	2 015.9	141.8	121.4	22.1	99.7	801.9	581.0	20.9

n.a.: data not available

Appendix 5: Calculation of the adsorption isotherms

Calculation of the isotherm parameters

To find the Langmuir and Freundlich isotherms for 30 g of clinoptilolite Equation (16) and (19) were used:

Langmuir:

$$q = q_{max}\frac{K_{ads}[A]}{1 + K_{ads}[A]} \qquad (16)$$

Freundlich:

$$q = K_f[A]^{1/n} \qquad (19)$$

To use Equation (16) and (19) the isotherm parameters needs to be determined. To determine these parameters the Langmuir and Freundlich isotherms were rearranged to a linear form, as seen from Equation (17) and (20):

Langmuir:

$$\frac{[A]}{q} = \frac{1}{K_{ads}q_{max}} + \frac{[A]}{q_{max}} \qquad (17)$$

Freundlich:

$$\log(q) = \log(K_f) + \left(\frac{1}{n}\right)\log([A]) \qquad (20)$$

The equation for the linear regression will be applied to find the parameters:

Langmuir isotherm parameters:

To find the isotherm parameters, C_A/q_A versus C_A was plotted against each other, along with a fitted linear regression. The Langmuir parameters were obtained by comparing Equation (17) with the results of the linear regression. The calculation of the parameters is as followed:

$$\frac{1}{q_{max}} = slope \qquad (17a)$$

$$\frac{1}{q_{max}K_{ads}} = intercept \qquad (17b)$$

Freundlich isotherm parameters

To find the isotherm parameters, *log* q_A versus *log [Me]* was plotted against each other, along with a fitted linear regression. The Freundlich parameters were obtained by comparing Equation (20) with the results of the linear regression. The calculation of the parameters is as followed:

$$\frac{1}{n} = slope \qquad (20a)$$

$$\log K_f = intercept \qquad (20b)$$

Calculation of the adsorption isotherms

The Langmuir and Freundlich isotherms will be calculated by using Equation (16) and (19). These two isotherms will be compared to the isotherm of the experimental data, which is found by the use of Equation (22):

$$q_e = \frac{V}{M}(C_i - C_e) \qquad (22)$$

Figure 21 shows the result from Folldal and Figure 22 the results from Løkken.

Folldal center:

Calculation of the isotherm parameters

Iron:

Table 28: Calculation of isotherm parameters, iron

Time [min]	Mass [g]	Volume [L]	$[Fe^{3+}]$ [mg/L]	q_A [mg/g]	$[Fe^{3+}]/q_A$ [L/g]	log $[Fe^{3+}]$	log q_A
0	30.007	0.100	869.118	0.000	n.a.	2.939	n.a.
15	30.007	0.100	749.498	0.399	1880.132	2.875	-0.399
30	30.007	0.095	708.867	0.534	1327.356	2.851	-0.272
60	30.007	0.090	638.521	0.768	830.889	2.805	-0.114
120	30.007	0.085	462.650	1.355	341.545	2.665	0.132
180	30.007	0.080	286.157	1.943	147.294	2.457	0.288

n.a.: data not available

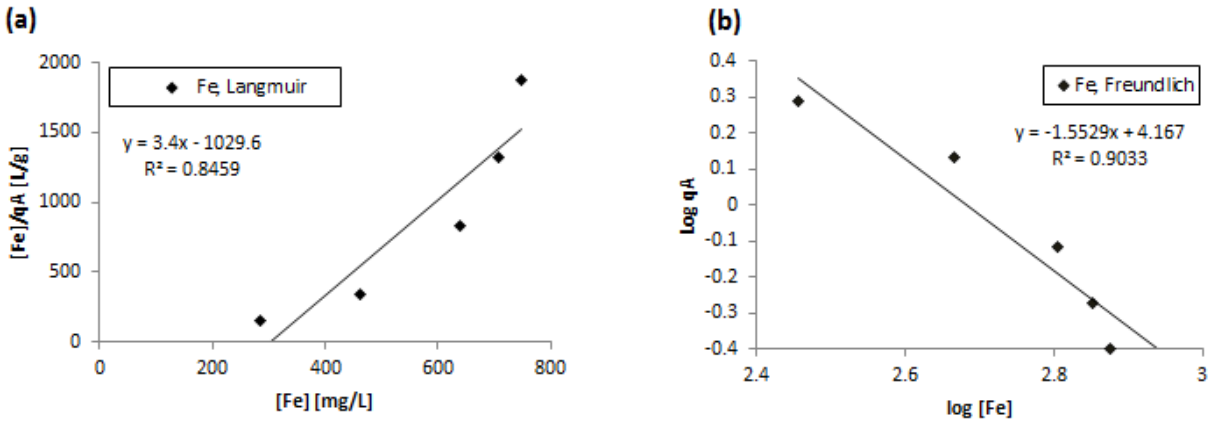

Figure 25: Linear regression to find isotherm parameters, iron

Copper:

Table 29: Calculation of isotherm parameters, copper

Time [min]	Mass [g]	Volume [L]	$[Cu^{2+}]$ [mg/L]	q_A [mg/g]	$[Cu^{2+}]/q_A$ [L/g]	log $[Cu^{2+}]$	log q_A
0	30.007	0.100	79.631	0.000	n.a.	1.901	n.a.
15	30.007	0.100	68.469	0.037	1840.579	1.835	-1.429
30	30.007	0.095	66.369	0.044	1501.632	1.822	-1.355
60	30.007	0.090	62.238	0.058	1073.747	1.794	-1.237
120	30.007	0.085	54.852	0.083	664.230	1.739	-1.083
180	30.007	0.080	53.046	0.089	598.728	1.725	-1.053

n.a.: data not available

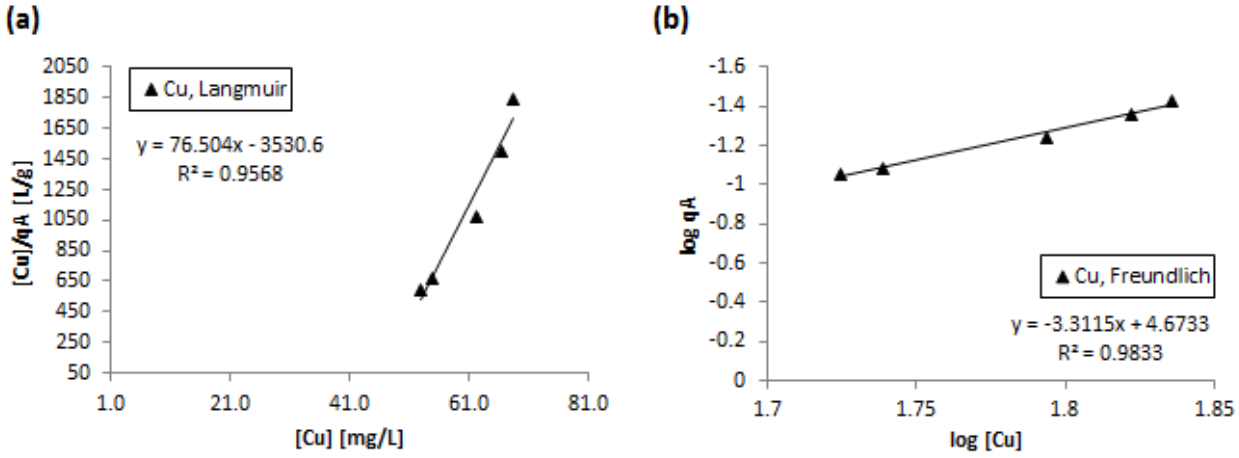

Figure 26: Linear regression to find isotherm parameters, copper

Zinc:

Table 30: Calculation of isotherm parameters, zinc

Time [min]	Mass [g]	Volume [L]	$[Zn^{2+}]$ [mg/g]	q_A [mg/g]	$[Zn^{2+}]/q_A$ [L/g]	log $[Zn^{2+}]$	log q_A
0	30.007	0.100	56.186	0.000	n.a.	1.750	n.a.
15	30.007	0.100	52.103	0.014	3829.381	1.717	-1.866
30	30.007	0.095	48.387	0.026	1861.762	1.685	-1.585
60	30.007	0.090	47.689	0.028	1684.146	1.678	-1.548
120	30.007	0.085	43.423	0.043	1020.936	1.638	-1.371
180	30.007	0.080	41.625	0.049	857.768	1.619	-1.314

n.a.: data not available

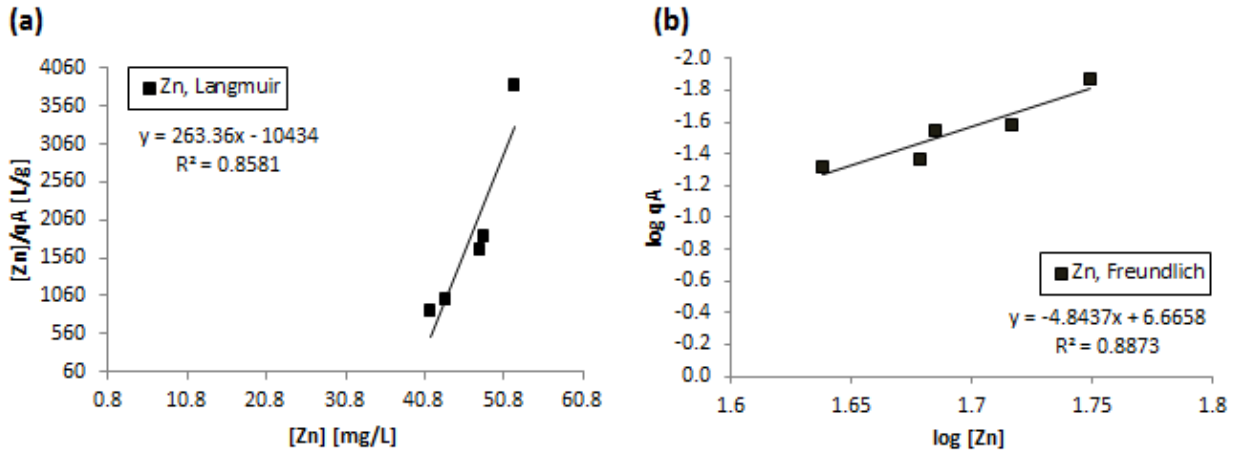

Figure 27: Linear regression to find isotherm parameters, zinc

Manganese:

Table 31: Calculation of isotherm parameters, manganese

Time [min]	Mass [g]	Volume [L]	$[Mn^{2+}]$[mg/L]	q_A [mg/g]	$[Mn^{2+}]/q_A$ [L/g]	log $[Mn^{2+}]$	log q_A
0	30.007	0.100	7.701	0.000	n.a.	0.887	n.a.
15	30.007	0.100	7.941	-0.001	-9929.160	0.900	n.a.
30	30.007	0.095	7.869	-0.001	-13993.128	0.896	n.a.
60	30.007	0.090	8.193	-0.002	-4995.187	0.913	n.a.
120	30.007	0.085	8.945	-0.004	-2156.773	0.952	n.a.
180	30.007	0.080	10.487	-0.009	-1129.419	1.021	n.a.

n.a.: data not available

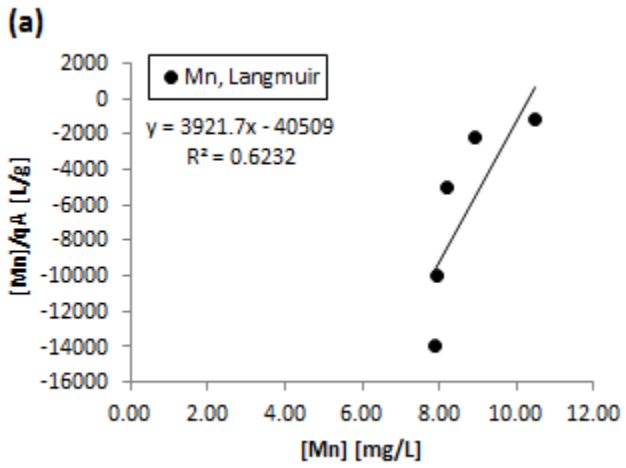

Figure 28: Linear regression to find isotherm parameters, manganese

The isotherm parameters for Folldal center can be seen in Table 6.

Calculation of the adsorption isotherms

Iron:

Table 32: Calculation of adsorption isotherms, iron

Time [min]	Mass [g]	Volume [L]	$[Fe^{3+}]$ [mg/L]	q_e	$q_{Langmuir}$	$q_{Freundlich}$
0	30.007	0.100	869.118	0.000	0.451	0.401
15	30.007	0.100	749.498	0.399	0.494	0.504
30	30.007	0.095	708.867	0.507	0.513	0.550
60	30.007	0.090	638.521	0.692	0.559	0.647
120	30.007	0.085	462.650	1.151	0.851	1.067
180	30.007	0.080	286.157	1.554	-5.050	2.250

Copper:

Table 33: Calculation of adsorption isotherms, copper

Time [min]	Mass [g]	Volume [L]	$[Cu^{2+}]$ [mg/L]	q_e	$q_{Langmuir}$	$q_{Freundlich}$
0	30.007	0.100	79.631	0.0000	0.0311	0.0239
15	30.007	0.100	68.469	0.0372	0.0401	0.0394
30	30.007	0.095	66.369	0.0420	0.0429	0.0436
60	30.007	0.090	62.238	0.0522	0.0506	0.0540
120	30.007	0.085	54.852	0.0702	0.0824	0.0820
180	30.007	0.080	53.046	0.0709	0.1005	0.0916

Zinc:

Table 34: Calculation of adsorption isotherms, zinc

Time [min]	Mass [g]	Volume [L]	$[Zn^{2+}]$ [mg/L]	q_e	$q_{Langmuir}$	$q_{Freundlich}$
0	30.007	0.100	56.186	0.00000	0.01288	0.01552
15	30.007	0.100	52.103	0.01361	0.01585	0.02237
30	30.007	0.095	48.387	0.02469	0.02095	0.03201
60	30.007	0.090	47.689	0.02548	0.02244	0.03434
120	30.007	0.085	43.423	0.03615	0.04334	0.05407
180	30.007	0.080	41.625	0.03882	0.07879	0.06637

Manganese:

Table 35: Calculation of adsorption isotherms, manganese

Time [min]	Mass [g]	Volume [L]	[Mn2+][mg/L]	q_e	$q_{Langmuir}$	$q_{Feundlich}$
0	30.007	0.100	7.701	0.00000	0.00011	n.a.
15	30.007	0.100	7.941	-0.00080	0.00011	n.a.
30	30.007	0.095	7.869	-0.00053	0.00011	n.a.
60	30.007	0.090	8.193	-0.00148	0.00011	n.a.
120	30.007	0.085	8.945	-0.00353	0.00012	n.a.
180	30.007	0.080	10.487	-0.00743	0.00013	n.a.

n.a.: data not available

Løkken works:

Calculation of the isotherm parameters

Iron:

Table 36: Calculation of the isotherm parameters, iron

Time [min]	Mass [g]	Volume [L]	$[Fe^{3+}]$ [mg/L]	q_A [mg/g]	$[Fe^{3+}]/q_A$ [L/g]	log $[Fe^{3+}]$	log q_A
0	30.013	0.100	2834.472	0.000	n.a.	3.452	n.a.
15	30.013	0.100	2248.374	1.953	1151.350	3.352	0.291
30	30.013	0.095	2326.420	1.693	1374.325	3.367	0.229
60	30.013	0.090	2311.225	1.743	1325.698	3.364	0.241
120	30.013	0.085	2177.304	2.190	994.379	3.338	0.340
180	30.013	0.080	2015.883	2.727	739.110	3.304	0.436

n.a.: data not available

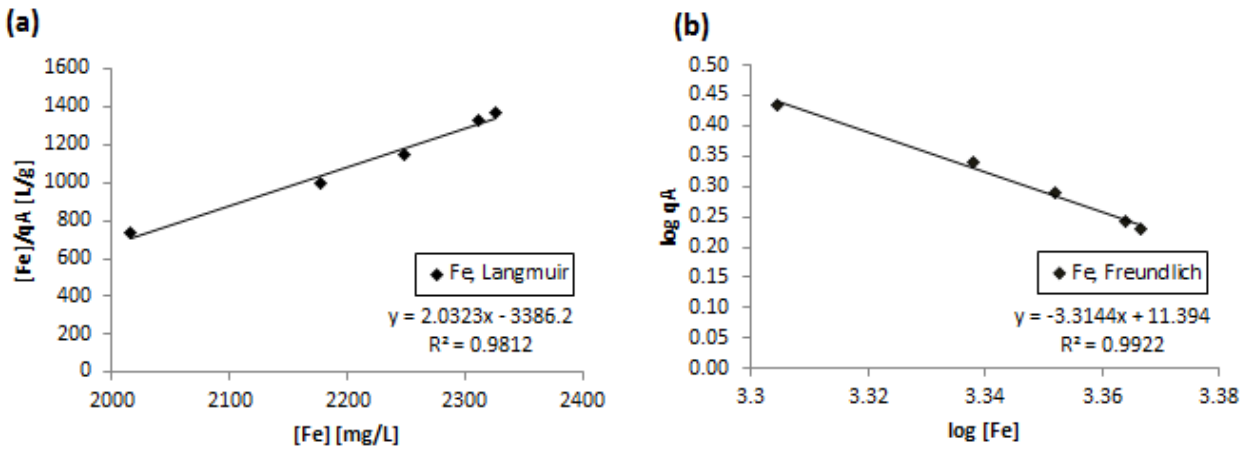

Figure 29: Linear regression to find isotherm parameters, iron

Copper:

Table 37: Calculation of isotherm parameters, copper

Time [min]	Mass [g]	Volume [L]	$[Cu^{2+}]$ [mg/L]	q_A [mg/g]	$[Cu^{2+}]/q_A$ [L/g]	log $[Cu^{2+}]$	log q_A
0	30.013	0.100	174.375	0.000	n.a.	2.241	n.a.
15	30.013	0.100	145.962	0.095	1541.772	2.164	-1.024
30	30.013	0.095	140.917	0.111	1264.041	2.149	-0.953
60	30.013	0.090	149.576	0.083	1810.232	2.175	-1.083
120	30.013	0.085	144.214	0.100	1435.026	2.159	-0.998
180	30.013	0.080	141.840	0.108	1308.445	2.152	-0.965

n.a.: data not available

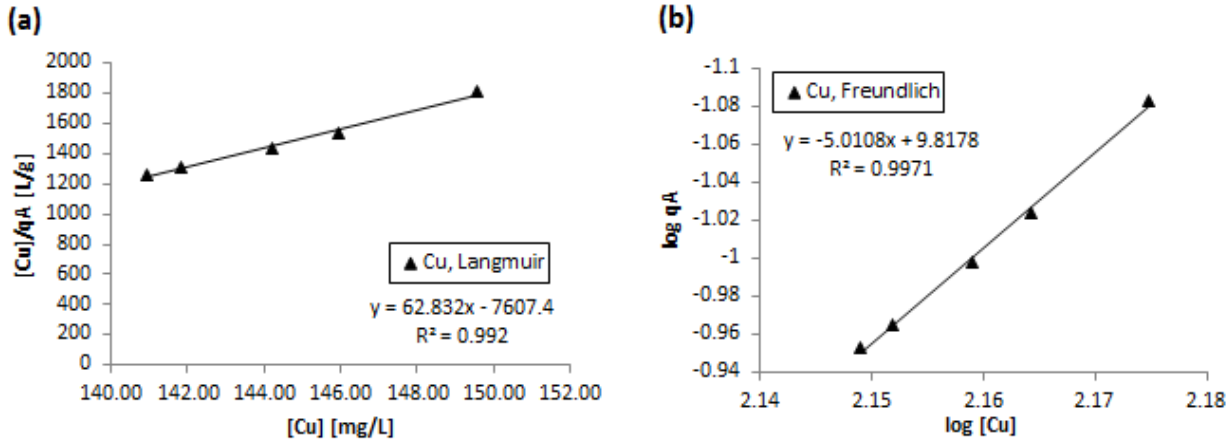

Figure 30: Linear regression to find isotherm parameters, copper

Zinc:

Table 38: Calculation of isotherm parameters, zinc

Time [min]	Mass [g]	Volume [L]	$[Zn^{2+}]$ [mg/g]	q_A [mg/g]	$[Zn^{2+}]/q_A$ [L/g]	log $[Zn^{2+}]$	log q_A
0	30.013	0.100	141.706	0.000	n.a	2.151	n.a.
15	30.013	0.100	135.803	0.020	6904.460	2.133	-1.706
30	30.013	0.095	129.446	0.041	3168.963	2.112	-1.389
60	30.013	0.090	125.262	0.055	2286.319	2.098	-1.261
120	30.013	0.085	124.167	0.058	2124.748	2.094	-1.233
180	30.013	0.080	121.441	0.068	1798.606	2.084	-1.171

n.a.: data not available

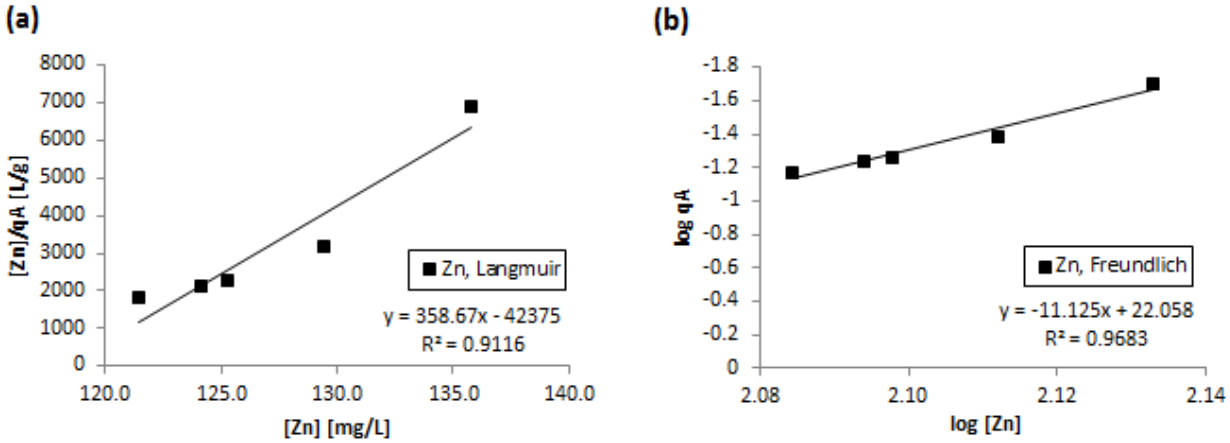

Figure 31: Linear regression to find isotherm parameters, zinc

Manganese:

Table 39: Calculation of isotherm parameters, manganese

Time [min]	Mass [g]	Volume [L]	$[Mn^{2+}]$[mg/L]	q_A [mg/g]	$[Mn^{2+}]/q_A$ [L/g]	log $[Mn^{2+}]$	log q_A
0	30.013	0.100	18.330	0.000	n.a.	1.263	n.a.
15	30.013	0.100	18.896	-0.002	-10024.057	1.276	n.a.
30	30.013	0.095	19.840	-0.005	-3944.897	1.298	n.a.
60	30.013	0.090	19.909	-0.005	-3785.214	1.299	n.a.
120	30.013	0.085	21.540	-0.011	-2014.221	1.333	n.a.
180	30.013	0.080	22.106	-0.013	-1757.266	1.345	n.a.

n.a.: data not available

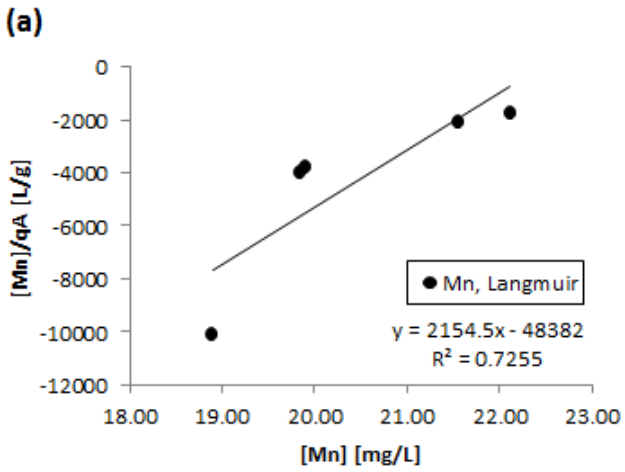

Figure 32: Linear regression to find the isotherm parameters, manganese

The isotherm parameters for Løkken works can be seen in Table 6.

Calculation of the adsorption isotherms

Iron:

Table 40: Calculation of the adsorption isotherms, iron

Time [min]	Mass [g]	Volume [L]	$[Fe^{3+}]$ [mg/L]	q_e	$q_{Langmuir}$	$q_{Freundlich}$
0	30.013	0.100	2834.472	0.000	1.194	0.894
15	30.013	0.100	2248.374	1.953	1.900	1.926
30	30.013	0.095	2326.420	1.608	1.734	1.720
60	30.013	0.090	2311.225	1.569	1.763	1.757
120	30.013	0.085	2177.304	1.861	2.096	2.142
180	30.013	0.080	2015.883	2.182	2.837	2.765

Copper:

Table 41: Calculation of the adsorption isotherms, copper

Time [min]	Mass [g]	Volume [L]	$[Cu^{2+}]$ [mg/L]	q_e	$q_{Langmuir}$	$q_{Frundlich}$
0	30.013	0.100	174.375	0.000	0.052	0.039
15	30.013	0.100	145.962	0.095	0.093	0.094
30	30.013	0.095	140.917	0.106	0.113	0.112
60	30.013	0.090	149.576	0.074	0.084	0.083
120	30.013	0.085	144.214	0.085	0.099	0.100
180	30.013	0.080	141.840	0.087	0.109	0.109

Zinc:

Table 42: Calculation of the adsorption isotherms, zinc

Time [min]	Mass [g]	Volume [L]	$[Zn^{2+}]$ [mg/L]	q_e	$q_{Langmuir}$	$q_{Freundlich}$
0	30.013	0.100	141.706	0.000	0.017	0.013
15	30.013	0.100	135.803	0.020	0.021	0.021
30	30.013	0.095	129.446	0.039	0.032	0.036
60	30.013	0.090	125.262	0.049	0.049	0.052
120	30.013	0.085	124.167	0.050	0.057	0.058
180	30.013	0.080	121.441	0.054	0.103	0.074

Manganese:

Table 43: Calculation of the adsorption isotherms, manganese

Time [min]	Mass [g]	Volume [L]	$[Mn^{2+}]$[mg/L]	q_e	$q_{Langmuir}$	$q_{Feundlich}$
0	30.013	0.100	18.330	0.000	-0.002	n.a.
15	30.013	0.100	18.896	-0.002	-0.002	n.a.
30	30.013	0.095	19.840	-0.005	-0.004	n.a.
60	30.013	0.090	19.909	-0.005	-0.004	n.a.
120	30.013	0.085	21.540	-0.009	-0.011	n.a.
180	30.013	0.080	22.106	-0.010	-0.029	n.a.

n.a.: data not available

Appendix 6: Log C – pH diagrams

To create Log C – pH diagrams the concentration of all metal hydroxides for the different pH values, need to be calculated. To find these concentrations the stability constant for complexation of metals by hydroxides was used. The stability constants from Stumm and Morgan (1996) were given as logβ_i and not as log* β_i. The difference between the two equilibrium constants is the way the chemical reaction is arranged. Equilibrium constants in the form β_i refer to reactions that are arranged to show the reaction between an uncomplexed ion and *i* ligands to form complexes of the type MeL_i. When using *β_i, the reaction is written with the ligand in a protonated form, with H^+ on the product side (Benjamin, 2002). The equilibrium constant has to be converted into the form of *β_i, since the required reactions should be written as follows:

$$Me^{i+} + nH_2O \leftrightarrow Me(OH)_n^i + nH^+ \qquad (27)$$

The relationship between β_i and *β_i is:

$$*\beta_i = \beta_i K_w^i \qquad (28)$$

Were K_w is the equilibrium constant for water, which at 25°C is10^{-14}.

The complexation reactions for the metals are as follows:

Ferric iron:

$$Fe^{3+} + H_2O \leftrightarrow FeOH^{2+} + H^+ \qquad (29a)$$

$$Fe^{3+} + 2H_2O \leftrightarrow Fe(OH)_2^+ + 2H^+ \qquad (29b)$$

$$Fe^{3+} + 3H_2O \leftrightarrow Fe(OH)_3^0 + 3H^+ \qquad (29c)$$

$$Fe^{3+} + 4H_2O \leftrightarrow Fe(OH)_4^- + 4H^+ \qquad (29d)$$

Copper:

$$Cu^{2+} + H_2O \leftrightarrow CuOH^+ + H^+ \qquad (29e)$$

$$Cu^{2+} + 2H_2O \leftrightarrow Cu(OH)_2^0 + 2H^+ \qquad (29f)$$

$$Cu^{2+} + 3H_2O \leftrightarrow Cu(OH)_3^- + 3H^+ \qquad (29g)$$

$$Cu^{2+} + 4H_2O \leftrightarrow Cu(OH)_4^{2-} + 4H^+ \qquad (29h)$$

Zinc:

$$n^{2+} + H_2O \leftrightarrow ZnOH^+ + H^+ \qquad (29i)$$

$$n^{2+} + 2H_2O \leftrightarrow Zn(OH)_2^0 + 2H^+ \qquad (29j)$$

$$n^{2+} + 3H_2O \leftrightarrow Zn(OH)_3^- + 3H^+ \qquad (29k)$$

$$n^{2+} + 4H_2O \leftrightarrow Zn(OH)_4^{2-} + 4H^+ \qquad (29l)$$

Manganese:

$$Mn^{2+} + H_2O \leftrightarrow MnOH^+ + H^+ \qquad (29m)$$

$$Mn^{2+} + 2H_2O \leftrightarrow Mn(OH)_2^0 + 2H^+ \qquad (29n)$$

$$Mn^{2+} + 3H_2O \leftrightarrow Mn(OH)_3^- + 3H^+ \qquad (29o)$$

$$Mn^{2+} + 4H_2O \leftrightarrow Mn(OH)_4^{2-} + 4H^+ \qquad (29p)$$

Concentration calculations:

For the reaction described in Equation (27) the expression for the equilibrium constant will be:

$$*\beta_i = \frac{\{Me(OH)_n^i\} \times \{H^+\}^n}{\{Me^{i+}\}} \qquad (30)$$

The equation for the metal hydroxide will then be:

$$\{Me(OH)_n^i\} = \frac{*\beta_i \times \{Me^{i+}\}}{\{H^+\}^n} \qquad (31)$$

To find the concentration of the metal hydroxide the concentration of the hydrogen and metal ion needs to be known. The concentration of the hydrogen ion is dependent on pH and can be found using Equation (32):

$$\{H^+\} = 10^{-pH} \qquad (32)$$

The total dissolved metal is given by Equation (33):

$$TOTMe = \{Me^{i+}\} \times (1 + \sum_{i=x}^{x} \frac{*\beta_i}{\{H^+\}^n}) \qquad (33)$$

The metal ion concentration is then found by rearranging Equation (33):

$$\{Me^{i+}\} = \frac{TOTMe}{1 + \sum_{i=x}^{x} \frac{* \beta_i}{\{H^+\}^n}} \qquad (33a)$$

The log values of all the concentrations are found and then they are plotted against the pH.

Below are the figures and tables for all the metals for Folldal and Løkken.

Folldal center:

Iron:

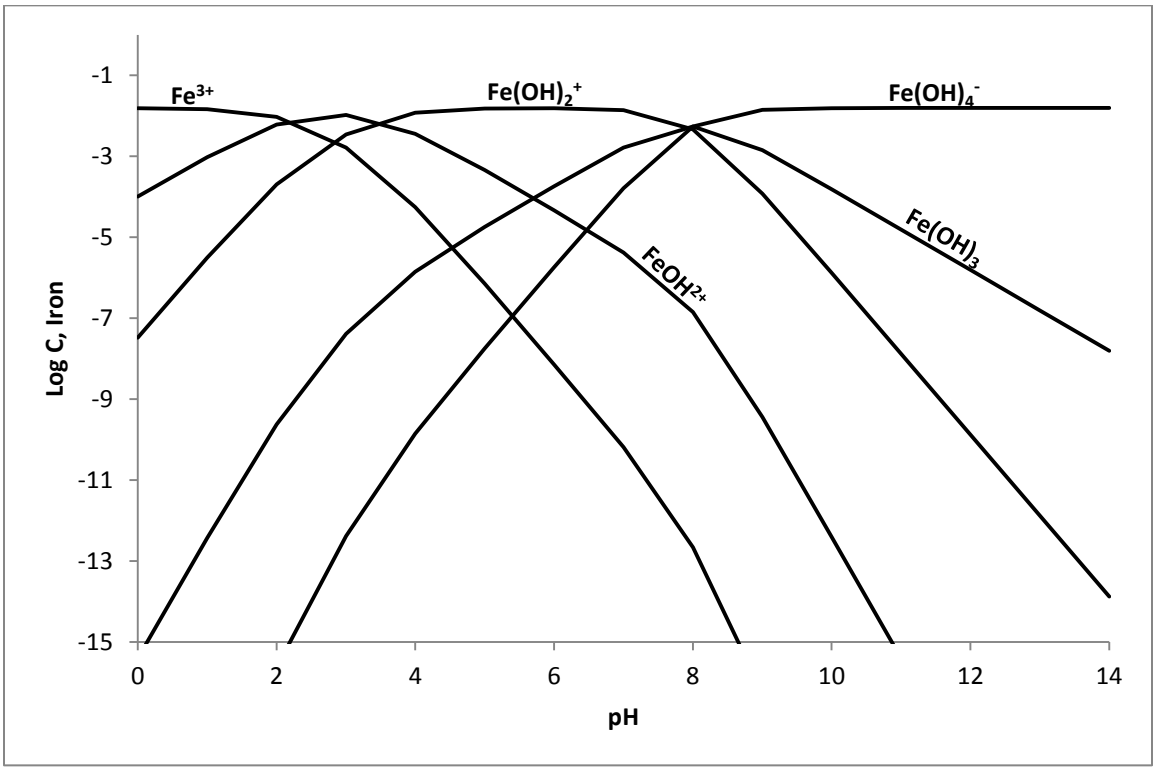

Figure 33: Log C-pH diagram for Fe in a system with 15.56 mM TOTFe, Folldal center

Table 44: Calculation of log C - pH diagram for iron, Folldal center

TOTFe [mol/L]	0.01556		
Log B1	-2.19	B1	6.46E-03
Log B2	-5.67	B2	2.14E-06
Log B3	-13.60	B3	2.51E-14
Log B4	-21.60	B4	2.51E-22

pH	$\{H^+\}$	$\{OH^-\}$	$B1/\{H^+\}^1$	$B2/\{H^+\}^2$	$B3/\{H^+\}^3$	$B4/\{H^+\}^4$	TOTFe,eq	$\{Fe^{3+}\}$	$Log\{Fe^{3+}\}$	$\{FeOH^{2+}\}$	$Log\{FeOH^{2+}\}$	$\{Fe(OH)_2^+\}$	$Log\{Fe(OH)_2^+\}$	$\{Fe(OH)_3^0\}$	$Log\{Fe(OH)_3^0\}$	$\{Fe(OH)_4^-\}$	$Log\{Fe(OH)_4^-\}$
0	1.00E+00	1.00E-14	6.46E-03	2.14E-06	2.51E-14	2.51E-22	1.01E+00	1.55E-02	-1.81E+00	9.98E-05	-4.00E+00	3.31E-08	-7.48E+00	3.88E-16	-1.54E+01	3.88E-24	-2.34E+01
1	1.00E-01	1.00E-13	6.46E-02	2.14E-04	2.51E-11	2.51E-18	1.06E+00	1.46E-02	-1.84E+00	9.44E-04	-3.03E+00	3.12E-06	-5.51E+00	3.67E-13	-1.24E+01	3.67E-20	-1.94E+01
2	1.00E-02	1.00E-12	6.46E-01	2.14E-02	2.51E-08	2.51E-14	1.67E+00	9.33E-03	-2.03E+00	6.03E-03	-2.22E+00	2.00E-04	-3.70E+00	2.34E-10	-9.63E+00	2.34E-16	-1.56E+01
3	1.00E-03	1.00E-11	6.46E+00	2.14E+00	2.51E-05	2.51E-10	9.59E+00	1.62E-03	-2.79E+00	1.05E-02	-1.98E+00	3.47E-03	-2.46E+00	4.07E-08	-7.39E+00	4.07E-13	-1.24E+01
4	1.00E-04	1.00E-10	6.46E+01	2.14E+02	2.51E-02	2.51E-06	2.79E+02	5.57E-05	-4.25E+00	3.60E-03	-2.44E+00	1.19E-02	-1.92E+00	1.40E-06	-5.85E+00	1.40E-10	-9.85E+00
5	1.00E-05	1.00E-09	6.46E+02	2.14E+04	2.51E+01	2.51E-02	2.21E+04	7.06E-07	-6.15E+00	4.56E-04	-3.34E+00	1.51E-02	-1.82E+00	1.77E-05	-4.75E+00	1.77E-08	-7.75E+00
6	1.00E-06	1.00E-08	6.46E+03	2.14E+06	2.51E+04	2.51E+02	2.17E+06	7.17E-09	-8.14E+00	4.63E-05	-4.33E+00	1.53E-02	-1.81E+00	1.80E-04	-3.74E+00	1.80E-06	-5.74E+00
7	1.00E-07	1.00E-07	6.46E+04	2.14E+08	2.51E+07	2.51E+06	2.41E+08	6.44E-11	-1.02E+01	4.16E-06	-5.38E+00	1.38E-02	-1.86E+00	1.62E-03	-2.79E+00	1.62E-04	-3.79E+00
8	1.00E-08	1.00E-06	6.46E+05	2.14E+10	2.51E+10	2.51E+10	7.16E+10	2.17E-13	-1.27E+01	1.40E-07	-6.85E+00	4.65E-03	-2.33E+00	5.46E-03	-2.26E+00	5.46E-03	-2.26E+00
9	1.00E-09	1.00E-05	6.46E+06	2.14E+12	2.51E+13	2.51E+14	2.78E+14	5.59E-17	-1.63E+01	3.61E-10	-9.44E+00	1.19E-04	-3.92E+00	1.40E-03	-2.85E+00	1.40E-02	-1.85E+00
10	1.00E-10	1.00E-04	6.46E+07	2.14E+14	2.51E+16	2.51E+18	2.54E+18	6.13E-21	-2.02E+01	3.96E-13	-1.24E+01	1.31E-06	-5.88E+00	1.54E-04	-3.81E+00	1.54E-02	-1.81E+00
11	1.00E-11	1.00E-03	6.46E+08	2.14E+16	2.51E+19	2.51E+22	2.51E+22	6.19E-25	-2.42E+01	4.00E-16	-1.54E+01	1.32E-08	-7.88E+00	1.55E-05	-4.81E+00	1.55E-02	-1.81E+00
12	1.00E-12	1.00E-02	6.46E+09	2.14E+18	2.51E+22	2.51E+26	2.51E+26	6.19E-29	-2.82E+01	4.00E-19	-1.84E+01	1.32E-10	-9.88E+00	1.56E-06	-5.81E+00	1.56E-02	-1.81E+00
13	1.00E-13	1.00E-01	6.46E+10	2.14E+20	2.51E+25	2.51E+30	2.51E+30	6.19E-33	-3.22E+01	4.00E-22	-2.14E+01	1.32E-12	-1.19E+01	1.56E-07	-6.81E+00	1.56E-02	-1.81E+00
14	1.00E-14	1.00E+00	6.46E+11	2.14E+22	2.51E+28	2.51E+34	2.51E+34	6.19E-37	-3.62E+01	4.00E-25	-2.44E+01	1.32E-14	-1.39E+01	1.56E-08	-7.81E+00	1.56E-02	-1.81E+00

Copper:

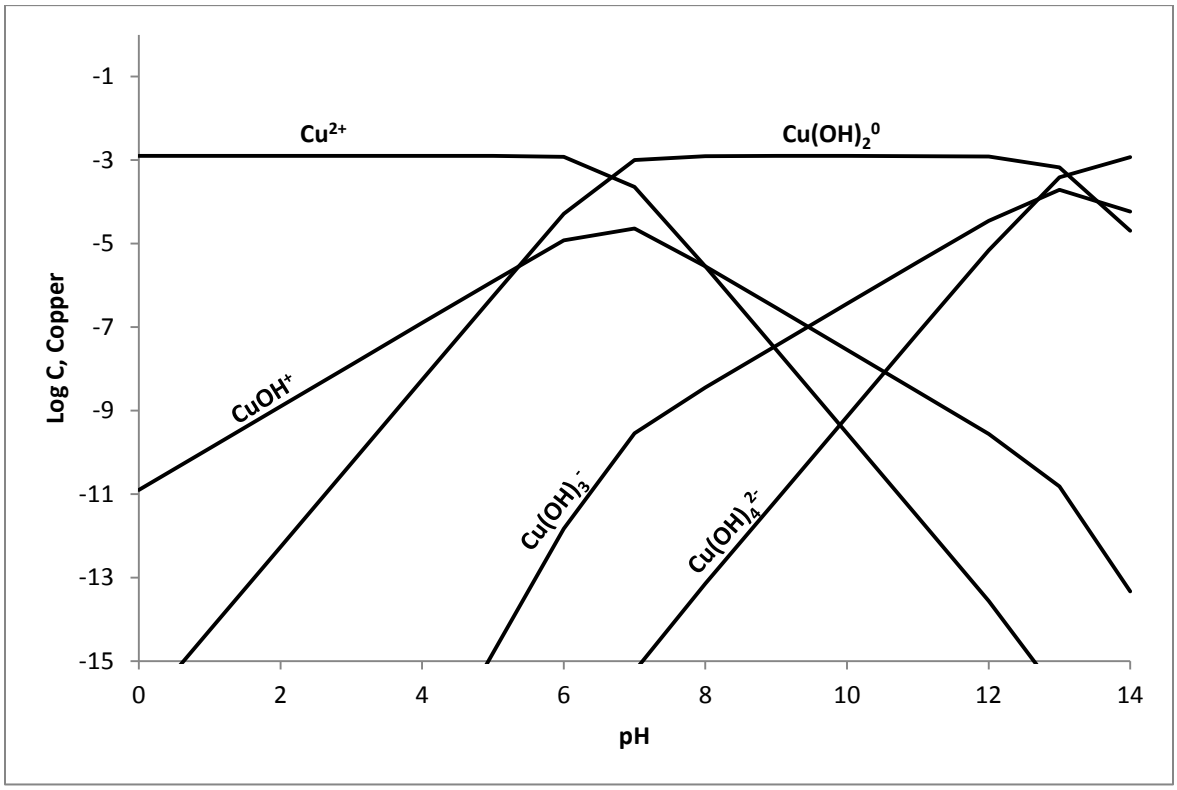

Figure 34: Log C-pH diagram for Cu in a system with 1.25 mM TOTCu, Folldal center

Table 45: Calculation of log C - pH diagram for copper, Folldal center

TOTCu [mol/L]	0.00125		
Log B1	-8	B1	1.00E-08
Log B2	-13.36	B2	4.37E-14
Log B3	-26.9	B3	1.26E-27
Log B4	-39.6	B4	2.51E-40

pH	$\{H^+\}$	$\{OH^-\}$	$B1/\{H^+\}^1$	$B2/\{H^+\}^2$	$B3/\{H^+\}^3$	$/B4\{H^+\}^4$	TOTCu, eq	$\{Cu^{2+}\}$	$Log\{Cu^{2+}\}$	$\{CuOH^+\}$	$Log\{CuOH^+\}$	$\{Cu(OH)_2^0\}$	$Log\{Cu(OH)_2^0\}$	$\{Cu(OH)_3^-\}$	$Log\{Cu(OH)_3^-\}$	$\{Cu(OH)_4^{2-}\}$	$Log\{Cu(OH)_4^{2-}\}$
0	1.00E+00	1.00E-14	1.00E-08	4.37E-14	1.26E-27	2.51E-40	1.00E+00	1.25E-03	-2.90E+00	1.25E-11	-1.09E+01	5.46E-17	-1.63E+01	1.57E-30	-2.98E+01	3.14E-43	-4.25E+01
1	1.00E-01	1.00E-13	1.00E-07	4.37E-12	1.26E-24	2.51E-36	1.00E+00	1.25E-03	-2.90E+00	1.25E-10	-9.90E+00	5.46E-15	-1.43E+01	1.57E-27	-2.68E+01	3.14E-39	-3.85E+01
2	1.00E-02	1.00E-12	1.00E-06	4.37E-10	1.26E-21	2.51E-32	1.00E+00	1.25E-03	-2.90E+00	1.25E-09	-8.90E+00	5.46E-13	-1.23E+01	1.57E-24	-2.38E+01	3.14E-35	-3.45E+01
3	1.00E-03	1.00E-11	1.00E-05	4.37E-08	1.26E-18	2.51E-28	1.00E+00	1.25E-03	-2.90E+00	1.25E-08	-7.90E+00	5.46E-11	-1.03E+01	1.57E-21	-2.08E+01	3.14E-31	-3.05E+01
4	1.00E-04	1.00E-10	1.00E-04	4.37E-06	1.26E-15	2.51E-24	1.00E+00	1.25E-03	-2.90E+00	1.25E-07	-6.90E+00	5.46E-09	-8.26E+00	1.57E-18	-1.78E+01	3.14E-27	-2.65E+01
5	1.00E-05	1.00E-09	1.00E-03	4.37E-04	1.26E-12	2.51E-20	1.00E+00	1.25E-03	-2.90E+00	1.25E-06	-5.90E+00	5.45E-07	-6.26E+00	1.57E-15	-1.48E+01	3.14E-23	-2.25E+01
6	1.00E-06	1.00E-08	1.00E-02	4.37E-02	1.26E-09	2.51E-16	1.05E+00	1.19E-03	-2.93E+00	1.19E-05	-4.93E+00	5.18E-05	-4.29E+00	1.49E-12	-1.18E+01	2.98E-19	-1.85E+01
7	1.00E-07	1.00E-07	1.00E-01	4.37E+00	1.26E-06	2.51E-12	5.47E+00	2.29E-04	-3.64E+00	2.29E-05	-4.64E+00	9.98E-04	-3.00E+00	2.88E-10	-9.54E+00	5.75E-16	-1.52E+01
8	1.00E-08	1.00E-06	1.00E+00	4.37E+02	1.26E-03	2.51E-08	4.39E+02	2.85E-06	-5.55E+00	2.85E-06	-5.55E+00	1.24E-03	-2.91E+00	3.59E-09	-8.45E+00	7.16E-14	-1.31E+01
9	1.00E-09	1.00E-05	1.00E+01	4.37E+04	1.26E+00	2.51E-04	4.37E+04	2.86E-08	-7.54E+00	2.86E-07	-6.54E+00	1.25E-03	-2.90E+00	3.60E-08	-7.44E+00	7.19E-12	-1.11E+01
10	1.00E-10	1.00E-04	1.00E+02	4.37E+06	1.26E+03	2.51E+00	4.37E+06	2.86E-10	-9.54E+00	2.86E-08	-7.54E+00	1.25E-03	-2.90E+00	3.60E-07	-6.44E+00	7.19E-10	-9.14E+00
11	1.00E-11	1.00E-03	1.00E+03	4.37E+08	1.26E+06	2.51E+04	4.38E+08	2.86E-12	-1.15E+01	2.86E-09	-8.54E+00	1.25E-03	-2.90E+00	3.59E-06	-5.44E+00	7.17E-08	-7.14E+00
12	1.00E-12	1.00E-02	1.00E+04	4.37E+10	1.26E+09	2.51E+08	4.52E+10	2.77E-14	-1.36E+01	2.77E-10	-9.56E+00	1.21E-03	-2.92E+00	3.48E-05	-4.46E+00	6.95E-06	-5.16E+00
13	1.00E-13	1.00E-01	1.00E+05	4.37E+12	1.26E+12	2.51E+12	8.14E+12	1.54E-16	-1.58E+01	1.54E-11	-1.08E+01	6.71E-04	-3.17E+00	1.93E-04	-3.71E+00	3.86E-04	-3.41E+00
14	1.00E-14	1.00E+00	1.00E+06	4.37E+14	1.26E+15	2.51E+16	2.68E+16	4.66E-20	-1.93E+01	4.66E-14	-1.33E+01	2.03E-05	-4.69E+00	5.87E-05	-4.23E+00	1.17E-03	-2.93E+00

Zinc:

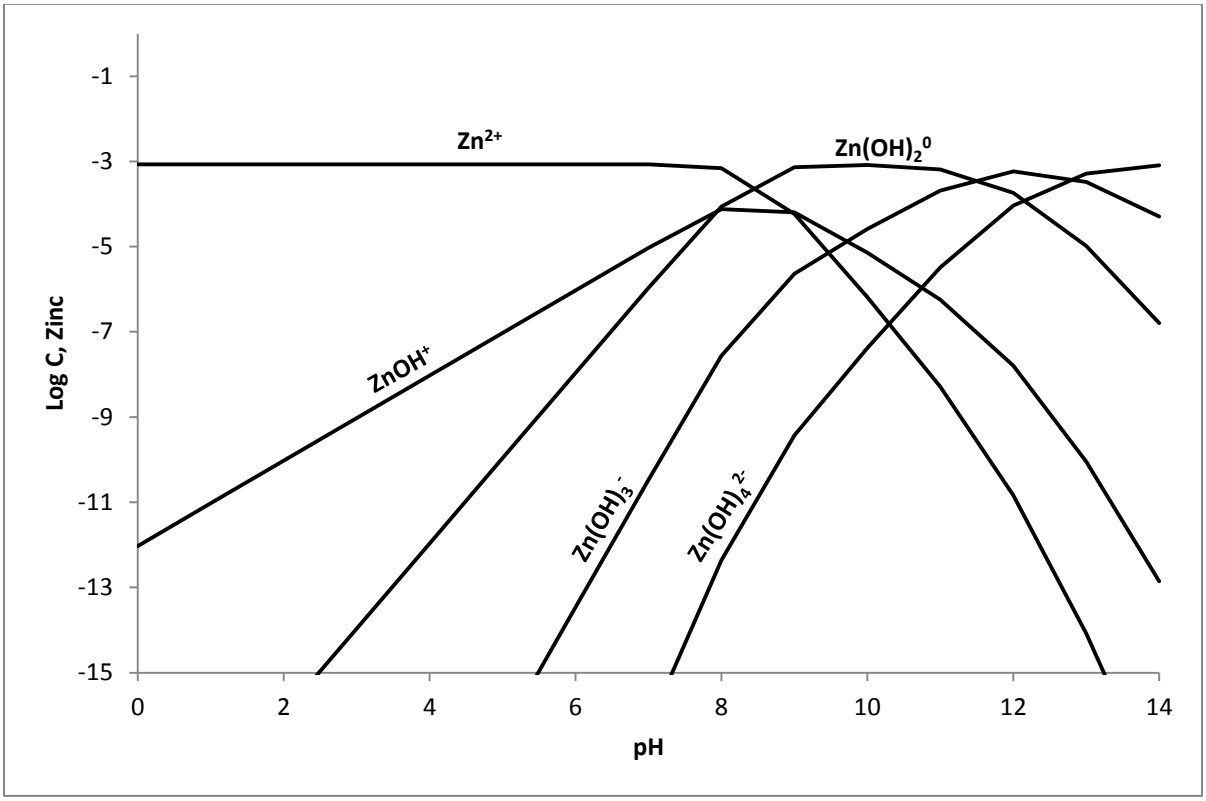

Figure 35: Log C-pH diagram for Zn in a system with 0.86 mM TOTZn, Folldal center

Table 46: Calculation of log C - pH diagram for zinc, Folldal center

TOTZn [mol/L]	0.00086		
Log B1	-8.96	B1	1.1E-09
Log B2	-16.9	B2	1.26E-17
Log B3	-28.4	B3	3.98E-29
Log B4	-41.2	B4	6.31E-42

pH	$\{H^+\}$	$\{OH^-\}$	$B1/\{H^+\}^1$	$B2/\{H^+\}^2$	$B3/\{H^+\}^3$	$/B4\{H^+\}^4$	TOTZn	$\{Zn^{2+}\}$	$Log\{Zn^{2+}\}$	$\{ZnOH^+\}$	$Log\{ZnOH^+\}$	$\{Zn(OH)_2^0\}$	$Log\{Zn(OH)_2^0\}$	$\{Zn(OH)_3^-\}$	$Log\{Zn(OH)_3^-\}$	$\{Zn(OH)_4^{2-}\}$	$Log\{Zn(OH)_4^{2-}\}$
0	1.00E+00	1.00E-14	1.10E-09	1.26E-17	3.98E-29	6.31E-42	1.00E+00	8.60E-04	-3.07E+00	9.43E-13	-1.20E+01	1.08E-20	-2.00E+01	3.42E-32	-3.15E+01	5.43E-45	-4.43E+01
1	1.00E-01	1.00E-13	1.10E-08	1.26E-15	3.98E-26	6.31E-38	1.00E+00	8.60E-04	-3.07E+00	9.43E-12	-1.10E+01	1.08E-18	-1.80E+01	3.42E-29	-2.85E+01	5.43E-41	-4.03E+01
2	1.00E-02	1.00E-12	1.10E-07	1.26E-13	3.98E-23	6.31E-34	1.00E+00	8.60E-04	-3.07E+00	9.43E-11	-1.00E+01	1.08E-16	-1.60E+01	3.42E-26	-2.55E+01	5.43E-37	-3.63E+01
3	1.00E-03	1.00E-11	1.10E-06	1.26E-11	3.98E-20	6.31E-30	1.00E+00	8.60E-04	-3.07E+00	9.43E-10	-9.03E+00	1.08E-14	-1.40E+01	3.42E-23	-2.25E+01	5.43E-33	-3.23E+01
4	1.00E-04	1.00E-10	1.10E-05	1.26E-09	3.98E-17	6.31E-26	1.00E+00	8.60E-04	-3.07E+00	9.43E-09	-8.03E+00	1.08E-12	-1.20E+01	3.42E-20	-1.95E+01	5.43E-29	-2.83E+01
5	1.00E-05	1.00E-09	1.10E-04	1.26E-07	3.98E-14	6.31E-22	1.00E+00	8.60E-04	-3.07E+00	9.43E-08	-7.03E+00	1.08E-10	-9.97E+00	3.42E-17	-1.65E+01	5.43E-25	-2.43E+01
6	1.00E-06	1.00E-08	1.10E-03	1.26E-05	3.98E-11	6.31E-18	1.00E+00	8.59E-04	-3.07E+00	9.42E-07	-6.03E+00	1.08E-08	-7.97E+00	3.42E-14	-1.35E+01	5.42E-21	-2.03E+01
7	1.00E-07	1.00E-07	1.10E-02	1.26E-03	3.98E-08	6.31E-14	1.01E+00	8.50E-04	-3.07E+00	9.32E-06	-5.03E+00	1.07E-06	-5.97E+00	3.38E-11	-1.05E+01	5.36E-17	-1.63E+01
8	1.00E-08	1.00E-06	1.10E-01	1.26E-01	3.98E-05	6.31E-10	1.24E+00	6.96E-04	-3.16E+00	7.63E-05	-4.12E+00	8.76E-05	-4.06E+00	2.77E-08	-7.56E+00	4.39E-13	-1.24E+01
9	1.00E-09	1.00E-05	1.10E+00	1.26E+01	3.98E-02	6.31E-06	1.47E+01	5.84E-05	-4.23E+00	6.40E-05	-4.19E+00	7.35E-04	-3.13E+00	2.33E-06	-5.63E+00	3.68E-10	-9.43E+00
10	1.00E-10	1.00E-04	1.10E+01	1.26E+03	3.98E+01	6.31E-02	1.31E+03	6.56E-07	-6.18E+00	7.19E-06	-5.14E+00	8.26E-04	-3.08E+00	2.61E-05	-4.58E+00	4.14E-08	-7.38E+00
11	1.00E-11	1.00E-03	1.10E+02	1.26E+05	3.98E+04	6.31E+02	1.66E+05	5.17E-09	-8.29E+00	5.67E-07	-6.25E+00	6.50E-04	-3.19E+00	2.06E-04	-3.69E+00	3.26E-06	-5.49E+00
12	1.00E-12	1.00E-02	1.10E+03	1.26E+07	3.98E+07	6.31E+06	5.87E+07	1.46E-11	-1.08E+01	1.61E-08	-7.79E+00	1.84E-04	-3.73E+00	5.83E-04	-3.23E+00	9.24E-05	-4.03E+00
13	1.00E-13	1.00E-01	1.10E+04	1.26E+09	3.98E+10	6.31E+10	1.04E+11	8.26E-15	-1.41E+01	9.05E-11	-1.00E+01	1.04E-05	-4.98E+00	3.29E-04	-3.48E+00	5.21E-04	-3.28E+00
14	1.00E-14	1.00E+00	1.10E+05	1.26E+11	3.98E+13	6.31E+14	6.71E+14	1.28E-18	-1.79E+01	1.41E-13	-1.29E+01	1.61E-07	-6.79E+00	5.10E-05	-4.29E+00	8.09E-04	-3.09E+00

Manganese:

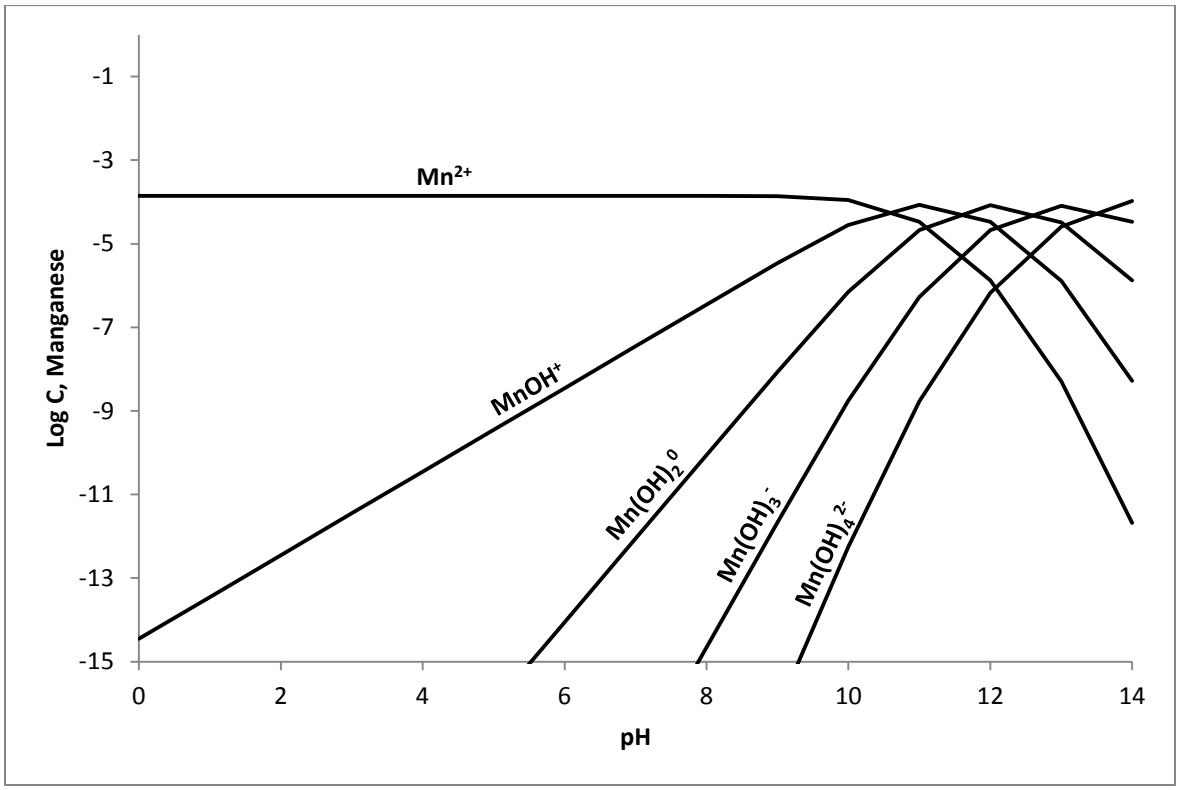

Figure 36: Log C-pH diagram for Mn in a system with 0.14 mM TOTMn, Folldal center

Table 47: Calculation of log C - pH diagram for manganese, Folldal center

TOTMn [mol/L]	0.00014		
Log B1	-8.96	B1	2.51E-11
Log B2	-16.9	B2	6.31E-23
Log B3	-28.4	B3	1.58E-35
Log B4	-41.2	B4	5.01E-49

pH	$\{H^+\}$	$\{OH^-\}$	$B1/\{H^+\}^1$	$B2/\{H^+\}^2$	$B3/\{H^+\}^3$	$/B4\{H^+\}^4$	TOTMn	$\{Mn^{2+}\}$	$Log\{Mn^{2+}\}$	$\{MnOH^+\}$	$Log\{MnOH^+\}$	$\{Mn(OH)_2^0\}$	$Log\{Mn(OH)_2^0\}$	$\{Mn(OH)_3^-\}$	$Log\{Mn(OH)_3^-\}$	$\{Mn(OH)_4^{2-}\}$	$Log\{Mn(OH)_4^{2-}\}$
0	1.00E+00	1.00E-14	2.51E-11	6.31E-23	1.58E-35	5.01E-49	1.00E+00	1.40E-04	-3.85E+00	3.52E-15	-1.45E+01	8.83E-27	-2.61E+01	2.22E-39	-3.87E+01	7.02E-53	-5.22E+01
1	1.00E-01	1.00E-13	2.51E-10	6.31E-21	1.58E-32	5.01E-45	1.00E+00	1.40E-04	-3.85E+00	3.52E-14	-1.35E+01	8.83E-25	-2.41E+01	2.22E-36	-3.57E+01	7.02E-49	-4.82E+01
2	1.00E-02	1.00E-12	2.51E-09	6.31E-19	1.58E-29	5.01E-41	1.00E+00	1.40E-04	-3.85E+00	3.52E-13	-1.25E+01	8.83E-23	-2.21E+01	2.22E-33	-3.27E+01	7.02E-45	-4.42E+01
3	1.00E-03	1.00E-11	2.51E-08	6.31E-17	1.58E-26	5.01E-37	1.00E+00	1.40E-04	-3.85E+00	3.52E-12	-1.15E+01	8.83E-21	-2.01E+01	2.22E-30	-2.97E+01	7.02E-41	-4.02E+01
4	1.00E-04	1.00E-10	2.51E-07	6.31E-15	1.58E-23	5.01E-33	1.00E+00	1.40E-04	-3.85E+00	3.52E-11	-1.05E+01	8.83E-19	-1.81E+01	2.22E-27	-2.67E+01	7.02E-37	-3.62E+01
5	1.00E-05	1.00E-09	2.51E-06	6.31E-13	1.58E-20	5.01E-29	1.00E+00	1.40E-04	-3.85E+00	3.52E-10	-9.45E+00	8.83E-17	-1.61E+01	2.22E-24	-2.37E+01	7.02E-33	-3.22E+01
6	1.00E-06	1.00E-08	2.51E-05	6.31E-11	1.58E-17	5.01E-25	1.00E+00	1.40E-04	-3.85E+00	3.52E-09	-8.45E+00	8.83E-15	-1.41E+01	2.22E-21	-2.07E+01	7.02E-29	-2.82E+01
7	1.00E-07	1.00E-07	2.51E-04	6.31E-09	1.58E-14	5.01E-21	1.00E+00	1.40E-04	-3.85E+00	3.52E-08	-7.45E+00	8.83E-13	-1.21E+01	2.22E-18	-1.77E+01	7.01E-25	-2.42E+01
8	1.00E-08	1.00E-06	2.51E-03	6.31E-07	1.58E-11	5.01E-17	1.00E+00	1.40E-04	-3.85E+00	3.51E-07	-6.45E+00	8.81E-11	-1.01E+01	2.21E-15	-1.47E+01	7.00E-21	-2.02E+01
9	1.00E-09	1.00E-05	2.51E-02	6.31E-05	1.58E-08	5.01E-13	1.03E+00	1.37E-04	-3.86E+00	3.43E-06	-5.46E+00	8.62E-09	-8.06E+00	2.16E-12	-1.17E+01	6.84E-17	-1.62E+01
10	1.00E-10	1.00E-04	2.51E-01	6.31E-03	1.58E-05	5.01E-09	1.26E+00	1.11E-04	-3.95E+00	2.80E-05	-4.55E+00	7.02E-07	-6.15E+00	1.76E-09	-8.75E+00	5.58E-13	-1.23E+01
11	1.00E-11	1.00E-03	2.51E+00	6.31E-01	1.58E-02	5.01E-05	4.16E+00	3.37E-05	-4.47E+00	8.46E-05	-4.07E+00	2.12E-05	-4.67E+00	5.34E-07	-6.27E+00	1.69E-09	-8.77E+00
12	1.00E-12	1.00E-02	2.51E+01	6.31E+01	1.58E+01	5.01E-01	1.06E+02	1.33E-06	-5.88E+00	3.33E-05	-4.48E+00	8.37E-05	-4.08E+00	2.10E-05	-4.68E+00	6.65E-07	-6.18E+00
13	1.00E-13	1.00E-01	2.51E+02	6.31E+03	1.58E+04	5.01E+03	2.74E+04	5.11E-09	-8.29E+00	1.28E-06	-5.89E+00	3.22E-05	-4.49E+00	8.09E-05	-4.09E+00	2.56E-05	-4.59E+00
14	1.00E-14	1.00E+00	2.51E+03	6.31E+05	1.58E+07	5.01E+07	6.66E+07	2.10E-12	-1.17E+01	5.28E-09	-8.28E+00	1.33E-06	-5.88E+00	3.33E-05	-4.48E+00	1.05E-04	-3.98E+00

Løkken works

Iron:

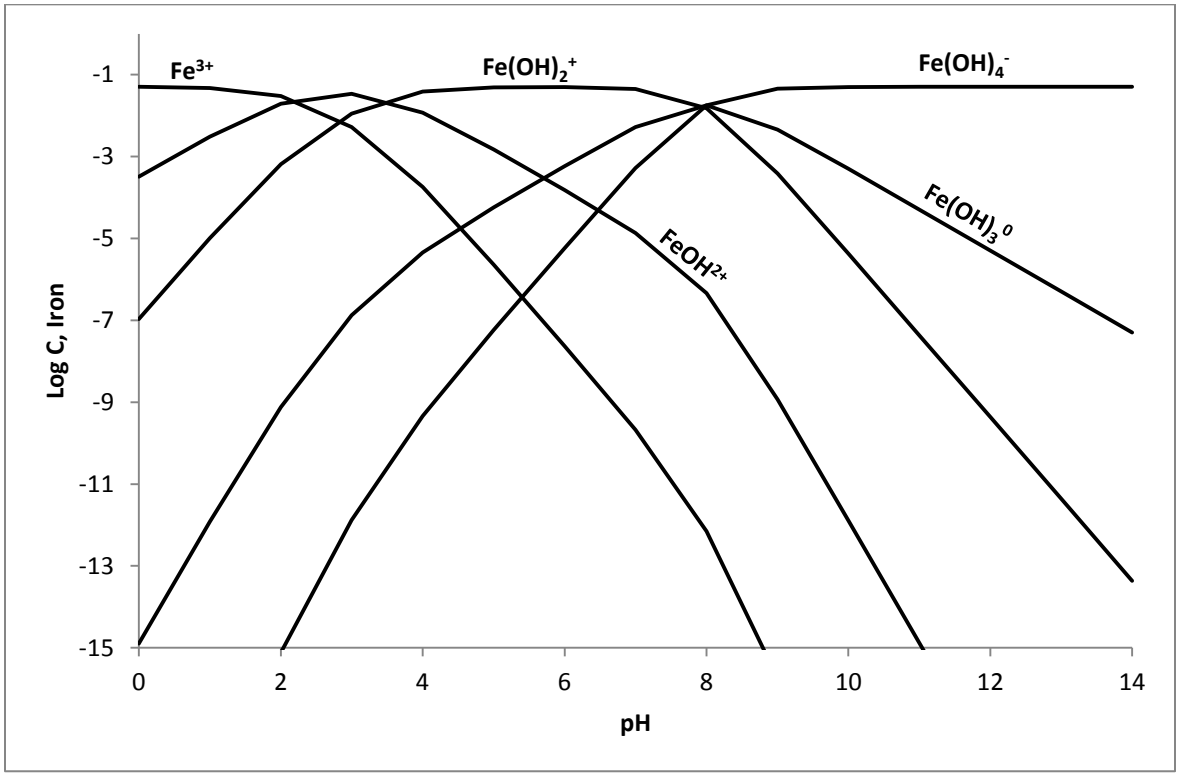

Figure 37: Log C-pH diagram for Fe in a system with 50.75 mM TOTFe, Løkken works

Table 48: Calculation of log C - pH diagram for iron, Løkken works

TOTFe [mol/L]	0.05075		
Log B1	-2.19	B1	6.46E-03
Log B2	-5.67	B2	2.14E-06
Log B3	-13.6	B3	2.51E-14
Log B4	-21.6	B4	2.51E-22

pH	$\{H^+\}$	$\{OH^-\}$	$B1/\{H^+\}^1$	$B2/\{H^+\}^2$	$B3/\{H^+\}^3$	$B4/\{H^+\}^4$	TOTFe,eq	$\{Fe^{3+}\}$	$Log\{Fe^{3+}\}$	$\{FeOH^{2+}\}$	$Log\{FeOH^{2+}$	$\{Fe(OH)_2^+\}$	$Log\{Fe(OH)_2^+$	$\{Fe(OH)_3^0\}$	$Log\{Fe(OH)_3^0\}$	$\{Fe(OH)_4^-\}$	$Log\{Fe(OH)_4^-\}$
0	1.00E+00	1.00E-14	6.46E-03	2.14E-06	2.51E-14	2.51E-22	1.01E+00	5.04E-02	-1.30E+00	3.26E-04	-3.49E+00	1.08E-07	-6.97E+00	1.27E-15	-1.49E+01	1.27E-23	-2.29E+01
1	1.00E-01	1.00E-13	6.46E-02	2.14E-04	2.51E-11	2.51E-18	1.06E+00	4.77E-02	-1.32E+00	3.08E-03	-2.51E+00	1.02E-05	-4.99E+00	1.20E-12	-1.19E+01	1.20E-19	-1.89E+01
2	1.00E-02	1.00E-12	6.46E-01	2.14E-02	2.51E-08	2.51E-14	1.67E+00	3.04E-02	-1.52E+00	1.97E-02	-1.71E+00	6.51E-04	-3.19E+00	7.65E-10	-9.12E+00	7.65E-16	-1.51E+01
3	1.00E-03	1.00E-11	6.46E+00	2.14E+00	2.51E-05	2.51E-10	9.59E+00	5.29E-03	-2.28E+00	3.42E-02	-1.47E+00	1.13E-02	-1.95E+00	1.33E-07	-6.88E+00	1.33E-12	-1.19E+01
4	1.00E-04	1.00E-10	6.46E+01	2.14E+02	2.51E-02	2.51E-06	2.79E+02	1.82E-04	-3.74E+00	1.17E-02	-1.93E+00	3.88E-02	-1.41E+00	4.56E-06	-5.34E+00	4.56E-10	-9.34E+00
5	1.00E-05	1.00E-09	6.46E+02	2.14E+04	2.51E+01	2.51E-02	2.21E+04	2.30E-06	-5.64E+00	1.49E-03	-2.83E+00	4.92E-02	-1.31E+00	5.78E-05	-4.24E+00	5.78E-08	-7.24E+00
6	1.00E-06	1.00E-08	6.46E+03	2.14E+06	2.51E+04	2.51E+02	2.17E+06	2.34E-08	-7.63E+00	1.51E-04	-3.82E+00	5.00E-02	-1.30E+00	5.88E-04	-3.23E+00	5.88E-06	-5.23E+00
7	1.00E-07	1.00E-07	6.46E+04	2.14E+08	2.51E+07	2.51E+06	2.41E+08	2.10E-10	-9.68E+00	1.36E-05	-4.87E+00	4.49E-02	-1.35E+00	5.28E-03	-2.28E+00	5.28E-04	-3.28E+00
8	1.00E-08	1.00E-06	6.46E+05	2.14E+10	2.51E+10	2.51E+10	7.16E+10	7.09E-13	-1.21E+01	4.58E-07	-6.34E+00	1.52E-02	-1.82E+00	1.78E-02	-1.75E+00	1.78E-02	-1.75E+00
9	1.00E-09	1.00E-05	6.46E+06	2.14E+12	2.51E+13	2.51E+14	2.78E+14	1.82E-16	-1.57E+01	1.18E-09	-8.93E+00	3.90E-04	-3.41E+00	4.58E-03	-2.34E+00	4.58E-02	-1.34E+00
10	1.00E-10	1.00E-04	6.46E+07	2.14E+14	2.51E+16	2.51E+18	2.54E+18	2.00E-20	-1.97E+01	1.29E-12	-1.19E+01	4.28E-06	-5.37E+00	5.02E-04	-3.30E+00	5.02E-02	-1.30E+00
11	1.00E-11	1.00E-03	6.46E+08	2.14E+16	2.51E+19	2.51E+22	2.51E+22	2.02E-24	-2.37E+01	1.30E-15	-1.49E+01	4.32E-08	-7.36E+00	5.07E-05	-4.29E+00	5.07E-02	-1.29E+00
12	1.00E-12	1.00E-02	6.46E+09	2.14E+18	2.51E+22	2.51E+26	2.51E+26	2.02E-28	-2.77E+01	1.30E-18	-1.79E+01	4.32E-10	-9.36E+00	5.07E-06	-5.29E+00	5.07E-02	-1.29E+00
13	1.00E-13	1.00E-01	6.46E+10	2.14E+20	2.51E+25	2.51E+30	2.51E+30	2.02E-32	-3.17E+01	1.30E-21	-2.09E+01	4.32E-12	-1.14E+01	5.07E-07	-6.29E+00	5.07E-02	-1.29E+00
14	1.00E-14	1.00E+00	6.46E+11	2.14E+22	2.51E+28	2.51E+34	2.51E+34	2.02E-36	-3.57E+01	1.30E-24	-2.39E+01	4.32E-14	-1.34E+01	5.07E-08	-7.29E+00	5.07E-02	-1.29E+00

Copper

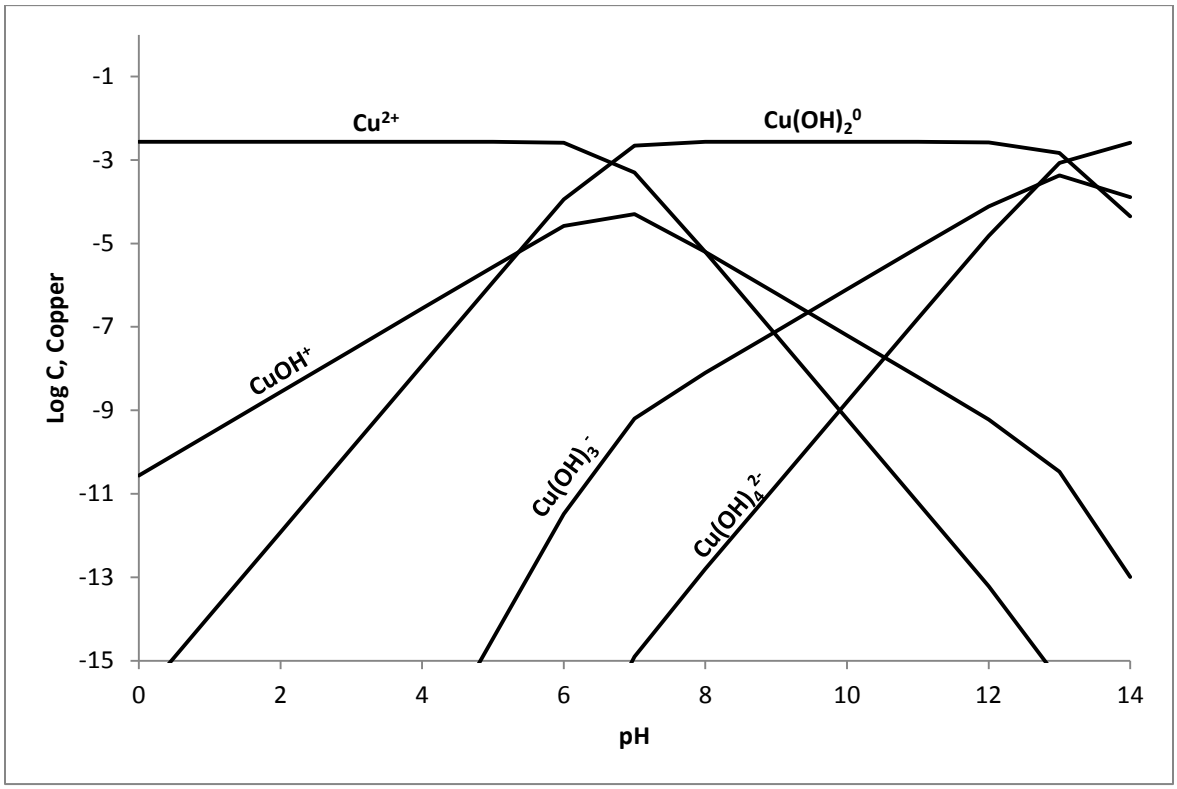

Figure 38: Log C-pH diagram for Cu in a system with 2.24 mM TOTCu, Løkken works

Table 49: Calculation of log C - pH diagram for copper, Løkken works

TOTCu [mol/L]	0.00274		
Log B1	-8	B1	1.00E-08
Log B2	-13.36	B2	4.37E-14
Log B3	-26.9	B3	1.26E-27
Log B4	-39.6	B4	2.51E-40

pH	$\{H^+\}$	$\{OH^-\}$	$B1/\{H^+\}^1$	$B2/\{H^+\}^2$	$B3/\{H^+\}^3$	$/B4\{H^+\}^4$	TOTCu, eq	$\{Cu^{2+}\}$	$Log\{Cu^{2+}\}$	$\{CuOH^+\}$	$Log\{CuOH^+\}$	$\{Cu(OH)_2^0\}$	$Log\{Cu(OH)_2^0\}$	$\{Cu(OH)_3^-\}$	$Log\{Cu(OH)_3^-\}$	$\{Cu(OH)_4^{2-}\}$	$Log\{Cu(OH)_4^{2-}\}$
0	1.00E+00	1.00E-14	1.00E-08	4.37E-14	1.26E-27	2.51E-40	1.00E+00	2.74E-03	-2.56E+00	2.74E-11	-1.06E+01	1.20E-16	-1.59E+01	3.45E-30	-2.95E+01	6.88E-43	-4.22E+01
1	1.00E-01	1.00E-13	1.00E-07	4.37E-12	1.26E-24	2.51E-36	1.00E+00	2.74E-03	-2.56E+00	2.74E-10	-9.56E+00	1.20E-14	-1.39E+01	3.45E-27	-2.65E+01	6.88E-39	-3.82E+01
2	1.00E-02	1.00E-12	1.00E-06	4.37E-10	1.26E-21	2.51E-32	1.00E+00	2.74E-03	-2.56E+00	2.74E-09	-8.56E+00	1.20E-12	-1.19E+01	3.45E-24	-2.35E+01	6.88E-35	-3.42E+01
3	1.00E-03	1.00E-11	1.00E-05	4.37E-08	1.26E-18	2.51E-28	1.00E+00	2.74E-03	-2.56E+00	2.74E-08	-7.56E+00	1.20E-10	-9.92E+00	3.45E-21	-2.05E+01	6.88E-31	-3.02E+01
4	1.00E-04	1.00E-10	1.00E-04	4.37E-06	1.26E-15	2.51E-24	1.00E+00	2.74E-03	-2.56E+00	2.74E-07	-6.56E+00	1.20E-08	-7.92E+00	3.45E-18	-1.75E+01	6.88E-27	-2.62E+01
5	1.00E-05	1.00E-09	1.00E-03	4.37E-04	1.26E-12	2.51E-20	1.00E+00	2.74E-03	-2.56E+00	2.74E-06	-5.56E+00	1.19E-06	-5.92E+00	3.44E-15	-1.45E+01	6.87E-23	-2.22E+01
6	1.00E-06	1.00E-08	1.00E-02	4.37E-02	1.26E-09	2.51E-16	1.05E+00	2.60E-03	-2.58E+00	2.60E-05	-4.58E+00	1.14E-04	-3.94E+00	3.27E-12	-1.15E+01	6.53E-19	-1.82E+01
7	1.00E-07	1.00E-07	1.00E-01	4.37E+00	1.26E-06	2.51E-12	5.47E+00	5.01E-04	-3.30E+00	5.01E-05	-4.30E+00	2.19E-03	-2.66E+00	6.31E-10	-9.20E+00	1.26E-15	-1.49E+01
8	1.00E-08	1.00E-06	1.00E+00	4.37E+02	1.26E-03	2.51E-08	4.39E+02	6.25E-06	-5.20E+00	6.25E-06	-5.20E+00	2.73E-03	-2.56E+00	7.87E-09	-8.10E+00	1.57E-13	-1.28E+01
9	1.00E-09	1.00E-05	1.00E+01	4.37E+04	1.26E+00	2.51E-04	4.37E+04	6.28E-08	-7.20E+00	6.28E-07	-6.20E+00	2.74E-03	-2.56E+00	7.90E-08	-7.10E+00	1.58E-11	-1.08E+01
10	1.00E-10	1.00E-04	1.00E+02	4.37E+06	1.26E+03	2.51E+00	4.37E+06	6.28E-10	-9.20E+00	6.28E-08	-7.20E+00	2.74E-03	-2.56E+00	7.90E-07	-6.10E+00	1.58E-09	-8.80E+00
11	1.00E-11	1.00E-03	1.00E+03	4.37E+08	1.26E+06	2.51E+04	4.38E+08	6.26E-12	-1.12E+01	6.26E-09	-8.20E+00	2.73E-03	-2.56E+00	7.88E-06	-5.10E+00	1.57E-07	-6.80E+00
12	1.00E-12	1.00E-02	1.00E+04	4.37E+10	1.26E+09	2.51E+08	4.52E+10	6.07E-14	-1.32E+01	6.07E-10	-9.22E+00	2.65E-03	-2.58E+00	7.64E-05	-4.12E+00	1.52E-05	-4.82E+00
13	1.00E-13	1.00E-01	1.00E+05	4.37E+12	1.26E+12	2.51E+12	8.14E+12	3.37E-16	-1.55E+01	3.37E-11	-1.05E+01	1.47E-03	-2.83E+00	4.24E-04	-3.37E+00	8.46E-04	-3.07E+00
14	1.00E-14	1.00E+00	1.00E+06	4.37E+14	1.26E+15	2.51E+16	2.68E+16	1.02E-19	-1.90E+01	1.02E-13	-1.30E+01	4.46E-05	-4.35E+00	1.29E-04	-3.89E+00	2.57E-03	-2.59E+00

Zinc:

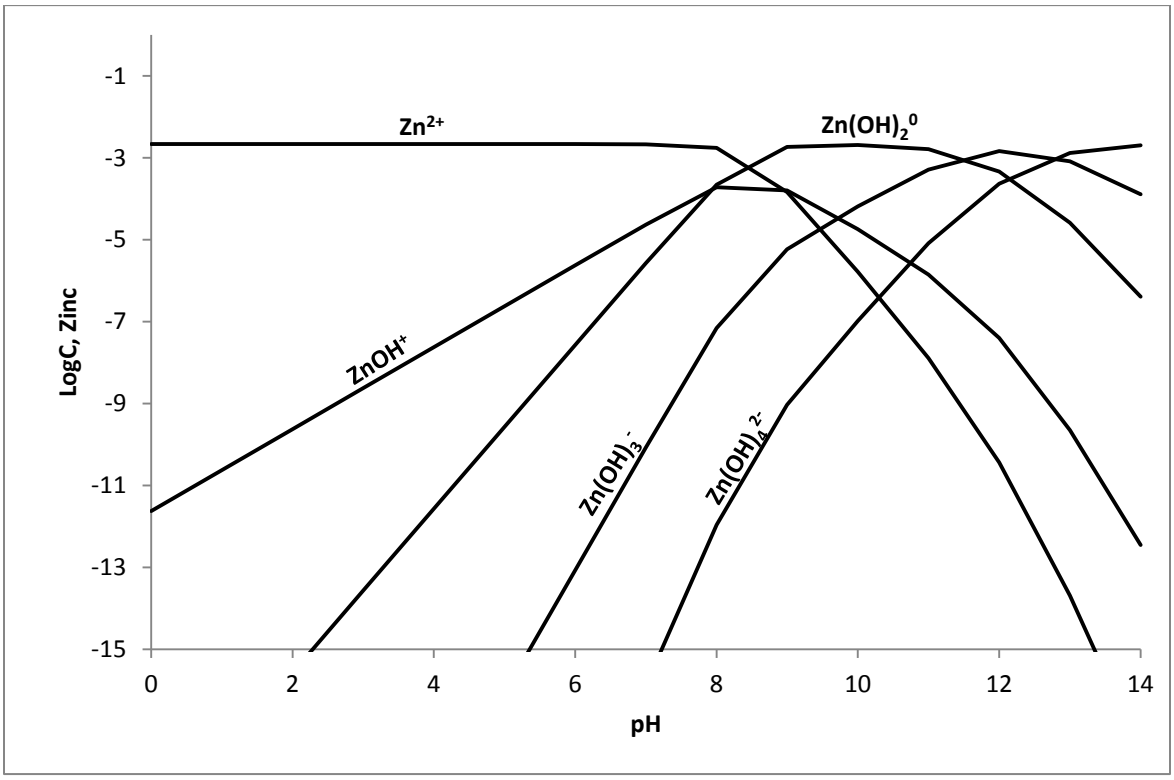

Figure 39: Log C-pH diagram for Zn in a system with 2.17 mM TOTZn, Løkken works

Table 50: Calculation of log C - pH diagram for zinc, Løkken works

TOTZn [mol/L]	0.00217		
Log B1	-8.96	B1	1.1E-09
Log B2	-16.9	B2	1.26E-17
Log B3	-28.4	B3	3.98E-29
Log B4	-41.2	B4	6.31E-42

pH	$\{H^+\}$	$\{OH^-\}$	$B1/\{H^+\}^1$	$B2/\{H^+\}^2$	$B3/\{H^+\}^3$	$/B4\{H^+\}^4$	TOTZn	$\{Zn^{2+}\}$	$Log\{Zn^{2+}\}$	$\{ZnOH^+\}$	$Log\{ZnOH^+\}$	$\{Zn(OH)_2^0\}$	$Log\{Zn(OH)_2^0\}$	$\{Zn(OH)_3^-\}$	$Log\{Zn(OH)_3^-\}$	$\{Zn(OH)_4^{2-}\}$	$Log\{Zn(OH)_4^{2-}\}$
0	1.00E+00	1.00E-14	1.10E-09	1.26E-17	3.98E-29	6.31E-42	1.00E+00	2.17E-03	-2.66E+00	2.38E-12	-1.16E+01	2.73E-20	-1.96E+01	8.64E-32	-3.11E+01	1.37E-44	-4.39E+01
1	1.00E-01	1.00E-13	1.10E-08	1.26E-15	3.98E-26	6.31E-38	1.00E+00	2.17E-03	-2.66E+00	2.38E-11	-1.06E+01	2.73E-18	-1.76E+01	8.64E-29	-2.81E+01	1.37E-40	-3.99E+01
2	1.00E-02	1.00E-12	1.10E-07	1.26E-13	3.98E-23	6.31E-34	1.00E+00	2.17E-03	-2.66E+00	2.38E-10	-9.62E+00	2.73E-16	-1.56E+01	8.64E-26	-2.51E+01	1.37E-36	-3.59E+01
3	1.00E-03	1.00E-11	1.10E-06	1.26E-11	3.98E-20	6.31E-30	1.00E+00	2.17E-03	-2.66E+00	2.38E-09	-8.62E+00	2.73E-14	-1.36E+01	8.64E-23	-2.21E+01	1.37E-32	-3.19E+01
4	1.00E-04	1.00E-10	1.10E-05	1.26E-09	3.98E-17	6.31E-26	1.00E+00	2.17E-03	-2.66E+00	2.38E-08	-7.62E+00	2.73E-12	-1.16E+01	8.64E-20	-1.91E+01	1.37E-28	-2.79E+01
5	1.00E-05	1.00E-09	1.10E-04	1.26E-07	3.98E-14	6.31E-22	1.00E+00	2.17E-03	-2.66E+00	2.38E-07	-6.62E+00	2.73E-10	-9.56E+00	8.64E-17	-1.61E+01	1.37E-24	-2.39E+01
6	1.00E-06	1.00E-08	1.10E-03	1.26E-05	3.98E-11	6.31E-18	1.00E+00	2.17E-03	-2.66E+00	2.38E-06	-5.62E+00	2.73E-08	-7.56E+00	8.63E-14	-1.31E+01	1.37E-20	-1.99E+01
7	1.00E-07	1.00E-07	1.10E-02	1.26E-03	3.98E-08	6.31E-14	1.01E+00	2.14E-03	-2.67E+00	2.35E-05	-4.63E+00	2.70E-06	-5.57E+00	8.53E-11	-1.01E+01	1.35E-16	-1.59E+01
8	1.00E-08	1.00E-06	1.10E-01	1.26E-01	3.98E-05	6.31E-10	1.24E+00	1.76E-03	-2.76E+00	1.93E-04	-3.72E+00	2.21E-04	-3.66E+00	6.99E-08	-7.16E+00	1.11E-12	-1.20E+01
9	1.00E-09	1.00E-05	1.10E+00	1.26E+01	3.98E-02	6.31E-06	1.47E+01	1.47E-04	-3.83E+00	1.62E-04	-3.79E+00	1.86E-03	-2.73E+00	5.87E-06	-5.23E+00	9.30E-10	-9.03E+00
10	1.00E-10	1.00E-04	1.10E+01	1.26E+03	3.98E+01	6.31E-02	1.31E+03	1.66E-06	-5.78E+00	1.82E-05	-4.74E+00	2.08E-03	-2.68E+00	6.59E-05	-4.18E+00	1.04E-07	-6.98E+00
11	1.00E-11	1.00E-03	1.10E+02	1.26E+05	3.98E+04	6.31E+02	1.66E+05	1.30E-08	-7.88E+00	1.43E-06	-5.84E+00	1.64E-03	-2.78E+00	5.19E-04	-3.28E+00	8.23E-06	-5.08E+00
12	1.00E-12	1.00E-02	1.10E+03	1.26E+07	3.98E+07	6.31E+06	5.87E+07	3.70E-11	-1.04E+01	4.05E-08	-7.39E+00	4.65E-04	-3.33E+00	1.47E-03	-2.83E+00	2.33E-04	-3.63E+00
13	1.00E-13	1.00E-01	1.10E+04	1.26E+09	3.98E+10	6.31E+10	1.04E+11	2.08E-14	-1.37E+01	2.28E-10	-9.64E+00	2.62E-05	-4.58E+00	8.29E-04	-3.08E+00	1.31E-03	-2.88E+00
14	1.00E-14	1.00E+00	1.10E+05	1.26E+11	3.98E+13	6.31E+14	6.71E+14	3.23E-18	-1.75E+01	3.55E-13	-1.25E+01	4.07E-07	-6.39E+00	1.29E-04	-3.89E+00	2.04E-03	-2.69E+00

Manganese:

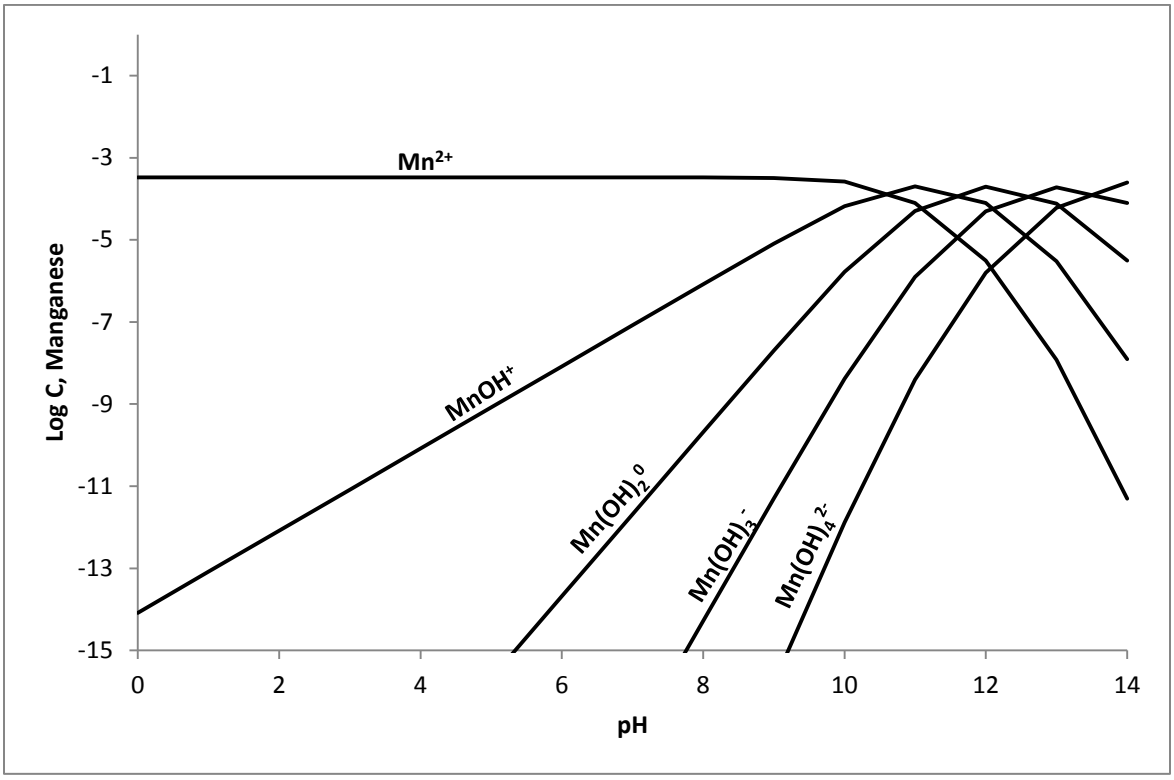

Figure 40: Log C-pH diagram for Mn in a system with 0.33 mM TOTMn, Løkken works

Table 51: Calculation of log C - pH diagram for manganese, Løkken works

TOTMn [mol/L]	0.00033		
Log B1		B1	2.51E-11
Log B2		B2	6.31E-23
Log B3		B3	1.58E-35
Log B4		B4	5.01E-49

pH	$\{H^+\}$	$\{OH^-\}$	$B1/\{H^+\}^1$	$B2/\{H^+\}^2$	$B3/\{H^+\}^3$	$/B4\{H^+\}^4$	TOTMn	$\{Mn^{2+}\}$	$Log\{Mn^{2+}\}$	$\{MnOH^+\}$	$Log\{MnOH^+$	$\{Mn(OH)_2^0\}$	$Log\{Mn(OH)_2$	$\{Mn(OH)_3^-$	$Log\{Mn(OH)_3^-$	$\{Mn(OH)_4^{2-}$	$Log\{Mn(OH)_4^{2-}$
0	1.00E+00	1.00E-14	2.51E-11	6.31E-23	1.58E-35	5.01E-49	1.00E+00	3.30E-04	-3.48E+00	8.29E-15	-1.41E+01	2.08E-26	-2.57E+01	5.23E-39	-3.83E+01	1.65E-52	-5.18E+01
1	1.00E-01	1.00E-13	2.51E-10	6.31E-21	1.58E-32	5.01E-45	1.00E+00	3.30E-04	-3.48E+00	8.29E-14	-1.31E+01	2.08E-24	-2.37E+01	5.23E-36	-3.53E+01	1.65E-48	-4.78E+01
2	1.00E-02	1.00E-12	2.51E-09	6.31E-19	1.58E-29	5.01E-41	1.00E+00	3.30E-04	-3.48E+00	8.29E-13	-1.21E+01	2.08E-22	-2.17E+01	5.23E-33	-3.23E+01	1.65E-44	-4.38E+01
3	1.00E-03	1.00E-11	2.51E-08	6.31E-17	1.58E-26	5.01E-37	1.00E+00	3.30E-04	-3.48E+00	8.29E-12	-1.11E+01	2.08E-20	-1.97E+01	5.23E-30	-2.93E+01	1.65E-40	-3.98E+01
4	1.00E-04	1.00E-10	2.51E-07	6.31E-15	1.58E-23	5.01E-33	1.00E+00	3.30E-04	-3.48E+00	8.29E-11	-1.01E+01	2.08E-18	-1.77E+01	5.23E-27	-2.63E+01	1.65E-36	-3.58E+01
5	1.00E-05	1.00E-09	2.51E-06	6.31E-13	1.58E-20	5.01E-29	1.00E+00	3.30E-04	-3.48E+00	8.29E-10	-9.08E+00	2.08E-16	-1.57E+01	5.23E-24	-2.33E+01	1.65E-32	-3.18E+01
6	1.00E-06	1.00E-08	2.51E-05	6.31E-11	1.58E-17	5.01E-25	1.00E+00	3.30E-04	-3.48E+00	8.29E-09	-8.08E+00	2.08E-14	-1.37E+01	5.23E-21	-2.03E+01	1.65E-28	-2.78E+01
7	1.00E-07	1.00E-07	2.51E-04	6.31E-09	1.58E-14	5.01E-21	1.00E+00	3.30E-04	-3.48E+00	8.29E-08	-7.08E+00	2.08E-12	-1.17E+01	5.23E-18	-1.73E+01	1.65E-24	-2.38E+01
8	1.00E-08	1.00E-06	2.51E-03	6.31E-07	1.58E-11	5.01E-17	1.00E+00	3.29E-04	-3.48E+00	8.27E-07	-6.08E+00	2.08E-10	-9.68E+00	5.22E-15	-1.43E+01	1.65E-20	-1.98E+01
9	1.00E-09	1.00E-05	2.51E-02	6.31E-05	1.58E-08	5.01E-13	1.03E+00	3.22E-04	-3.49E+00	8.09E-06	-5.09E+00	2.03E-08	-7.69E+00	5.10E-12	-1.13E+01	1.61E-16	-1.58E+01
10	1.00E-10	1.00E-04	2.51E-01	6.31E-03	1.58E-05	5.01E-09	1.26E+00	2.62E-04	-3.58E+00	6.59E-05	-4.18E+00	1.66E-06	-5.78E+00	4.16E-09	-8.38E+00	1.32E-12	-1.19E+01
11	1.00E-11	1.00E-03	2.51E+00	6.31E-01	1.58E-02	5.01E-05	4.16E+00	7.94E-05	-4.10E+00	1.99E-04	-3.70E+00	5.01E-05	-4.30E+00	1.26E-06	-5.90E+00	3.98E-09	-8.40E+00
12	1.00E-12	1.00E-02	2.51E+01	6.31E+01	1.58E+01	5.01E-01	1.06E+02	3.13E-06	-5.51E+00	7.85E-05	-4.11E+00	1.97E-04	-3.71E+00	4.95E-05	-4.31E+00	1.57E-06	-5.81E+00
13	1.00E-13	1.00E-01	2.51E+02	6.31E+03	1.58E+04	5.01E+03	2.74E+04	1.20E-08	-7.92E+00	3.02E-06	-5.52E+00	7.59E-05	-4.12E+00	1.91E-04	-3.72E+00	6.03E-05	-4.22E+00
14	1.00E-14	1.00E+00	2.51E+03	6.31E+05	1.58E+07	5.01E+07	6.66E+07	4.95E-12	-1.13E+01	1.24E-08	-7.90E+00	3.13E-06	-5.50E+00	7.85E-05	-4.10E+00	2.48E-04	-3.60E+00

Comparing theoretical and practical dry matter content in AMD

Folldal center

Practical amount:

Table 52: Practical amount of dry matter in 100 ml AMD from Folldal center

Weight of beaker [g]	65.4
Weight of magnet [g]	2.0
Weight of beaker, magnet and dry matter [g]	68.2
Dry matter [g]	***0.9***
Dry matter [mg]	***899.6***

Theoretical amount:

Table 53: Theoretical amount of dry matter in 100 ml AMD from Folldal center

	Initial metal conc. [mol/L]	**Conc. of soluble metal hydroxides at pH 6 [mol/L]**	**Conc. of precipitate metal hydroxides at pH 6 [mol/L]**	**Molar mass [g/mol]**	**Conc. precipitated metal hydroxides at pH 6 [mg/L]**	**Amount dry matter in 100 ml AMD [mg]**
$Fe(OH)_3^0$	1.56E-02	1.80E-04	1.54E-02	106.87	1.64E+03	1.64E+02
$Cu(OH)_2^0$	1.25E-03	5.18E-05	1.20E-03	97.56	1.17E+02	1.17E+01
$Zn(OH)_2^0$	8.60E-04	1.08E-08	8.60E-04	99.40	8.55E+01	8.55E+00
$Mn(OH)_2^0$	1.40E-04	8.83E-15	1.40E-04	88.95	1.25E+01	1.25E+00
Dry matter [mg]						***185.85***

Løkken works

Practical amount:

Table 54: Practical amount of dry matter in 100 ml AMD from Løkken works

Weight of beaker [g]	69.4
Weight of magnet [g]	2.0
Weight of beaker, magnet and dry matter [g]	73.7
Dry matter [g]	***2.3***
Dry matter [mg]	***2337.9***

Theoretical amount:

Table 55: Theoretical amount of dry matter in 100 ml AMD from Løkken works

	Initial metal conc. [mol/L]	Conc. of soluble metal hydroxides at pH 6 [mol/L]	Conc. of precipitate metal hydroxides at pH 6 [mol/L]	Molar mass [g/mol]	Conc. precipitated metal hydroxides at pH 6 [mg/L]	Amount dry matter in 100 ml AMD [mg]
$Fe(OH)_3^0$	0.05075	5.88E-04	5.02E-02	106.87	5.36E+03	5.36E+02
$Cu(OH)_2^0$	0.00274	1.14E-04	2.63E-03	97.56	2.56E+02	2.56E+01
$Zn(OH)_2^0$	0.00217	2.73E-08	2.17E-03	99.40	2.16E+02	2.16E+01
$Mn(OH)_2^0$	0.00033	2.08E-15	3.30E-04	88.95	2.94E+01	2.94E+00
Dry matter [mg]						***586.20***